Univerzita Karlova

1. lékařská fakulta

Studijní program: Biochemie a patobiochemie

Ing. Kateřina, Žížalová

Metabolické účinky žlučových lipidů

Metabolic effects of bile lipids

Typ závěrečné práce:

Disertační

Vedoucí závěrečné práce/Školitel: MUDr. Martin Leníček, Ph.D

Praha, 2023

Prohlášení:

Prohlašuji, že jsem závěrečnou práci zpracoval/a samostatně a že jsem řádně uvedla a citovala všechny použité prameny a literaturu. Současně prohlašuji, že práce nebyla využita k získání jiného nebo stejného titulu

Souhlasím s trvalým uložením elektronické verze mé práce v databázi systému meziuniverzitního projektu Theses.cz za účelem soustavné kontroly podobnosti kvalifikačních prací.

V Praze, 14. 06. 2023

Kateřina Žížalová

Podpis

Identifikační záznam:

ŽÍŽALOVÁ, Kateřina. *Metabolické účinky žlučových lipidů*. Praha, 2023. Disertační práce. Univerzita Karlova, 1. lékařská fakulta, Ústav lékařské biochemie a laboratorní diagnostiky. Vedoucí práce Martin Leníček.

Klíčová slova: *žlučové kyseliny, portální hypertenze, bakteriální modifikace*

Keywords: *bile acids, portal hypertension, bacterial modification*

Poděkování:
Na tomto místě bych ráda poděkovala všem, kdo mi při vypracování i splnění cílů disertační práce pomohli. Můj dík patří zejména všem současným i bývalým členům Laboratoře pro výzkum nemocí jater a metabolismu hemu. Jmenovitě prof. MUDr. Liboru Vítkovi Ph.D. za její vedení i cenné rady, mému školiteli MUDr. Martinu Leníčkovi Ph.D. za ochotu, nápady i trpělivost v průběhu všech let a RNDr. Aleši Dvořákovi Ph.D. za korektury i podporu.
Dále bych ráda poděkovala zaměstnancům IV. interní kliniky VFN za poskytnuté vzorky i četné konzultace, obzvláště prof. MUDr. Radanu Brůhovi CSc., MUDr. Václavu Šmídovi Ph.D. a MUDr. Barboře Novákové. V neposlední řadě děkuji MUDr. Marku Veckovi Ph.D. z Laboratoře pro výzkum aterosklerózy za rady i ochotu.
Nakonec bych ráda poděkovala Nadačnímu fondu České hepatologické společnosti za finanční podporu k účasti na řadě konferencí.

Obsah

1. Úvod 6
1.1 Historie poznání 6
1.2 Struktura žlučových kyselin 8
1.3 Fyzikálně-chemické vlastnosti žlučových kyselin 9
1.4 Biosyntéza žlučových kyselin 10
1.5 Biotransformace žlučových kyselin 13
1.5.1 Konjugace 13
1.5.2 Sulfatace 15
1.5.3 Glukuronidace 17
1.5.4 Bakteriální transformace 17
1.6 Enterohepatální oběh 20
1.7 Metody stanovení žlučových kyselin 22
1.7.1 Chromatografické metody 22
1.7.2 Enzymatické stanovení 24
1.7.3 Imunochemické metody 25
1.7.4 Nukleární magnetická rezonanční spektroskopie 26
2. Cíle práce 27
3. Publikace 29
4. Diskuse 30
5. Citace 38
Seznam zkratek 47
Příloha 1 48
Příloha 2 55
Příloha 3 67
Příloha 4 89
Příloha 5 93

1. Úvod

1.1 Historie poznání

Podávání žlučových kyselin ve formě medvědí žluči bylo součástí tradiční čínské (a později i korejské a japonské) medicíny již před mnoha staletími. Medvědí žluč byla doporučována pro detoxikaci organismu, při zánětu jater, ale také na snížení bolesti, horečky či při hemeroidech (Feng et al., 2009). V té době se ale nevědělo, že hlavní účinnou složkou medvědí žluči je kyselina ursodeoxycholová, tu západní medicína objevila až v osmdesátých letech 20. století (Podda et al., 1989; Salen, 1988).

Vědecky se jako první žlučovými kyselinami zabýval Adolph Strecker. Tento významný chemik 19. století kromě jiného zkoumal složení volské a prasečí žluči. V roce 1848 popsal izolaci kyseliny cholové a zároveň správně určil její sumární vzorec $C_{24}H_{40}O_5$ (Strecker, 1848; Zeisel, 2012). Strukturu této kyseliny jako první popsal Heinrich Otto Wieland, za což získal Nobelovu cenu za rok 1927 (*The Nobel Prize in Chemistry 1927*). Jím popsaná struktura však nebyla zcela správná, Wieland nesprávně určil druhý kruh jako cyklopentan a nesprávně umístil i postranní řetězec (Obrázek 1). Skutečnou chemickou strukturu žlučových kyselin popsal až O. Rosenheim v roce 1932 (Rosenheim & King, 1932).

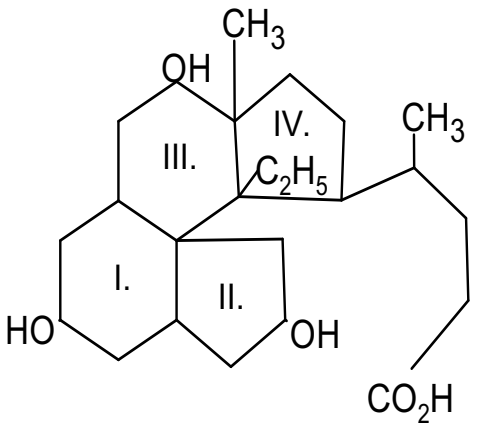

Obrázek 1: Struktura žlučové kyseliny navržená H.Wielandem Upraveno z: (Wieland, 1924)

Rosenheim popsal strukturu jako redukovaný fenantren, ke kterému je připojen čtvrtý cyklopentanový kruh s postranním řetězcem na C17, tedy nikoliv na C10, jak předpokládal Wieland (Obrázek 2) (Rosenheim & King, 1932).

Rosenheim k výzkumu žlučových kyselin přispěl ještě jedním objevem, kdy správně lokalizoval druhou hydroxylovou skupinu kyseliny deoxycholové na C12 (Rosenheim & King, 1932). Její struktura byla objevena jako poslední z majoritních lidských žlučových kyselin.

Heinrich Wieland popsal i izolaci kyseliny cholové z volské žluče (Wieland, 1924). Následně přesvědčil manžela své sestřenice Alberta Boehringera, který vlastnil farmacetickou společnost, aby začala kyselinu cholovou vyrábět komerčně podle jeho postupu. V té době se věřilo, že kyselina cholová podporuje funkci jater a funguje jako laxativum. Nebylo to však podložené žádnou studií, výzkum žlučových kyselin byl v té době spíše na okraji zájmu. Ve 40. letech 20. století začala být ve velkém vyráběna i kyselina deoxycholová, ta však jako prekurzor kortisonu (Hofmann & Hagey, 2014).

Až po druhé světové válce se skupina z laboratoře Sune Bergstroma začala zabývat metabolismem žlučových kyselin v různých organismech (Bergstrom et al., 1960; Bergstrom et al., 1959; Gustafsson et al., 1957). Z této skupiny pocházel i Jan Sjovall, který popsal metody stanovení žlučových kyselin pomocí plynové chromatografie (GC) s hmotnostní detekcí (MS) (Eneroth et al., 1966). Tuto metodu využil k řadě objevů během následujících 40 let, mimo jiné k odlišení žlučových kyselin na primární a sekundární (Norman & Sjovall, 1958). Historie poznání by však jistě nebyla kompletní bez Alana Fredericka Hofmanna, který celý svůj profesní život zasvětil výzkumu žlučových kyselin a jehož objevy se dají jen těžko shrnout do jedné věty. Namátkou popsal fylogenezi žlučových kyselin, enterohepatální oběh nebo využití

žlučových kyselin při rozpouštění žlučových kamenů (Hofmann, 2009), citace jeho publikací se prolínají celou disertační prací.

1.2 Struktura žlučových kyselin

Žlučové kyseliny se skládají z jádra a postranního řetězce. Jádro tvoří jeden cyklopentanový a tři cyklohexanové kruhy, postranní řetězec je pak tvořen alifatickým uhlovodíkem s karboxylovou skupinou (Obrázek 2). Jednotlivé žlučové kyseliny

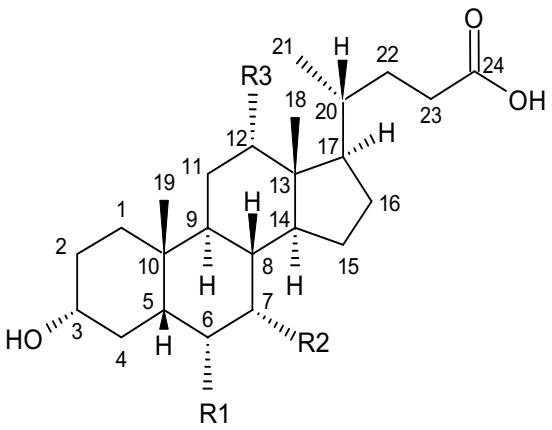

	kyselina	R1	R2	R3
AlloCA*	allocholová		7α	12α
CA	cholová		7α	12α
CDCA	chenodeoxycholová		7α	
DCA	deoxycholová			12α
HCA	hyocholová	6α	7α	
HDCA	hyodeoxycholová	6α		
LCA	lithocholová			
MDCA	murideoxycholová	6β		
UDCA	ursodeoxycholová		7α	
α-MCA	α-muricholová	6β	7α	
β-MCA	β-muricholová	6β	7α	
ω-MCA	ω-muricholová	6α	7α	

Obrázek 2. Struktura žlučové kyseliny. Tabulka popisuje pozici hydroxylových skupin pro jednotlivé žlučové kyseliny. V pozicích, které jsou volné je na příslušný uhlík navázán vodík, pro přehlednost je však neuvádím. Dále v textu používám výše uvedené zkratky, v případě konjugace (viz dále) používám před zkratkou žlučové kyseliny G pro glycin a T pro taurin.

**Na obrázku je znázorněna konformace cis. Předpona allo se používá pro žlučové kyseliny v pozici trans.*

se mohou lišit jak délkou postranního řetězce, tak substituenty na něm i na jádře (Hofmann & Roda, 1984). Všechny žlučové kyseliny však obsahují hydroxylovou skupinu na C3 v pozici α, na rozdíl od cholesterolu, který ji má v pozici β. U lidí se postranní řetězec nemění, lidské žlučové kyseliny tvoří vždy 24 uhlíkatá kostra. Lišit se mohou tedy konjugací na postranním řetězci (viz dále) a počtem hydroxylových skupin (Hofmann et al., 2010). Majoritními lidskými žlučovými kyselinami jsou kyselina cholová (CA), kyselina chenodeoxcholová (CDCA), kyselina

deoxcholová (DCA) a kyselina lithocholová (LCA). Strukturu těchto (i dalších žlučových kyselin použitých v naší práci) znázorňuje (Obrázek 2).

Pokud se podíváme na stereochemii molekuly, kruhy A a B mohou zaujímat jak pozici *cis*, tak *trans*, což je dáno postavením vodíku na C5. Většina v přírodě se vyskytujících žlučových kyselin zaujímá pozici *cis.* Pro žlučové kyseliny s kruhy A/B v pozici *trans* byla zavedena předpona *allo* (Fieser & Fieser, 1959; Hofmann & Hagey, 2014).

1.3 Fyzikálně-chemické vlastnosti žlučových kyselin

Žlučové kyseliny jsou planární amfipatické molekuly. Skládají se z hydrofobní (steroidní jádro) a hydrofilní (hydroxylové a karboxylové skupiny) části (Hofmann, 2009) (Obrázek 3). Obecně je rozpustnost přirozeně se vyskytujících C24 žlučových

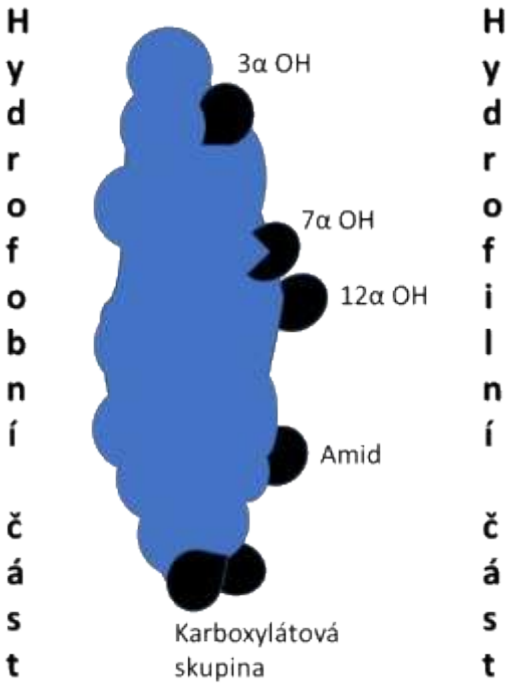

Obrázek 3: Uspořádání molekuly kyseliny cholové. [Upraveno z:(Hofmann & Hagey, 2014)]

kyselin ve vodě velmi malá, pro základní lidské žlučové kyseliny se pohybuje od 0,05 μmol/l (LCA) přes 28 μmol/l (CDCA a DCA) po 273 μmol/l (CA) (Roda & Fini, 1984).

V roztoku se mohou žlučové kyseliny vyskytovat v protonované formě, zároveň jako slabé kyseliny v roztoku částečně disociují a tvoří soli zejména s kationty vápníku nebo sodíku (Hofmann & Mysels, 1992). Pokud koncentrace žlučových kyselin dosáhne tzv. kritické micelární koncentrace, anionty žlučových kyselin se samovolně spojují a tvoří agregáty obsahující od 4 do 40 molekul (Cabral, 1989). Hodnota kritické micelární koncentrace se odvíjí zejména od počtu hydroxylových skupin žlučových kyselin, dále od jejich pozice a orientace. Také se mění s přítomností kationtů nebo dalších lipofilních látek, a to i v závislosti na koncentraci (Hofmann & Mysels, 1992). Například v séru se žlučové kyseliny vyskytují pod svou micelární koncentrací, shlukují se pak s polárními lipidy a tvoří micely složené (Hofmann, 2009; Natalini et al., 2014; Tamesue & Juniper, 1967). Předpokládá se, že ve žluči se žlučové kyseliny vyskytují ve všech formách, tedy ve formě monomerů, jednoduchých i složených micel (Hofmann & Hagey, 2014).

1.4 Biosyntéza žlučových kyselin

Na syntéze žlučových kyselin se podílí přes 17 enzymů, které jsou lokalizovány v cytosolu, endoplasmatickém retikulu, mitochondriích a peroxisomech. U lidí probíhá zejména dvěma drahami: první nazýváme klasickou (též neutrální), druhou pak alternativní (kyselou) (Russell, 2003; Vaz & Ferdinandusse, 2017). Žlučové kyseliny vzniklé biosyntézou nazýváme jako primární. Klasickou cestou vzniká zejména kyselina cholová, na konci té alternativní je pak kyselina chenodeoxycholová. U obou

těchto drah je výchozí molekulou cholesterol. Dochází ke zkrácení postranního řetězce, oxidaci na karboxylovou kyselinu, změně pozice 3β hydroxylové skupiny na 3α a k hydroxylaci C7, případně C12 (Chiang, 1998; Vaz & Ferdinandusse, 2017). Jednotlivé kroky obou drah viz (Obrázek 4)**Chyba! Nenalezen zdroj odkazů.**. Každý den se v játrech přemění na žlučové kyseliny asi 500 mg cholesterolu (Russell, 2003). Kromě toho byly popsány dvě další dráhy, nazývají se Yamasakiho a 25-hydroxylační. Tyto dráhy sdílejí většinu reakcí i enzymů s drahami uvedenými výše, kombinují reakce těchto dvou drah či jejich pořadí (více Duane et al., 1988; Setchell et al., 1988). U všech výše uvedených drah není dodnes znám přesný počet meziproduktů, všechny enzymy ani lokalizace všech reakcí (Sarenac & Mikov, 2018).

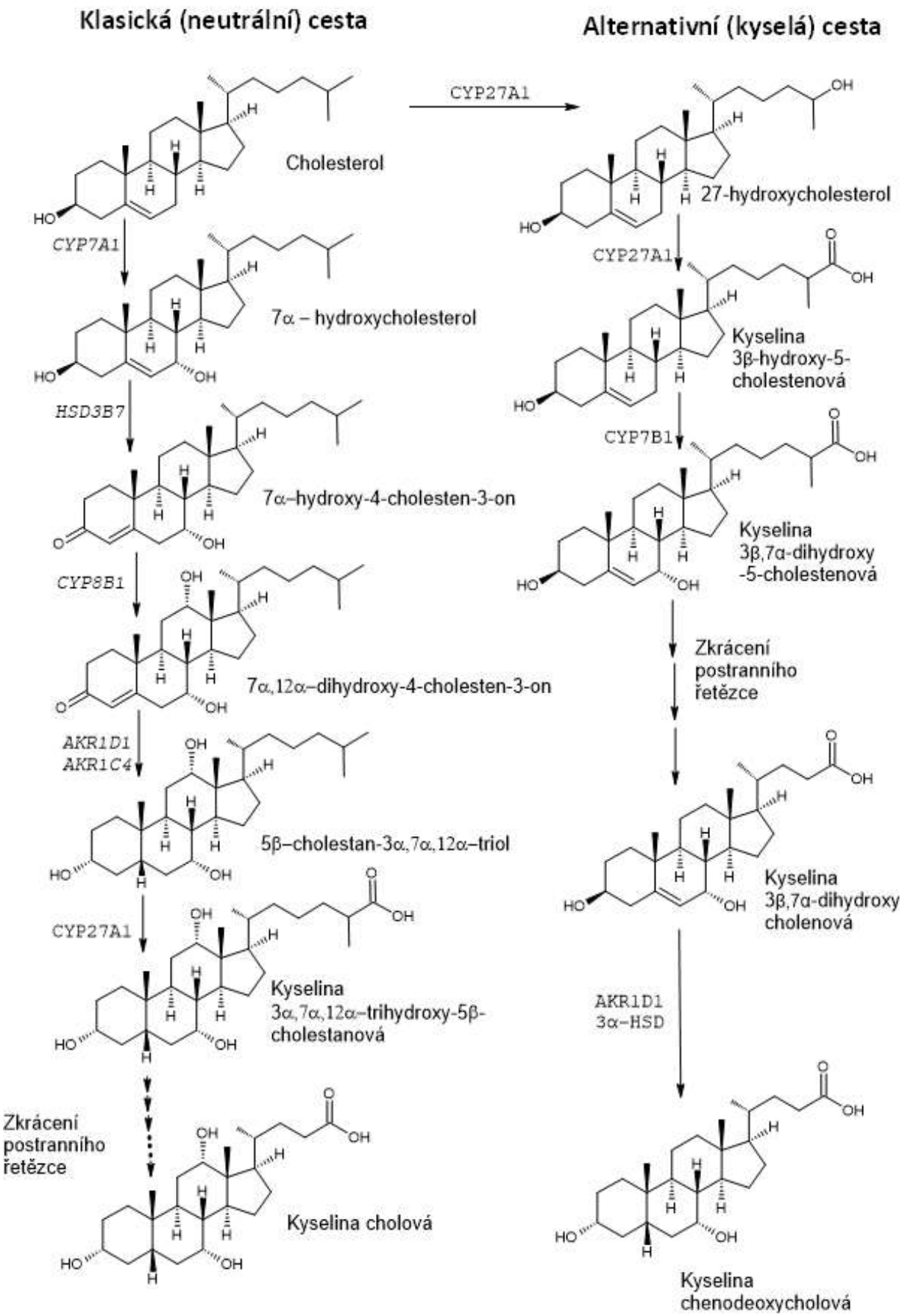

Obrázek 4: Biosyntéza žlučových kyselin

1.5 Biotransformace žlučových kyselin

K biotransformaci žlučových kyselin dochází jak endogenně v játrech, tak činností střevních bakterií. Endogenní modifikace zlepšují detergentní vlastnosti žlučových kyselin (konjugace) či usnadňují jejich vylučovaní z organismu (sulfatace, glukuronidace). Bakterie zase části žlučových kyselin využívají ke své potřebě či je modifikují s cílem snížit jejich toxicitu (Hofmann & Hagey, 2014; Pedersen et al., 2022; Philipp, 2011).

1.5.1 Konjugace

Konjugací se v případě žlučových kyselin rozumí N-acyl amidace. Jedná se o II. fázi biotransformace, při které dochází ke vzniku kovalentní vazby mezi karboxylovou skupinou žlučové kyseliny a glycinem nebo taurinem (Hofmann & Hagey, 2014). Konjugace žlučových kyselin s těmito aminokyselinami snižuje jejich pKa. Nekojugované žlučové kyseliny jsou tak nejslabší kyselinou (pKa= 5), následují glykokonjugáty (pKa= 4) a nakonec taurokonjugáty (pKa= 2) (Fini & Roda, 1987). V lumen tenkého střeva se uvádí pH kolem 6,5. To znamená, že nekonjugované kyseliny nejhůře disociují a jsou tedy nejméně rozpustné ve vodě (Hofmann, 1963). Proces konjugace probíhá jak v hepatocytech, tak v cholangiocytech, nicméně konjugace v hepatocytech výrazně převažuje (Hylemon et al., 1990). Klíčovým enzymem je Bile acid-CoA:amino-acid N-acyltransferase (BAAT, EC: 2.3.1.65), která je lokalizována v peroxisomech i cytosolu. Podle posledních prací však dochází ke konjugaci pouze v peroxisomech, kde se konjugují jak nově vzniklé žlučové kyseliny, tak ty přicházejících portální žílou (Styles et al., 2007, Rembacz et al., 2010). Konjugace probíhá ve dvou základních krocích, v prvním dochází ke vzniku thioesteru, ve druhém je připojen taurin nebo glycin (Obrázek 5).

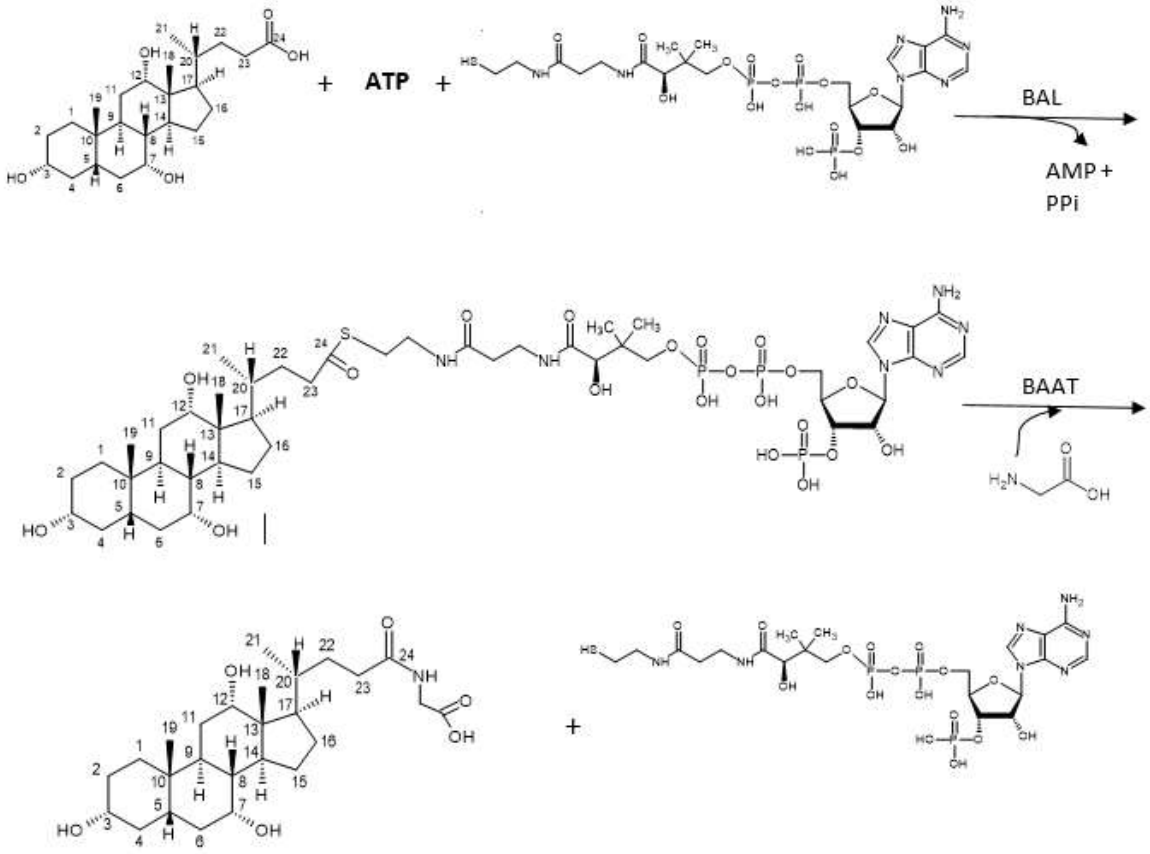

Obrázek 5: Při konjugaci dochází ke vzniku thioesteru z postranního řetězce žlučové kyseliny a koenzymu A v přítomnosti enzymu BAL (Bile acid CoA ligase, EC 6.2.1.7). V druhé fázi BAAT odštěpí koenzym A a místo něj je na acylový zbytek kovalentně připojen taurin nebo glycin (Kirilenko et al., 2019; Sfakianos et al., 2002).

BAAT na žlučové kyseliny přenáší výhradně taurin nebo glycin, a tak jsou u vyšších obratlovců i přes variabilitu aminokyselin syntetizovány výhradně glyko nebo taurokonjugáty. *In vitro* experimenty ukazují, že BAAT upřednostňuje konjugaci s taurinem. Tomu odpovídá i fakt, že taurokonjugáty u většiny vyšších obratlovců dominují (Killenberg & Jordan, 1978). V živočišné říši existuje však několik výjimek, kde převažují glykokonjugáty, mezi ně patří i *homo sapiens*. U lidí se poměr glyko : tauro konjugátům standardně uvádí asi 3:1. Tento poměr je však značně závislý na dostupnosti taurinu, při jeho podávání se podíl taurokonjugátů dramaticky zvyšuje (Sjovall, 1959). Naopak vyšší poměr se pojí například

s vegetariánskou/veganskou stravou, což je dáno nedostatkem taurinu (Hardison, 1978; Trefflich et al., 2020).

Důvody proč lidská BAAT konjuguje žlučové kyseliny výhradně s glycinem nebo taurinem zkoumal A. Hofmann ve své práci (Huijghebaert & Hofmann, 1986). V té se zabývali stabilitou synteticky připravených konjugátů s ostatními aminokyselinami a zjistili, že pakreatická šťáva (izolovaná od pacientů) štěpí amidovou vazbu se všemi aminokyselinami kromě právě glycinu a taurinu. Nabízí se otázka: Proč? Existují dvě hlavní karboxypeptidasy: karboxypeptidasa B, která štěpí peptidovou vazbu na C-konci bazických L-α-aminokyselin, a karboxypeptidasa A. Ta štěpí neutrální L-α-aminokyseliny, nicméně téměř neštěpí peptidovou vazbu, které se účastní glycin (Ambler, 1972). V případě taurinu je pak popisována nízká afinita karboxypeptidas k β-aminokyselinám (Snoke & Neurath, 1949). Konjugáty taurinu a glycinu jsou tak jako jediné z neutrálních a bazických aminokyselin rezistentní ke štěpení pankreatickými (A) i sérovými (B) karboxypeptidasami. Konjugace znemožňuje pasivní difuzi a absence transportérů způsobuje, že konjugáty glycinu a taurinu se nevstřebávají příliš brzy, konkrétně už v proximální části tenkého střeva (Huijghebaert & Hofmann, 1986).

1.5.2 Sulfatace

Sulfatace žlučových kyselin je katalyzována skupinou enzymů, které nazýváme sulfotransferasy (Glatt, 2000), a spočívá v přenosu sulfonové skupiny z 3´fosfoadenosin 5´fosfosulfátu (PAPS) na hydroxylovou, amino nebo karboxylovou skupinu. Přidáním sulfoskupiny, která nese negativní náboj (pKa < 1), se zvyšuje rozpustnost žlučových kyselin ve vodě (Glatt, 2000) a zároveň se snižuje jejich

vstřebávání ze střeva. Sulfatované žlučové kyseliny jsou tak méně toxické a snadněji se vylučují močí i stolicí (Alnouti, 2009).

Za fyziologických podmínek je sulfatovaných 40-70 % žlučových kyselin vyloučených močí. Množství žlučových kyselin vyloučených močí je však menší než 1 μmol za den. Zastoupení sulfatovaných žlučových kyselin v séru je u zdravých lidí pravděpodobně velmi variabilní, v literatuře se uvádí hodnoty mezi 5-32 % (Alnouti, 2009). Ve žluči je jejich zastoupení zanedbatelné (0 až 4 % ze všech žlučových kyselin). Intenzita sulfatace se mění s počtem hydroxylových skupin, LCA se vyskytuje téměř výhradně v sulfatované formě, naopak CA spíše výjimečně. Důvodem je snaha organismu eliminovat toxické žlučové kyseliny zejména právě LCA (Obrázek 6). Význam sulfatace vzrůstá při cholestatických a hepatobiliárních onemocněních, kdy vylučování sulfatovaných žlučových kyselin močí vzrůstá až 100krát a stává se tak jednou z hlavních cest eliminace žlučových kyselin (Alnouti, 2009; Stiehl et al., 1985).

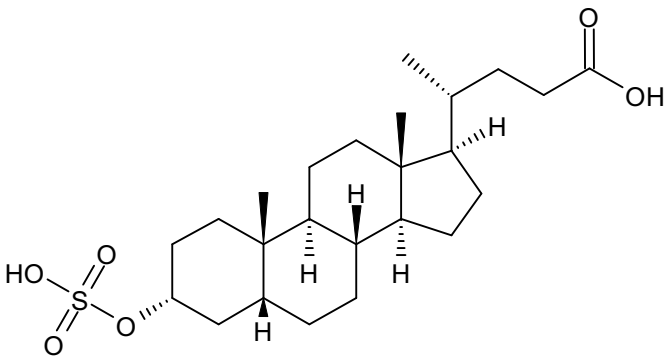

Obrázek 6: LCA-S (kyselina 3-sulfolitocholová)

1.5.3 Glukuronidace

Glukuronidace je u lidí jednou z hlavních cest zvýšení polarity molekul. V případě žlučových kyselin ji u lidí poprvé prokázali Alme a Sjovall (Alme et al., 1978). Ti u své pacientky popsali, že 20 % žlučových kyselin vyloučených močí je glukuronidováno, přičemž 90 % původně neslo hydroxylovou skupinu na C6 (zcela majoritní je kyselina hyodeoxycholová) (Alme et al., 1978). Později bylo popsáno, že glukuronidace je hlavní cestou eliminace exogenně podávané HDCA (Obrázek 7) (Radominska-Pyrek et al., 1987; Sacquet et al., 1983). Dnes víme, že u lidí může být glukuronidovaná většina žlučových kyselin (CA, CDCA, LCA, DCA, HCA a HDCA) (Barbier et al., 2009). Glukuronidované žlučové kyseliny tvoří u zdravých jedinců 12-36 % celkových žlučových kyselin vyloučených močí (Alme & Sjovall, 1980). Význam glukoronidace stoupá při cholestáze, kdy se stává důležitou eliminační cestou a glukuronidované žlučové kyseliny tvoří až 2/3 žlučových kyselin vyloučených močí (Perreault et al., 2013).

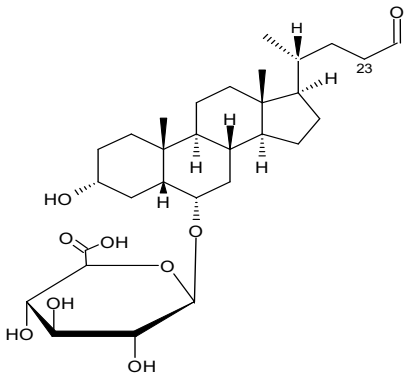

Obrázek 7 : Glukuronidovaná HDCA

Zajímavé je, že glukuronidace žlučových kyselin nebyla popsána u jiného živočišného druhu než u člověka (Hofmann & Hagey, 2014).

1.5.4 Bakteriální transformace

Při průchodu trávicím traktem podléhají žlučové kyseliny řadě chemických modifikací, jako je dekonjugace, dehydroxylace, oxidace, epimerace a rekonjugace. Ke všem těmto modifikacím dochází činností bakteriálních enzymů (Pedersen et al., 2022).

Transformací žlučových kyselin se bakterie brání před jejich toxickým působením. Se zvyšující se koncentrací žlučových kyselin dochází u bakterií k solubilizaci membrán, disociaci integrálních membránových proteinů a unikání obsahu z buněk (Dunne et al., 2001; Kumar et al., 2006; Ridlon et al., 2016).

Žlučové kyseliny bakterie zároveň využívají jako akceptor elektronů vzniklých fermentací (Philipp, 2011).

1.5.4.1 Dekonjugace

Dekonjugace je vůbec nejčastější bakteriální transformací. To ilustruje fakt, že žlučové kyseliny vyloučené stolicí jsou téměř výhradně nekonjugované (Ridlon et al., 2006). Dekonjugace je zprostředkována mikrobiálními hydrolásami žlučových solí (BSH, EC 3.5.1.24). BSH jsou široce rozšířené u grampozitivních bakterií, byly popsány u *Clostridií, Enterokoků, Bifidobacterií i Lactobacillů*, naproti tomu u gramnegativních bakterií se pravděpodobně vyskytují jen u rodu *Bacteroides* (Ridlon et al., 2016). Jejich vnější membrána tvoří přirozenou ochranu před působením detergentů, a tak gramnegativní koliformní bakterie enzymovou ochranu nepotřebují (Kramer et al., 1980).

Není však zcela jasné, proč bakterie žlučové kyseliny dekonjugují. BSH jsou lokalizovány intracelulárně, k dekonjugaci tedy dochází uvnitř buněk. Žlučové kyseliny způsobují uvnitř buněk acidifikaci, což pro bakterie představuje energetickou zátěž (De Smet et al., 1995). Nicméně dekonjugované a dehydroxylované žlučové kyseliny ve střevě precipitují, což by mohla být hlavní výhoda, protože tím se žlučové kyseliny stávají pro bakterie neškodné (De Boever & Verstraete, 1999).

Zároveň se zdá, že některé bakterie dokážou využít odštěpené aminokyseliny ke své potřebě (Huijghebaert & Eyssen, 1982; Van Eldere et al., 1996). Pro některé je dokonce tento zdroj zcela zásadní (Devkota et al., 2012).

1.5.4.2 Dehydroxylace

Další charakteristickou modifikací žlučových kyselin zprostředkovanou bakteriálními enzymy je dehydroxylace. Žlučové kyseliny vzniklé činností bakterií nazýváme jako sekundární, většinou jsou však za sekundární považovány pouze ty vzniklé 7α-dehydroxylací. I dehydroxylace vede ke zvýšení hydrofobicity žlučových kyselin, což způsobuje jejich precipitaci (De Boever & Verstraete, 1999; Ridlon et al., 2016; Schubert et al., 1983). Ač u člověka sekundární žlučové kyseliny tvoří většinu žlučových kyselin ve stolici, byla tato dráha popsána jen u asi 0,0001 % všech střevních bakterií, a to zejména rodu *Clostridium (Ridlon et al., 2006).*

1.5.4.3 Epimerace

Epimerace hydroxyskupiny žlučových kyselin je reverzibilní stereochemickou změnou konfigurace z α na β (či *vice versa*), při které dochází i k tvorbě stabilního meziproduktu oxo žlučové kyseliny. Epimerace vyžaduje součinnost dvou polohově specifických, ale stereochemicky odlišných hydroxysteroiddehydrogenas (HSD) vnitrodruhového nebo mezidruhového původu (Sutherland & Macdonald, 1982). Tato schopnost byla popsána napříč všemi hlavními kmeny tedy *Firmicutes, Bacteroidetes, Actinobacter, Proteobacter* a také metanogenních archaeí (Doden et al., 2021).

1.5.4.4 Další možnosti konjugace

V posledních letech se ukazuje, že činností střevního mikrobiomu mohou vznikat i konjugáty s jinými aminokyselinami (Quinn et al., 2020). Jako první byly ve výše zmíněné práci popsány konjugáty s leucinem, tyrosinem a phenylalaninem nalezené v ileu, duodenu a jejunu myší se střevem kolonizovaným kmenem *Blautia producta.* Od té doby byly popsány desítky dalších konjugátů produkovaných desítkami různých bakteriálních kmenů (zatím byla konjugace popsána u 27 kmenů) (Lucas et al., 2021).

Výzkumy naznačují, že tyto konjugáty by mohly být ligandy receptorů žlučových kyselin (Ay et al., 2022). Jejich skutečný vliv na střevní mikrobiom a lidský organismus je však zatím spíše otázkou.

1.6 Enterohepatální oběh

Konjugované žlučové kyseliny jsou přenášeny přes kanalikulární membránu hepatocytu aktivně transportérem BSEP (Bile Salt Export Pump, TCDB: 3.A.1.201.2). Na této membráně se sice nacházejí i další transportéry schopné přenášet žlučové kyseliny (MRP2, MDR1 a BCRP), ale předpokládá se, že fyziologicky nehrají v transportu žlučových kyselin významnou roli. Dokážou však obstarat transport v případě BSEP deficience (Akita et al., 2001).

Žlučové kyseliny se dostávají do žluče a jsou koncentrovány ve žlučníku. Kontrakcí žlučníku se pak dostávají do duodena. V celém tenkém střevě působí jako detergenty, podporují solubilizaci, trávení a vstřebávání lipidů a vitamínů rozpustných v tucích. Vysoké koncentrace žlučových kyselin nalézáme v duodenu, jejunu a proximálním ileu, právě zde totiž dochází k trávení a absorpci tuků (Ridlon et al., 2006). Až 90 % žlučových kyselin je vstřebáno v konjugované formě v distální části ilea (Hofmann, 1999). Dále je zapotřebí aktivního transportu, proto je vstup žlučových kyselin do enterocytů zprostředkován transportním proteinem ASBT (Apical sodium-dependent bile acid transporter, TCDB: 2.A.28.1.2) (Wong et al., 1994). Tento transportér přesouvá konjugované žlučové kyseliny z lumen tenkého střeva přes apikální membránu. Dále jsou žlučové kyseliny transportovány přes basolaterální membránu do portálního oběhu pomocí transportního proteinu OSTα a OSTβ (Organic solute transporter α a β, TCDB: 2.A.82.1.1) (Dawson et al., 2009).

Portálním řečištěm jsou odváděny jak konjugované žlučové kyseliny, tak nekonjugované žlučové kyseliny vstřebané pasivním transportem z tlustého střeva. Všechny žlučové kyseliny jsou účinně vychytány hepatocyty. Předpokládá se, že většina žlučových kyselin je transportována prostřednictvím NTCP (Na^+-taurocholate cotransporting polypeptide, TCDB: 2.A.28.1.9). Na basolaterální membráně se vyskytuje celá řada dalších transportérů schopných přenášet žlučové kyseliny, patří sem například OATP1A2, OATP1B1, OATP1B3 nebo OATP1C1 (TCDB: 2.A.60.1.14, 2.A.60.1.5, 2.A.60.1.12, 2.A.60.1.15). Jejich význam v transportu žlučových kyselin však není zcela znám (Hofmann & Hagey, 2014). Fyziologicky jsou přednostně vychytávány konjugáty kyseliny cholové. Poločas jakékoliv plasmatické žlučové kyseliny je však menší než 5 minut (Dawson et al., 2009). Schéma enterohepálního oběhu znázorňuje Obrázek 8.

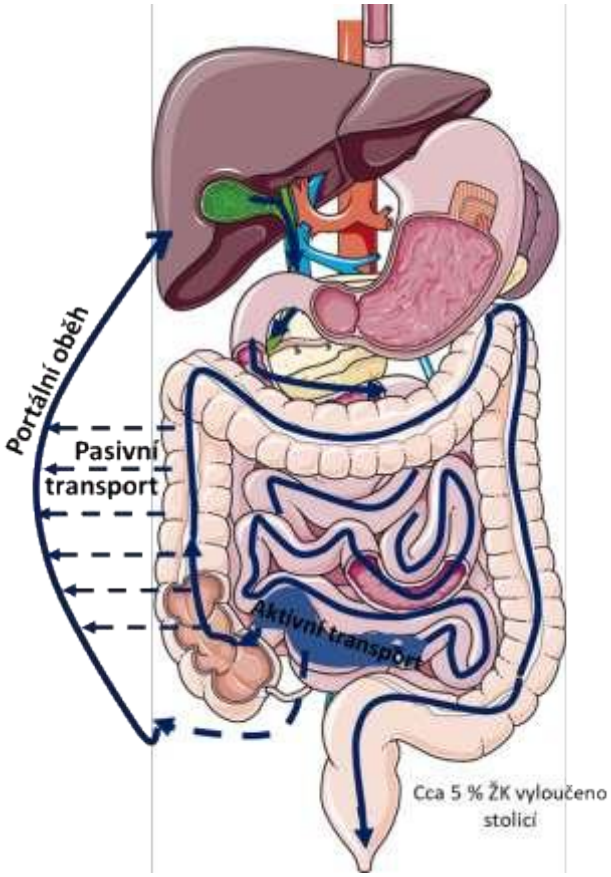

Obrázek 8: Schéma enterohepatálního oběhu žlučových kyselin. Použitý obrázek (Servier Medical Art, Servier, licence Creative Commons Attribution 3.0), upraven z (Hylemon et al., 2009)

1.7 Metody stanovení žlučových kyselin

Za vůbec první popsané stanovení se považuje důkaz kyseliny cholové sacharózou v koncentrované kyselině sírové. Reakci popsal v roce 1844 Max von Pettenkoffer (Pettenkofer, 1844). Žlučové kyseliny zde dávají růžové zbarvení, a tak je na počátku dvacátého století vidět snaha tuto reakci využít a měřit je kolorimetricky. To však naráží na řadu interferencí v analyzovaných matricích, jako jsou krev a žluč (Aldrich, 1928). Žlučové kyseliny jsou poměrně heterogenní skupinou, a tak se velice záhy ukazuje, že právě separace z matrice bude minimálně stejně složitým úkolem jako jejich stanovení. To změnil až rozvoj chromatografických metod.

1.7.1 Chromatografické metody

První, kdo použil chromatografii k analýze žlučových kyselin, byl Jan Sjovall, který separoval 9 nekonjugovaných žlučových kyselin kapalinovou rozdělovací chromatografií na reverzní fázi (Sjovall, 1953). V 60. letech začala být široce dostupná chromatografie na tenké vrstvě (TLC) díky komerční výrobě adsorbentů např. oxidu hlinitého nebo kyseliny ortokřemičité. V případě žlučových kyselin našla TLC široké uplatnění jako semikvantitatvní metoda při separaci jednotlivých skupin konjugátů i jednotlivých žlučových kyselin (Hofmann, 1961; Hofmann & Hagey, 2014). Do dnešního dne byla samozřejmě popsána řada modifikací. Za zlatý standard se považuje separace na silikagelu s mobilní fází n-hexan/ethyl-acetát/methanol/kyselina octová v poměru 20:20:5:2 s detekcí kyselinou sírovou nebo fosfomolybdenovou (Pyka, 2008*)*. TLC však později začaly vytlačovat jiné chromatografické metody s vyšší účinností a menší náročností na množství materiálu. I dnes má však tato metoda své místo zejména pro rychlou orientaci.

1.7.1.1 Plynová chromatografie

Historicky byla plynová chromatografie bezpochyby nejčastěji využívanou metodou k analýze profilu žlučových kyselin. Tuto metodu popsala už v roce 1953 skupina kolem Jana Sjovalla (Griffiths & Sjovall, 2010). Jedná se o metodu extrakce na aniotovém iontoměniči, následovanou hydrolytickým štěpením amidové vazby, derivatizací diazomethanem a přečištěním. K chromatografii byla použita fluor-silikonová (QF-1) kolona a k detekci plamenový ionizační detektor (Sandberg et al., 1965; Sjovall, 1953).

Plynová chromatografie se k měření žlučových kyselin používá dodnes. Nejčastěji ve spojení s hmotnostním detektorem, má však řadu nevýhod. Žlučové kyseliny jsou pro tuto metodu teplotně nestabilní a málo volatilní. Proto je nutné je hydrolyzovat a derivatizovat, k čemuž se nejčastěji používá převedení karboxylové skupiny na methylester. Proto je tato metoda zdlouhavá a zároveň přicházíme o informace ohledně konjugace (Zhao et al., 2022).

1.7.1.2 Kapalinová chromatografie

HPLC (high-performance liquid chromatography; vysokoúčinná kapalinová chromatografie) byla vyvinuta v 70. letech a velmi záhy byla použita k analýze žlučových kyselin. Nevýhodou byl tehdy používaný UV detektor. Konjugované žlučové kyseliny lze sice detekovat při 205 nm (absorpční maximum amidové vazby), ale nekojugované a sulfatované žlučové kyseliny takto detekovat nelze. Nevýhodou jsou i vysoké požadavky na množství vzorku (Linnet et al., 1984). Dnes se nejčastěji používá chromatografie na reverzní fázi (Griffiths & Sjovall, 2010). Pro kompletní analýzu profilu žlučových kyselin je v současné době jedinou možnou metodou spojení kapalinové chromatografie s tandemovým hmotnostním detektorem (Hofmann &

Hagey, 2014). LC-MS/MS je pro analýzu žlučových kyselin relativně citlivá, nenáročná na množství materiálu i extrakci, což umožňuje měřit žlučové kyseliny v různých matricích jako je sérum, žluč i jaterní tkáň. V tomto uspořádání lze měřit konjugované, nekonjugované, sulfatované i glukuronidované žlučové kyseliny (Yang et al., 2017). Pro všechny tyto výhody, spolu se zvětšující se dostupností přístrojového vybavení, začíná LC-MS/MS vytlačovat ostatní metody analýzy žlučových kyselin.

1.7.2 Enzymatické stanovení

Tuto metodu popsal jako první Iwata (Iwata & Yamasaki, 1964), který využil 3α-hydroxysteroiddehydrogenasy (EC 1.1.1.50) izolované z *Comamonas testosteroni* (dříve *Pseudomonas testosteroni*). Tento enzym oxiduje 3α-hydroxyskupinu žlučových kyselin a je NAD dependentní, dochází tedy k redukci na NADH. To je pak měřeno buď přímo v UV spektru nebo následují spřažené reakce, při kterých vzniká barevný produkt (Obrázek 9) (Griffiths & Sjovall, 2010; Hofmann & Hagey, 2014). Takovým měřením získáváme informaci nejen o celkové koncentraci žlučových kyselin s 3α-hydroxyskupinou, ale i ostatních 3α-hydroxysteroidů. Těch jsou v séru nicméně za fyziologických podmínek zanedbatelné koncentrace. Nevýhodou je, že se nedozvídáme nic o profilu žlučových kyselin, ale jen o jejich celkové sumě. Zároveň tato metoda neměří ty, u kterých je 3α hydroxylová skupina modifikovaná, například sulfatací nebo glukuronidací.

Byly popsány i modifikace s dalšími enzymy jako například se 7α-hydroxysteroiddehydrogenasou, ty se však používají velmi zřídka (Zhao et al., 2022).

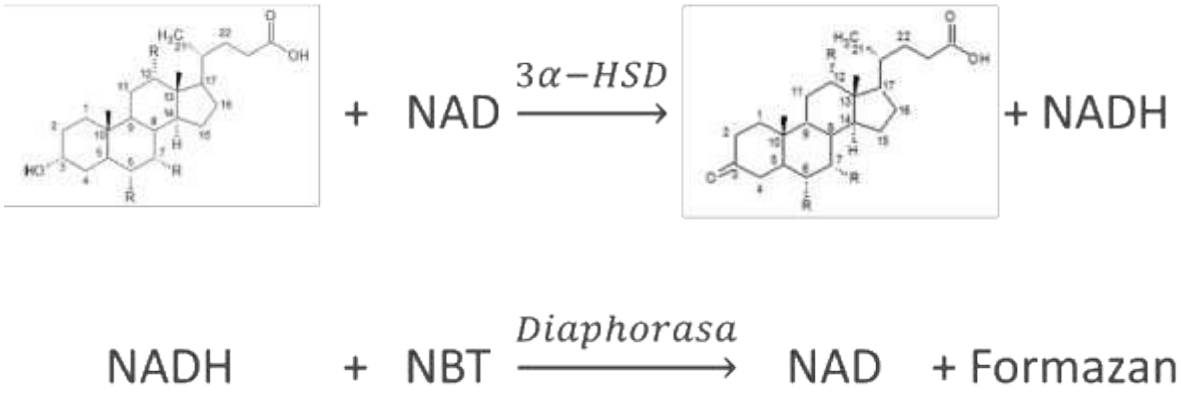

Obrázek 9: Princip enzymatické analýzy žlučových kyselin

1.7.3 Imunochemické metody

Metody, které využívají imunochemických reakcí, jsou k analýze žlučových kyselin používány velice zřídka. Popsána byla detekce žlučových kyselin radioimunoanalýzou, tu popsal v roce 1973 Simmonds. V té době byla hlavní výhodou metody možnost měřit konjugáty žlučových kyselin, k tomu se však dnes využívají jiné metody (Simmonds et al., 1973).

Druhou metodou je ELISA, ale její použití není obvyklé a k analýze žlučových kyselin byla použita ve 2 % publikací z celkového počtu 105 sledovaných (Zhao et al., 2022). Existuje metoda, která v jedné analýze dokáže detekovat 5 žlučových kyselin CA, DCA, CDCA, UDCA, HDCA. Pro svou jednoduchost je někdy používána v rutinních provozech u matric, ve kterých není vhodné použití enzymatického kitu (De Corso et al., 2007; Liu et al., 2017; Zhao et al., 2022). Takovou matricí by mohly být například sliny, protože enzymatická metoda výsledky ve slinách pravděpodobně podhodnocuje (De Corso et al., 2007).

1.7.4 Nukleární magnetická rezonanční spektroskopie

Tato metoda se zatím v detekci žlučových kyselin příliš neuplatňuje. Její využití poprvé popsal Duarte v roce 2009 k analýze složek žluči. V tomto uspořádání však nebylo možné rozlišit tauro a glykokonjugáty. To se změnilo až s nástupem 2D nukleární magnetické rezonance. Zajímavé by mohlo být uplatnění této metody k měření žlučových kyselin *in vivo* (Kunnecke et al., 2007; Prescot et al., 2003). Takto by bylo možné nukleární magnetickou rezonanci použít k detekci složení žlučových kamenů nebo distribuci žlučových kyselin ve složených micelách (Zhao et al., 2022).

2. Cíle práce

LC-MS/MS se v současné době jeví jako nejpřesnější a nejspolehlivější metoda pro měření žlučových kyselin. přičemž se nejčastěji používá pro výzkumné účely. Pro svou jednoduchost a rychlost má ale i své zastoupení enzymatická metoda stanovení celkových žlučových kyselin. Cílem mé práce bylo ověřit, nakolik je tato metoda spolehlivá pro jednotlivé žlučové kyseliny. Vzhledem k tomu o jak heterogenní skupinu se jedná, jsme předpokládali, že by se účinnost přeměny 3α-HSD mohla pro jednotlivé žlučové kyseliny lišit. To by pak mohlo mít vliv na spolehlivost metody u vzorků s odlišným spektrem či u experimentů, kde změny ve spektru žlučových kyselin očekáváme. Výsledky jsme popsali v publikaci **Enzymatic methods may underestimate the total serum bile acid concentration.**

Kvůli pochybám o spolehlivosti enzymatické metody, jsem zavedla metodu stanovení žlučových kyselin na LC-MS/MS. Tuto metodu jsme využili k měření žlučových kyselin při přetížení potkanů železem. Akumulace železa provází celou řadu genetických onemocnění, jako jsou hereditární hemochromatóza nebo β-talasémie. Vzniká ale i sekundárně například po opakovaných krevních transfúzích. U takového přetížení bylo popsáno, že se mění metabolismus cholesterolu. Jaký vliv to má na metabolismus žlučových kyselin, však dosud popsáno nebylo. My jsme to popsali v práci **Iron overload reduces synthesis and elimination of bile acids in rat liver.**

Střevní bakterie modifikují žlučové kyseliny mnoha cestami a vytváří tím i selekční tlak mezi sebou. Konkrétně bakterie *Eggerthella lenta* zmírňuje toxické účinky některých žlučových kyselin pro ostatní bakterie. Postihnout tyto změny pomocí LC-MS/MS jsme se pokusili v práci **Eggerthella lenta DSM 2243 alleviates bile acid stress response in Clostridium ramosum and Anaerostipes caccae by transformation of bile**

acids. Naší hypotézou bylo, že *Eggerthella lenta* přeměňuje tyto žlučové kyseliny na jejich méně toxické varianty a jejich identifikace byla předmětem naší práce. Zároveň jsme chtěli ověřit, zda *E. lenta* disponuje enzymy schopnými vytvářet amidovou vazbu mezi žlučovými kyselinami a jinými aminokyselinami, než je taurin nebo glycin. Jak se zmiňuji v kapitole ¨Další možnosti konjugace¨, v roce 2020 bylo popsáno, že střevní bakterie mohou tuto amidovou vazbu tvořit.

Pro metabolismus žlučových kyselin je samozřejmě klíčová i jejich biosyntéza. Jako marker její aktivity se používá jeden z meziproduktů této dráhy, a to 7-alpha-hydroxy-4-cholesten-3-on (C4). Pro jeho měření na LC-MS/MS je potřeba jej nejprve izolovat ze séra. K tomu se používá řada metod. Cílem naší práce bylo popsané metody porovnat. Tedy jak jsou dané metody schopny odstranit proteiny, fosfolipidy, s jakou účinností izolují samotný C4, ale i jakou mají časovou náročnost. To jsme popsali v práci **Comparison of simple extraction procedures in liquid chromatography-mass spectrometry based determination of serum 7alpha-hydroxy-4-cholesten-3-one, a surrogate marker of bile acid synthesis.**

Posledním bodem mé disertační práce bylo využití žlučových kyselin jako klinického markeru. Konkrétně ověřit hypotézu, zda by sérové koncentrace žlučových kyselin nemohly odrážet hodnoty portálního tlaku u nemocných s cirhózou jater. Při portální hypertenzi dochází ke vzniku porto-systémových spojek. Proto nás zajímalo, zda by poměr krve obcházející játra mohl odpovídat výši portální hypertenze, s ohledem k vysokému first-pass efektu žlučových kyselin. O tom pojednává práce **Serum concentration of taurochenodeoxycholic acid predicts clinically significant portal hypertension.**

3. Publikace

Zizalova, K., Vecka, M., Vitek, L., & Lenicek, M. (2020). Enzymatic methods may underestimate the total serum bile acid concentration. *PLoS One*, *15*(7), e0236372. https://doi.org/10.1371/journal.pone.0236372

- **Příloha 1**

Prasnicka, A., Lastuvkova, H., Alaei Faradonbeh, F., Cermanova, J., Hroch, M., Mokry, J., Dolezelova, E., Pavek, P., Zizalova, K., Vitek, L., Nachtigal, P., & Micuda, S. (2019). Iron overload reduces synthesis and elimination of bile acids in rat liver. *Sci Rep*, *9*(1), 9780. https://doi.org/10.1038/s41598-019-46150-7

- **Příloha 2**

Pedersen, K. J., Haange, S. B., Zizalova, K., Viehof, A., Clavel, T., Lenicek, M., Engelmann, B., Wick, L. Y., Schaap, F. G., Jehmlich, N., Rolle-Kampczyk, U., & von Bergen, M. (2022). Eggerthella lenta DSM 2243 Alleviates Bile Acid Stress Response in Clostridium ramosum and Anaerostipes caccae by Transformation of Bile Acids. *Microorganisms*, *10*(10). https://doi.org/10.3390/microorganisms10102025

- **Příloha 3**

Lenicek, M., Vecka, M., Zizalova, K., & Vitek, L. (2016). Comparison of simple extraction procedures in liquid chromatography-mass spectrometry based determination of serum 7alpha-hydroxy-4-cholesten-3-one, a surrogate marker of bile acid synthesis. *J Chromatogr B Analyt Technol Biomed Life Sci*, *1033-1034*, 317-320. https://doi.org/10.1016/j.jchromb.2016.08.046

- **Příloha 4**

Zizalova, K., Novakova, B., Vecka, M., Petrtyl, J., Lanska, V., Pelinkova, K., Smid, V., Bruha, R., Vitek, L., & Lenicek, M. (2023). Serum concentration of taurochenodeoxycholic acid predicts clinically significant portal hypertension. *Liver Int*, *43*(4), 888-895. https://doi.org/10.1111/liv.15481

- **Příloha 5**

4. Diskuse

Ke stanovení žlučových kyselin se používá řada metod, jednou z nich je enzymatická metoda. V literatuře, která tuto metodu používá, se často objevuje tvrzení, že enzymatická metoda stanovení pravděpodobně není stejně účinná pro všechny žlučové kyseliny. Tedy že enzym 3α-hydroxysteroiddehydrogenasa nereaguje s jednotlivými žlučovými kyselinami se stejnou rychlostí (Iwata & Yamasaki, 1964; Mashige et al., 1981). Této problematice jsme se věnovali v práci **Enzymatic methods may underestimate the total serum bile acid concentration** (Zizalova et al., 2020). V té jsme popsali, že účinnost tohoto enzymu se opravdu značně liší od nejlépe reagující kyseliny glykocholové po nejhůře reagující α-muricholovou, které enzym přemění jen pětinu za stejnou časovou jednotku oproti GCDCA. Naše zjištění jsou v souladu s dříve publikovanými daty pro hlavní lidské žlučové kyseliny CA > CDCA > DCA > LCA (Engert & Turner, 1973).

Z našich dat dále vyplývá, že u jednotlivých žlučových kyselin se liší zejména rychlost reakce katalyzovaná 3α-hydroxysteroiddehydrogenasou. S prodloužením času reakce se rozdíl mezi GCA a α-MCA zmenšuje, nicméně nikdy se zcela nevyrovná. Enzymatická metoda stanovení žlučových kyselin je hojně využívanou metodou, jedná se o metodu rychlou, jednoduchou a nenáročnou na vybavení. Ve světle těchto odlišností je však jasné, že se musí lišit výsledky podle toho na jakou žlučovou kyselinu je kalibrujeme. Tím se zabývali ve své práci Danese a spolupracovníci (Danese et al., 2017). Zde měřili stejné vzorky třemi různými komerčními kity a LC-MS jako referenční metodou. Výsledky se ve všech třech případech signifikantně liší. Výrobci však složení kalibrátorů nedeklarují. Problematické mohou být rovněž vzorky, u kterých předpokládáme změny ve spektru žlučových kyselin. Na možné zkreslení výsledků v multicentrické klinické studii na pacientkách s intrahepatalní cholestázou těhotných

(Hague et al., 2021) poukazuje Leníček (Lenicek, 2021). Ve studii porovnávali pacientky po podání UDCA nebo rifampicinu se zdravými kontrolami. V případě obou těchto terapií dochází ke dramatické změně spektra žlučových kyselin, a získáváme tak pravděpodobně podhodnocené výsledky.

I přes své nedostatky je v klinické praxi enzymatická metoda stanovení žlučových kyselin většinou dostačující. Měli bychom si však být jejich limitů vědomi. Zároveň se z těchto důvodů nezdá příliš vhodnou pro výzkumné účely.

Pro naše další měření se vhodnější zdála metoda LC-MS/MS. V případě této analýzy bylo nutné zvolit vhodnou preanalytickou přípravu. Kromě jiného jsme potřebovali otestovat extrakci 7-alpha-hydroxy-4-cholesten-3-onu (C4) ze séra. C4 je jedním z meziproduktů biosyntézy žlučových kyselin a používá se jako její marker (Freudenberg et al., 2013; Lyutakov et al., 2021). K porovnání jsme vybrali 4 metody popsané v literatuře a výsledky sepsali do práce **Comparison of simple extraction procedures in liquid chromatography–mass spectrometry based determination of serum 7α-hydroxy-4-cholesten-3-one, a surrogate marker of bile acid synthesis (Lenicek et al., 2016).** V publikaci jsme porovnávali schopnost deproteinace, odsolení, odstranění fosfolipidů, přesnost, opakovatelnost a časovou náročnost. Všechny 4 metody dosahují přijatelných výsledků ve všech těchto parametrech, variační koeficient pod 10 %, opakovatelnost mezi 88 a 97 %, nepřítomnost fosfolipidů a zbytkový protein maximálně 1 %. Metody se ale liší ve schopnosti odsolení a jsou různě časově náročné. Z hlediska odsolení dosahuje zdaleka nejlepších výsledků metoda s použitím směsi chloroform/methanol. Nejrychlejší je metoda využívající k vysrážení proteinů acetonitril. Právě tuto metodu jsme se rozhodli používat i pro extrakci C4 i žlučových kyselin při měření na LC-MS. To, že je na to tato metoda vhodná popisují ve své práci i Tagliacozzi a spolupracovníci

(Tagliacozzi et al., 2003). Extrakce acetonitrilem se často používá ve spojení s SPE (solid phase extraction) při analýze řady hydrofobních látek, například steroidů (Wang et al., 2019) nebo perfluorovaných sloučenin (Yeung et al., 2009). Zařazením SPE získáváme čistší vzorek, ale v komplexnějších analýzách můžeme o některé analyty přicházet. Zároveň tím samozřejmě prodlužujeme dobu analýzy (Gosetti et al., 2013). Dle našich zjištění získáváme extrakcí acetonitrilem dostatečně čistý vzorek pro LC-MS analýzu. A řada publikací, ve kterých SPE krok vynechávají, to potvrzuje (Janzen et al., 2011; Thomas et al., 2010; Yang et al., 2017).

Žlučové kyseliny byly dlouhá léta považovány za pouhé detergenty, až s rozvojem molekulárně genetických metod bylo objeveno, že ovlivňují celou řadu nukleárních receptorů. Tím významně ovlivňují metabolismus, a naopak řada látek má vliv na jejich expresi i vylučování (Vitek & Haluzik, 2016). My jsme se v publikaci **Iron overload reduces synthesis and elimination of bile acids in rat liver (Prasnicka et al., 2019)** zabývali změnou v obratu žlučových kyselin u potkanů při nadměrném podávání železa. Jak jsme zjistili, u těchto potkanů dochází pravděpodobně k redukci biosyntézy žlučových kyselin. Předávkování železem vede v játrech k signifikantnímu snížení koncentrací téměř všech měřených žlučových kyselin s výjimkou GCA. V plasmě se však nemění spektrum ani koncentrace měřených žlučových kyselin. Naše data tedy ukazují, že předávkování železem vede u potkanů spíše k potlačení syntézy žlučových kyselin a zároveň ke zvýšení celkového cholesterolu v krevní plasmě. Tomu odpovídají i snížené exprese enzymů CYP7A1 i CYP8B1, klíčových enzymů biosyntézy žlučových kyselin. Blokáda této dráhy v organismu způsobuje vyšší koncentrace cholesterolu (Heubi et al., 2007). V plasmě těchto potkanů je cholesterol skutečně signifikantně zvýšený. Spoluautoři nicméně změřili, že vysoké dávky železa mají vliv i na expresi celé řady transportérů asociovaných se žlučovými kyselinami. Jejich

změny odpovídají změnám v expresi při cholestázách, nejblíže pak obstrukční cholestáze (s výjimkou BSEP, který se nemění) (Geier et al., 2007).

V takovém případě bychom však očekávali zvýšené koncentrace žlučových kyselin v játrech případně v séru (Arab et al., 2017), naše zjištění jsou však zcela opačná. Stejně tak jako při cholestázách dochází i zde k výraznému zvýšení exprese HMG-CoA reduktasy (asi 2,5x), klíčového enzymu v biosyntéze cholesterolu (Chisholm et al., 1999; Kattermann & Creutzfeldt, 1970). Předávkování železem i cholestáza mají jednoho společného jmenovatele, a tím je oxidační stres (Copple et al., 2010; Philippe et al., 2007). To ostatně potvrzuje i naše práce, ve které jsme pozorovali zvýšené koncentrace glutationu i jeho oxidované formy u potkanů s vysokým příjmem železa. Hypercholesterolémie je v souvislosti s vysokými koncentracemi železa často zmiňována. Vztah těchto dvou molekul je však spíše nejasný. (Herbert, 1994; Sullivan, 1996). Často je diskutován v souvislosti s neurodegerativními onemocněními, které jsou spojovány s hypercholestrolémií, oxidačním stresem i vyššími koncentracemi železa v mozku (Ong & Halliwell, 2004). Souhrnně lze říct, že vysoké dávky železa u potkanů způsobí blokádu syntézy žlučových kyselin, což vede k nárůstu koncentrací cholesterolu. Zda vysoké koncentrace cholesterolu způsobují další oxidační stres či oxidační stres způsobený vysokými dávkami železa zvyšuje koncentrace cholesterolu je však otázka dalšího výzkumu.

Žlučové kyseliny výrazně ovlivňují střevní mikrobiom a naopak jsou jím významně ovlivňovány (Collins et al., 2022). Jeho součástí je i *Eggerthella lenta,* tato anaerobní grampozitivní bakterie se běžně vyskytuje v trávicím traktu člověka (Eggerth, 1935). Disponuje celou řadou enzymů modifikující žlučové kyseliny (Hirano & Masuda, 1981). Jak bylo popsáno dříve, kokultivace s touto bakterií poskytuje výhodu i dalším bakteriím (Edenharder & Schneider, 1985). Jak naznačuje naše práce

***Eggerthella lenta* DSM 2243 alleviates bile acid stress response in *Clostridium ramosum* and *Anaerostipes caccae* by transformation of bile acids (Pedersen et al., 2022)**, *E. lenta* by mohla ovlivňovat růst dalších bakterií cestou změn ve spektru žlučových kyselin. Jak bylo zjištěno, stres způsobený vysokými koncentracemi DCA inhibuje růst 4 bakterií, a sice *B. longum, B. producta, C. butyricum and C. ramosum*, nicméně kokultivace s *E. lenta* tento stres zmírňuje. Reakce bakterií na tento stres se dají částečně předvídat. Jak je uvedeno v kapitole o bakteriální transformaci, gramnegativní bakterie (jako je *E. coli*) disponují mechanismem, který je chrání proti detergentnímu působení žlučových kyselin (Ridlon et al., 2016). My se blíže zaměřili na 3 bakteriální druhy, a sice *E. coli* (nízká stresová reakce), *A. caccae* (střední reakce) a *C. ramosum* (vysoká míra stresu). Spoluautoři určovali míru stresu pomocí zeta potenciálu, který měří změny v permeabilitě membrán (Ferreyra Maillard et al., 2021). Měření ukázalo u *C. ramosum* značně zvýšenou permeabilitu membrán v případě kultivace v médiu s DCA. Tento efekt však zcela mizí v případě kokultivace s *E. lenta*. Zajímalo nás, jakým mechanismem toho tato bakterie dosahuje. Jednou z možností by mohla být transformace žlučových kyselin na jiné, méně toxické. Měřením ketoderivátů žlučových kyselin a isomerů žlučových kyselin jsme zjistili, že při kokultivaci *E. lenta* a *C. ramosum* je více než polovina DCA transformována na 7keto-LCA a DCA isomery. Ketoderiváty žlučových kyselin mají vyšší kritickou micelární koncentraci než jejich hydroxylované či dehydroxylované varianty (Sewell et al., 1980). Nižší schopnost tvořit micely by mohla mít za následek obtížnější prostup bakteriální stěnou, a tak vysvětlovat benefity kokultivace s *E. lenta* pro *C. ramosum*. Stejná vlastnost a s tím i související nižší toxicita byla popsána u isoDCA (Devlin & Fischbach, 2015).

Současně jsme testovali, kolik z výše zmíněných bakteriálních druhů je schopných konjugovat žlučové kyseliny, a vytvářet tak konjugáty nejen s taurinem nebo glycinem, ale také s dalšími aminokyselinami. Jak je uvedeno v kapitole "Další možnosti amidace“, dlouho se myslelo, že v lidském těle vznikají jen konjugáty s glycinem a taurinem (Huijghebaert & Hofmann, 1986). Až s rozvojem citlivějších analytických metod (a jejich schopností měřit konjugáty žlučových kyseliny) se zjistilo, že činností střevního mikrobiomu vzniká celá řada konjugátů s dalšími aminokyselinami (Lucas et al., 2021). V naší práci jsme zjistili, že vytvářet amidovou vazbu mezi kyselinou cholovou a tyrosinem, phenylalaninem nebo leucinem dokáže všech 8 zkoumaných bakteriálních druhů (s výjimkou TyrCA u *C. ramosum* a *E. coli*). V případě DCA je situace obdobná, jen jsme nenašli měřitelné hodnoty u *E. coli*, *C. butyricum,* ani *L. plantarum.* V případě kokultivace všech 8 bakterií s *E. lenta* jsme pozorovali spíše pokles koncentrace těchto konjugátů, nikoliv však signifikantní. Koncentrace těchto konjugátů se pohybují v rozmezí od 5 do 200 nmol/L, pravděpodobně tedy nemají na snížení toxicity DCA výrazný vliv.

V klinické praxi se stanovení žlučových kyselin u pacientů příliš nepoužívá, v doporučeních české lékařské společnosti JEP figuruje pouze k diagnostice intrahepatální cholestázy těhotných (ČGPS, 2017). Nejinak je tomu i v doporučeních Evropské asociace pro studium jater (Archer et al., 2022). Přitom diagnostický potenciál žlučových kyselin se zdá mnohem větší. Jako endogenní molekuly s výrazným first-pass efektem jsou silně ovlivňovány stavem jater (Aldini et al., 1982), navíc jejich spektrum odráží stav střevního mikrobiomu (Ramirez-Perez et al., 2017). Byla publikována řada prací, které navrhují, jak je možné změřené koncentrace žlučových kyselin využít v diagnostice. Zvýšené koncentrace žlučových kyselin v cirkulaci jsou silně asociovány například s těžkým poškozením jater, jejich

rakovinou (Farhat et al., 2022) či cirhózou (Mannes et al., 1986). Ve studii, na které aktuálně spolupracuji, zase pozorujeme potenciál k odlišení NAFLD a NASH pomocí sérových koncentrací sulfatované GCDCA. V již publikované práci **Serum concentration of taurochenodeoxycholic acid predicts clinically significant portal hypertension (Zizalova et al., 2023)** jsme chtěli ověřit hypotézu, zda by sérové koncentrace žlučových kyselin nemohly odrážet hodnoty portálního tlaku právě z důvodu first-pass efektu, který je při portální hypertenzi narušený vznikem portosystémových spojek (Moller & Bendtsen, 2018). Použili jsme explorativní kohortu 21 pacientů, u kterých jsme měli k dispozici jak portální, tak periferní krev. V obou těchto vzorcích jsme změřili 23 žlučových kyselin na LC-MS/MS. Porovnáním portální a periferní krve jsme však zjistili, že v případě našich pacientů je vstřebávání žlučových kyselin vážně narušeno a koncentrace v portální a periferní krvi se téměř neliší (jen asi o 10 %). Za fyziologických podmínek by rozdíl mezi portální a periferní krvi by měl být mezi 70 % a 90 % (LaRusso et al., 1978; Marin et al., 2015). V případě cirhózy se však naše zjištění shodují s literaturou (Lindblad et al., 1977).

Na explorativní kohortě jsme zároveň zjistili, že s hodnotami portálních tlaků (HVPG) korelují sérové koncentrace 2 žlučových kyselin, a to GCDCA a TCDCA. Jako nejspolehlivější se ukázala jejich schopnost predikovat klinicky významnou portální hypertenzi. Za tu jsou považovány hodnoty vyšší než 10 mm Hg (Garcia-Tsao, 2016). Pozorovali jsme i dramatickou změnu v poměru CA a CDCA. Zatímco fyziologicky se tyto dvě žlučové kyseliny vyskytují v poměru 3:1 (Carey, 1958), u našich pacientů nalézáme poměr 1:3. Schopnost GCDCA a TCDCA predikovat klinicky významnou portální hypertenzi jsme následně ověřili na validační kohortě 214 pacientů. Na té jsme potvrdili, že obě tyto žlučové kyseliny jsou schopné odlišit portální tlak nad 10 mm Hg s vysokou specifitou a senzitivitou. V další fázi jsme ověřovali, zda by se prediktivní

schopnost těchto žlučových kyselin nedala zlepšit přidáním některého z markerů portální hypertenze popsaných v literatuře. Konkrétně sérových koncentrací albuminu (Harjai et al., 1995), kyseliny hyaluronové (Kropf et al., 1991), bilirubinu (Park et al., 2009), poměru AST/ALT (Heart Protection Study Collaborative, 2002), kreatininu (Garcia-Pagan et al., 2020), osteopontinu (Bruha et al., 2016) a průměru sleziny (měřeného ultrasonograficky) (Gonzalez-Ojeda et al., 2014). Všechny tyto parametry, s výjimkou kreatininu, korelují s portálním tlakem i u naší validační kohorty. Na základě logistické regrese jsme zjistili, že nejvýznamnějšími prediktory (z výše uvedených) jsou sérové koncentrace TCDCA, AST/ALT a průměr sleziny. S pomocí těchto dat jsme se definovali vztah:

Průměr sleziny [mm] / 42 + 2,3 AST/ALT + 0,6 TCDCA ≥ 6.

Hodnoty vyšší nebo rovno 6 predikují klinicky významnou portální hypertenzi s 95 % senzitivitou a 76 % specificitou (AUROC 0,93 ± 0,04). Teoreticky bychom tak s tímto modelem mohli z odebrané krve diagnostikovat klinicky významnou portální hypertenzi namísto používané katetrizace jaterních žil (de Franchis & Baveno, 2015), což by odstranilo zdravotní rizika tohoto vyšetření a umožnilo intenzivnější sledování pacientů s možností lépe reagovat na případné změny zdravotního stavu.

Intenzivnější výzkum v oblasti žlučových kyselin probíhá až od 50. let 20.století. Od té doby bylo zjištěno, že žlučové kyseliny v organismu neplní jen svou detergentní funkci, ale výrazným způsobem ovlivňují střevní mikrobiom a cestou transkripčních faktorů i řadu metabolických pochodů. Zároveň dnes víme, že se jedná o poměrně heterogenní skupinu, značně se lišící svými vlastnostmi a tím i působením v organismu (Hofmann & Hagey, 2014). Výzkum v této oblasti však není zdaleka u konce, a ani to, co už víme, jsme ještě nedokázali v klinické praxi naplno využít. Snad by se to mohlo povést s rozvojem citlivých analytických metod a jejich zavedením do rutinní praxe.

5. Citace

Akita, H., Suzuki, H., Ito, K., Kinoshita, S., Sato, N., Takikawa, H., & Sugiyama, Y. (2001). Characterization of bile acid transport mediated by multidrug resistance associated protein 2 and bile salt export pump. *Biochim Biophys Acta*, *1511*(1), 7-16. https://doi.org/10.1016/s0005-2736(00)00355-2

Aldini, R., Roda, A., Labate, A. M., Cappelleri, G., Roda, E., & Barbara, L. (1982). Hepatic bile acid uptake: effect of conjugation, hydroxyl and keto groups, and albumin binding. *J Lipid Res*, *23*(8), 1167-1173. https://www.ncbi.nlm.nih.gov/pubmed/7175373

Aldrich, M. B., Mary Sue. (1928). STUDIES IN THE METABOLISM OF THE BILE. *The Journal of Biological Chemistry*, *77*, 519-537.

Alme, B., Norden, A., & Sjovall, J. (1978). Glucuronides of unconjugated 6-hydroxylated bile acids in urine of a patient with malabsorption. *Clin Chim Acta*, *86*(3), 251-259. https://doi.org/10.1016/0009-8981(78)90379-0

Alme, B., & Sjovall, J. (1980). Analysis of bile acid glucuronides in urine. Identification of 3 alpha, 6 alpha, 12 alpha-trihydroxy-5 beta-cholanoic acid. *J Steroid Biochem*, *13*(8), 907-916. https://doi.org/10.1016/0022-4731(80)90164-8

Alnouti, Y. (2009). Bile Acid sulfation: a pathway of bile acid elimination and detoxification. *Toxicol Sci*, *108*(2), 225-246. https://doi.org/10.1093/toxsci/kfn268

Ambler, R. P. (1972). [10] Enzymatic hydrolysis with carboxypeptidases. *Methods Enzymol*, *25*, 143-154. https://doi.org/10.1016/S0076-6879(72)25012-1

Arab, J. P., Cabrera, D., & Arrese, M. (2017). Bile Acids in Cholestasis and its Treatment. *Ann Hepatol*, *16*(Suppl. 1: s3-105.), s53-s57. https://doi.org/10.5604/01.3001.0010.5497

Archer, A. J., Belfield, K. J., Orr, J. G., Gordon, F. H., & Abeysekera, K. W. (2022). EASL clinical practice guidelines: non-invasive liver tests for evaluation of liver disease severity and prognosis. *Frontline Gastroenterol*, *13*(5), 436-439. https://doi.org/10.1136/flgastro-2021-102064

Ay, U., Lenicek, M., Classen, A., Olde Damink, S. W. M., Bolm, C., & Schaap, F. G. (2022). New Kids on the Block: Bile Salt Conjugates of Microbial Origin. *Metabolites*, *12*(2). https://doi.org/10.3390/metabo12020176

Barbier, O., Trottier, J., Kaeding, J., Caron, P., & Verreault, M. (2009). Lipid-activated transcription factors control bile acid glucuronidation. *Mol Cell Biochem*, *326*(1-2), 3-8. https://doi.org/10.1007/s11010-008-0001-5

Bergstrom, S., Danielsson, H., & Kazuno, T. (1960). Bile acids and steroids. 98. The metabolism of bile acids in python and constrictor snakes. *J Biol Chem*, *235*, 983-988. https://www.ncbi.nlm.nih.gov/pubmed/13799458

Bergstrom, S., Lindstedt, S., & Samuelsson, B. (1959). Bile acids and steroids. LXXXII. On the mechanism of deoxycholic acid formation in the rabbit. *J Biol Chem*, *234*(8), 2022-2025. https://www.ncbi.nlm.nih.gov/pubmed/13673007

Bruha, R., Jachymova, M., Petrtyl, J., Dvorak, K., Lenicek, M., Urbanek, P., Svestka, T., & Vitek, L. (2016). Osteopontin: A non-invasive parameter of portal hypertension and prognostic marker of cirrhosis. *World J Gastroenterol*, *22*(12), 3441-3450. https://doi.org/10.3748/wjg.v22.i12.3441

Cabral, D. J. S., D.M. (1989). Physical chemistry of bile. In F. Schultz, Rauner (Ed.), *In Handbook of Physiology. The Gastrointestinal System* (pp. 621-662). American Physiological Society.

Carey, J. B., Jr. (1958). The serum trihydroxy-dihydroxy bile acid ratio in liver and biliary tract disease. *J Clin Invest*, *37*(11), 1494-1503. https://doi.org/10.1172/JCI103741

Collins, S. L., Stine, J. G., Bisanz, J. E., Okafor, C. D., & Patterson, A. D. (2022). Bile acids and the gut microbiota: metabolic interactions and impacts on disease. *Nat Rev Microbiol*. https://doi.org/10.1038/s41579-022-00805-x

Copple, B. L., Jaeschke, H., & Klaassen, C. D. (2010). Oxidative stress and the pathogenesis of cholestasis. *Semin Liver Dis*, *30*(2), 195-204. https://doi.org/10.1055/s-0030-1253228
ČGPS, Č. g. a. p. s. (2017). Intrahepatální cholestáza v těhotenství. Doporučený postup. *Česká gynekologie 2*.
Danese, E., Salvagno, G. L., Negrini, D., Brocco, G., Montagnana, M., & Lippi, G. (2017). Analytical evaluation of three enzymatic assays for measuring total bile acids in plasma using a fully-automated clinical chemistry platform. *PLoS One*, *12*(6), e0179200. https://doi.org/10.1371/journal.pone.0179200
Dawson, P. A., Lan, T., & Rao, A. (2009). Bile acid transporters. *J Lipid Res*, *50*(12), 2340-2357. https://doi.org/10.1194/jlr.R900012-JLR200
De Boever, P., & Verstraete, W. (1999). Bile salt deconjugation by lactobacillus plantarum 80 and its implication for bacterial toxicity. *J Appl Microbiol*, *87*(3), 345-352. https://doi.org/10.1046/j.1365-2672.1999.00019.x
De Corso, E., Baroni, S., Agostino, S., Cammarota, G., Mascagna, G., Mannocci, A., Rigante, M., & Galli, J. (2007). Bile acids and total bilirubin detection in saliva of patients submitted to gastric surgery and in particular to subtotal Billroth II resection. *Ann Surg*, *245*(6), 880-885. https://doi.org/10.1097/01.sla.0000255574.22821.a1
de Franchis, R., & Baveno, V. I. F. (2015). Expanding consensus in portal hypertension: Report of the Baveno VI Consensus Workshop: Stratifying risk and individualizing care for portal hypertension. *J Hepatol*, *63*(3), 743-752. https://doi.org/10.1016/j.jhep.2015.05.022
De Smet, I., Van Hoorde, L., Vande Woestyne, M., Christiaens, H., & Verstraete, W. (1995). Significance of bile salt hydrolytic activities of lactobacilli. *J Appl Bacteriol*, *79*(3), 292-301. https://doi.org/10.1111/j.1365-2672.1995.tb03140.x
Devkota, S., Wang, Y., Musch, M. W., Leone, V., Fehlner-Peach, H., Nadimpalli, A., Antonopoulos, D. A., Jabri, B., & Chang, E. B. (2012). Dietary-fat-induced taurocholic acid promotes pathobiont expansion and colitis in Il10-/- mice. *Nature*, *487*(7405), 104-108. https://doi.org/10.1038/nature11225
Devlin, A. S., & Fischbach, M. A. (2015). A biosynthetic pathway for a prominent class of microbiota-derived bile acids. *Nat Chem Biol*, *11*(9), 685-690. https://doi.org/10.1038/nchembio.1864
Doden, H. L., Wolf, P. G., Gaskins, H. R., Anantharaman, K., Alves, J. M. P., & Ridlon, J. M. (2021). Completion of the gut microbial epi-bile acid pathway. *Gut Microbes*, *13*(1), 1-20. https://doi.org/10.1080/19490976.2021.1907271
Duane, W. C., Pooler, P. A., & Hamilton, J. N. (1988). Bile acid synthesis in man. In vivo activity of the 25-hydroxylation pathway. *J Clin Invest*, *82*(1), 82-85. https://doi.org/10.1172/JCI113605
Dunne, C., O'Mahony, L., Murphy, L., Thornton, G., Morrissey, D., O'Halloran, S., Feeney, M., Flynn, S., Fitzgerald, G., Daly, C., Kiely, B., O'Sullivan, G. C., Shanahan, F., & Collins, J. K. (2001). In vitro selection criteria for probiotic bacteria of human origin: correlation with in vivo findings. *Am J Clin Nutr*, *73*(2 Suppl), 386S-392S. https://doi.org/10.1093/ajcn/73.2.386s
Edenharder, R., & Schneider, J. (1985). 12 beta-dehydrogenation of bile acids by Clostridium paraputrificum, C. tertium, and C. difficile and epimerization at carbon-12 of deoxycholic acid by cocultivation with 12 alpha-dehydrogenating Eubacterium lentum. *Appl Environ Microbiol*, *49*(4), 964-968. https://doi.org/10.1128/aem.49.4.964-968.1985
Eggerth, A. H. (1935). The Gram-positive Non-spore-bearing Anaerobic Bacilli of Human Feces. *J Bacteriol*, *30*(3), 277-299. https://doi.org/10.1128/jb.30.3.277-299.1935
Eneroth, P., Gordon, B., Ryhage, R., & Sjovall, J. (1966). Identification of mono- and dihydroxy bile acids in human feces by gas-liquid chromatography and mass spectrometry. *J Lipid Res*, *7*(4), 511-523. https://www.ncbi.nlm.nih.gov/pubmed/5966634
Engert, R., & Turner, M. D. (1973). Problems in the measurement of bile acids with 3 -hydroxysteroid dehydrogenase. *Anal Biochem*, *51*(2), 399-407. https://doi.org/10.1016/0003-2697(73)90493-4
Farhat, Z., Freedman, N. D., Sampson, J. N., Falk, R. T., Koshiol, J., Weinstein, S. J., Albanes, D., Sinha, R., & Loftfield, E. (2022). A prospective investigation of serum bile acids with risk of liver

cancer, fatal liver disease, and biliary tract cancer. *Hepatol Commun*, *6*(9), 2391-2399. https://doi.org/10.1002/hep4.2003
Feng, Y., Siu, K., Wang, N., Ng, K. M., Tsao, S. W., Nagamatsu, T., & Tong, Y. (2009). Bear bile: dilemma of traditional medicinal use and animal protection. *J Ethnobiol Ethnomed*, *5*, 2. https://doi.org/10.1186/1746-4269-5-2
Fieser, L. F., & Fieser, M. A. (1959). *Steroids* (New ed.).
Fini, A., & Roda, A. (1987). Chemical properties of bile acids. IV. Acidity constants of glycine-conjugated bile acids. *J Lipid Res*, *28*(7), 755-759. https://www.ncbi.nlm.nih.gov/pubmed/3625035
Freudenberg, F., Gothe, F., Beigel, F., Rust, C., & Koletzko, S. (2013). Serum 7-alpha-hydroxy-4-cholesten-3-one as a marker for bile acid loss in children. *J Pediatr*, *163*(5), 1367-1371 e1361. https://doi.org/10.1016/j.jpeds.2013.06.083
Garcia-Pagan, J. C., Saffo, S., Mandorfer, M., & Garcia-Tsao, G. (2020). Where does TIPS fit in the management of patients with cirrhosis? *JHEP Rep*, *2*(4), 100122. https://doi.org/10.1016/j.jhepr.2020.100122
Garcia-Tsao, G. (2016). Beta blockers in cirrhosis: The window re-opens. *J Hepatol*, *64*(3), 532-534. https://doi.org/10.1016/j.jhep.2015.12.012
Geier, A., Wagner, M., Dietrich, C. G., & Trauner, M. (2007). Principles of hepatic organic anion transporter regulation during cholestasis, inflammation and liver regeneration. *Biochim Biophys Acta*, *1773*(3), 283-308. https://doi.org/10.1016/j.bbamcr.2006.04.014
Glatt, H. (2000). Sulfotransferases in the bioactivation of xenobiotics. *Chem Biol Interact*, *129*(1-2), 141-170. https://doi.org/10.1016/s0009-2797(00)00202-7
Gonzalez-Ojeda, A., Cervantes-Guevara, G., Chavez-Sanchez, M., Davalos-Cobian, C., Ornelas-Cazares, S., Macias-Amezcua, M. D., Chavez-Tostado, M., Ramirez-Campos, K. M., Ramirez-Arce Adel, R., & Fuentes-Orozco, C. (2014). Platelet count/spleen diameter ratio to predict esophageal varices in Mexican patients with hepatic cirrhosis. *World J Gastroenterol*, *20*(8), 2079-2084. https://doi.org/10.3748/wjg.v20.i8.2079
Gosetti, F., Mazzucco, E., Gennaro, M. C., & Marengo, E. (2013). Ultra high performance liquid chromatography tandem mass spectrometry determination and profiling of prohibited steroids in human biological matrices. A review. *J Chromatogr B Analyt Technol Biomed Life Sci*, *927*, 22-36. https://doi.org/10.1016/j.jchromb.2012.12.003
Griffiths, W. J., & Sjovall, J. (2010). Bile acids: analysis in biological fluids and tissues. *J Lipid Res*, *51*(1), 23-41. https://doi.org/10.1194/jlr.R001941-JLR200
Gustafsson, B. E., Bergstrom, S., Lindstedt, S., & Norman, A. (1957). Turnover and nature of fecal bile acids in germfree and infected rats fed cholic acid-24-14C; bile acids and steroids 41. *Proc Soc Exp Biol Med*, *94*(3), 467-471. https://doi.org/10.3181/00379727-94-22981
Hague, W. M., Callaway, L., Chambers, J., Chappell, L., Coat, S., de Haan-Jebbink, J., Dekker, M., Dixon, P., Dodd, J., Fuller, M., Gordijn, S., Graham, D., Heikinheimo, O., Hennessy, A., Kaaja, R., Khong, T. Y., Lampio, L., Louise, J., Makris, A., . . . Williamson, C. (2021). A multi-centre, open label, randomised, parallel-group, superiority Trial to compare the efficacy of URsodeoxycholic acid with RIFampicin in the management of women with severe early onset Intrahepatic Cholestasis of pregnancy: the TURRIFIC randomised trial. *BMC Pregnancy Childbirth*, *21*(1), 51. https://doi.org/10.1186/s12884-020-03481-y
Hardison, W. G. (1978). Hepatic taurine concentration and dietary taurine as regulators of bile acid conjugation with taurine. *Gastroenterology*, *75*(1), 71-75. https://www.ncbi.nlm.nih.gov/pubmed/401099
Harjai, K. J., Kamble, M. S., Ashar, V. J., Anklesaria, P. S., Ratnam, K. L., & Abraham, P. (1995). Portal venous pressure and the serum-ascites albumin concentration gradient. *Cleve Clin J Med*, *62*(1), 62-67. https://doi.org/10.3949/ccjm.62.1.62
Heart Protection Study Collaborative, G. (2002). MRC/BHF Heart Protection Study of cholesterol lowering with simvastatin in 20,536 high-risk individuals: a randomised placebo-controlled trial. *Lancet*, *360*(9326), 7-22. https://doi.org/10.1016/S0140-6736(02)09327-3

Herbert, V. (1994). Iron worsens high-cholesterol-related coronary artery disease. *Am J Clin Nutr*, *60*(2), 299-300. https://doi.org/10.1093/ajcn/60.2.299
Heubi, J. E., Setchell, K. D., & Bove, K. E. (2007). Inborn errors of bile acid metabolism. *Semin Liver Dis*, *27*(3), 282-294. https://doi.org/10.1055/s-2007-985073
Hirano, S., & Masuda, N. (1981). Transformation of bile acids by Eubacterium lentum. *Appl Environ Microbiol*, *42*(5), 912-915. https://doi.org/10.1128/aem.42.5.912-915.1981
Hofmann, A. F. (1961). Thin-layer adsorption chromatography of free and conjugated bile acids on silicic acid. *Journal of Lipid Research*, *3*(1), 127-128.
Hofmann, A. F. (1963). The Function of Bile Salts in Fat Absorption. The Solvent Properties of Dilute Micellar Solutions of Conjugated Bile Salts. *Biochem J*, *89*, 57-68. https://doi.org/10.1042/bj0890057
Hofmann, A. F. (1999). The continuing importance of bile acids in liver and intestinal disease. *Arch Intern Med*, *159*(22), 2647-2658. https://doi.org/10.1001/archinte.159.22.2647
Hofmann, A. F. (2009). Bile acids: trying to understand their chemistry and biology with the hope of helping patients. *Hepatology*, *49*(5), 1403-1418. https://doi.org/10.1002/hep.22789
Hofmann, A. F., & Hagey, L. R. (2014). Key discoveries in bile acid chemistry and biology and their clinical applications: history of the last eight decades. *J Lipid Res*, *55*(8), 1553-1595. https://doi.org/10.1194/jlr.R049437
Hofmann, A. F., Hagey, L. R., & Krasowski, M. D. (2010). Bile salts of vertebrates: structural variation and possible evolutionary significance. *J Lipid Res*, *51*(2), 226-246. https://doi.org/10.1194/jlr.R000042
Hofmann, A. F., & Mysels, K. J. (1992). Bile acid solubility and precipitation in vitro and in vivo: the role of conjugation, pH, and Ca2+ ions. *J Lipid Res*, *33*(5), 617-626. https://www.ncbi.nlm.nih.gov/pubmed/1619357
Hofmann, A. F., & Roda, A. (1984). Physicochemical properties of bile acids and their relationship to biological properties: an overview of the problem. *J Lipid Res*, *25*(13), 1477-1489. https://www.ncbi.nlm.nih.gov/pubmed/6397555
Huijghebaert, S. M., & Eyssen, H. J. (1982). Specificity of bile salt sulfatase activity from Clostridium sp. strains S1. *Appl Environ Microbiol*, *44*(5), 1030-1034. https://doi.org/10.1128/aem.44.5.1030-1034.1982
Huijghebaert, S. M., & Hofmann, A. F. (1986). Pancreatic carboxypeptidase hydrolysis of bile acid-amino conjugates: selective resistance of glycine and taurine amidates. *Gastroenterology*, *90*(2), 306-315. https://doi.org/10.1016/0016-5085(86)90925-x
Hylemon, P. B., Bohdan, P. M., Sirica, A. E., Heuman, D. M., & Vlahcevic, Z. R. (1990). Cholesterol and bile acid metabolism in cultures of primary rat bile ductular epithelial cells. *Hepatology*, *11*(6), 982-988. https://doi.org/10.1002/hep.1840110612
Hylemon, P. B., Zhou, H., Pandak, W. M., Ren, S., Gil, G., & Dent, P. (2009). Bile acids as regulatory molecules. *J Lipid Res*, *50*(8), 1509-1520. https://doi.org/10.1194/jlr.R900007-JLR200
Chiang, J. Y. (1998). Regulation of bile acid synthesis. *Front Biosci*, *3*, d176-193. https://doi.org/10.2741/a273
Chisholm, J. W., Nation, P., Dolphin, P. J., & Agellon, L. B. (1999). High plasma cholesterol in drug-induced cholestasis is associated with enhanced hepatic cholesterol synthesis. *Am J Physiol*, *276*(5), G1165-1173. https://doi.org/10.1152/ajpgi.1999.276.5.G1165
Iwata, T., & Yamasaki, K. (1964). Enzymatic Determination and Thin-Layer Chromatography of Bile Acids in Blood. *J Biochem*, *56*, 424-431. https://doi.org/10.1093/oxfordjournals.jbchem.a128013
Janzen, N., Sander, S., Terhardt, M., Steuerwald, U., Peter, M., Das, A. M., & Sander, J. (2011). Rapid steroid hormone quantification for congenital adrenal hyperplasia (CAH) in dried blood spots using UPLC liquid chromatography-tandem mass spectrometry. *Steroids*, *76*(13), 1437-1442. https://doi.org/10.1016/j.steroids.2011.07.013

Kattermann, R., & Creutzfeldt, W. (1970). The effect of experimental cholestasis on the negative feedback regulation of cholesterol synthesis in rat liver. *Scand J Gastroenterol*, *5*(5), 337-342. https://www.ncbi.nlm.nih.gov/pubmed/5455818

Killenberg, P. G., & Jordan, J. T. (1978). Purification and characterization of bile acid-CoA:amino acid N-acyltransferase from rat liver. *J Biol Chem*, *253*(4), 1005-1010. https://www.ncbi.nlm.nih.gov/pubmed/624713

Kirilenko, B. M., Hagey, L. R., Barnes, S., Falany, C. N., & Hiller, M. (2019). Evolutionary Analysis of Bile Acid-Conjugating Enzymes Reveals a Complex Duplication and Reciprocal Loss History. *Genome Biol Evol*, *11*(11), 3256-3268. https://doi.org/10.1093/gbe/evz238

Kramer, V. C., Calabrese, D. M., & Nickerson, K. W. (1980). Growth of Enterobacter cloacae in the presence of 25% sodium dodecyl sulfate. *Appl Environ Microbiol*, *40*(5), 973-976. https://doi.org/10.1128/aem.40.5.973-976.1980

Kropf, J., Gressner, A. M., & Tittor, W. (1991). Logistic-regression model for assessing portal hypertension by measuring hyaluronic acid (hyaluronan) and laminin in serum. *Clin Chem*, *37*(1), 30-35. https://www.ncbi.nlm.nih.gov/pubmed/1988206

Kumar, R. S., Brannigan, J. A., Prabhune, A. A., Pundle, A. V., Dodson, G. G., Dodson, E. J., & Suresh, C. G. (2006). Structural and functional analysis of a conjugated bile salt hydrolase from Bifidobacterium longum reveals an evolutionary relationship with penicillin V acylase. *J Biol Chem*, *281*(43), 32516-32525. https://doi.org/10.1074/jbc.M604172200

LaRusso, N. F., Hoffman, N. E., Korman, M. G., Hofmann, A. F., & Cowen, A. E. (1978). Determinants of fasting and postprandial serum bile acid levels in healthy man. *Am J Dig Dis*, *23*(5), 385-391. https://doi.org/10.1007/BF01072919

Lenicek, M. (2021). Mathematical recalibration of total bile acids: comparing the incomparable? *Clin Chem Lab Med*, *59*(12), 1889-1890. https://doi.org/10.1515/cclm-2021-0793

Lenicek, M., Vecka, M., Zizalova, K., & Vitek, L. (2016). Comparison of simple extraction procedures in liquid chromatography-mass spectrometry based determination of serum 7alpha-hydroxy-4-cholesten-3-one, a surrogate marker of bile acid synthesis. *J Chromatogr B Analyt Technol Biomed Life Sci*, *1033-1034*, 317-320. https://doi.org/10.1016/j.jchromb.2016.08.046

Lindblad, L., Lundholm, K., & Schersten, T. (1977). Bile acid concentrations in systemic and portal serum in presumably normal man and in cholestatic and cirrhotic conditions. *Scand J Gastroenterol*, *12*(4), 395-400. https://doi.org/10.3109/00365527709181679

Linnet, K., Andersen, J. R., & Hesselfeldt, P. (1984). Concentrations of glycine- and taurine-conjugated bile acids in portal and systemic venous serum in man. *Scand J Gastroenterol*, *19*(4), 575-578. https://www.ncbi.nlm.nih.gov/pubmed/6463582

Liu, S., Zhang, Y., Qu, B., Qin, G., Cheng, J., Lu, F., Qu, H., & Zhao, Y. (2017). Detection of total bile acids in biological samples using an indirect competitive ELISA based on four monoclonal antibodies [10.1039/C6AY03243E]. *Analytical Methods*, *9*(4), 625-633. https://doi.org/10.1039/C6AY03243E

Lucas, L. N., Barrett, K., Kerby, R. L., Zhang, Q., Cattaneo, L. E., Stevenson, D., Rey, F. E., & Amador-Noguez, D. (2021). Dominant Bacterial Phyla from the Human Gut Show Widespread Ability To Transform and Conjugate Bile Acids. *mSystems*, e0080521. https://doi.org/10.1128/mSystems.00805-21

Lyutakov, I., Lozanov, V., Sugareva, P., Valkov, H., & Penchev, P. (2021). Serum 7-alfa-hydroxy-4-cholesten-3-one and fibroblast growth factor-19 as biomarkers diagnosing bile acid malabsorption in microscopic colitis and inflammatory bowel disease. *Eur J Gastroenterol Hepatol*, *33*(3), 380-387. https://doi.org/10.1097/MEG.0000000000001925

Mannes, G. A., Thieme, C., Stellaard, F., Wang, T., Sauerbruch, T., & Paumgartner, G. (1986). Prognostic significance of serum bile acids in cirrhosis. *Hepatology*, *6*(1), 50-53. https://doi.org/10.1002/hep.1840060110

Marin, J. J., Macias, R. I., Briz, O., Banales, J. M., & Monte, M. J. (2015). Bile Acids in Physiology, Pathology and Pharmacology. *Curr Drug Metab*, *17*(1), 4-29. https://doi.org/10.2174/1389200216666151103115454

Mashige, F., Tanaka, N., Maki, A., Kamei, S., & Yamanaka, M. (1981). Direct spectrophotometry of total bile acids in serum. *Clin Chem*, *27*(8), 1352-1356. https://www.ncbi.nlm.nih.gov/pubmed/6895053

Moller, S., & Bendtsen, F. (2018). The pathophysiology of arterial vasodilatation and hyperdynamic circulation in cirrhosis. *Liver Int*, *38*(4), 570-580. https://doi.org/10.1111/liv.13589

Natalini, B., Sardella, R., Gioiello, A., Ianni, F., Di Michele, A., & Marinozzi, M. (2014). Determination of bile salt critical micellization concentration on the road to drug discovery. *J Pharm Biomed Anal*, *87*, 62-81. https://doi.org/10.1016/j.jpba.2013.06.029

The Nobel Prize in Chemistry 1927. <https://www.nobelprize.org/prizes/chemistry/1927/summary/>

Norman, A., & Sjovall, J. (1958). On the transformation and enterohepatic circulation of cholic acid in the rat: bile acids and steroids 68. *J Biol Chem*, *233*(4), 872-885. https://www.ncbi.nlm.nih.gov/pubmed/13587508

Ong, W. Y., & Halliwell, B. (2004). Iron, atherosclerosis, and neurodegeneration: a key role for cholesterol in promoting iron-dependent oxidative damage? *Ann N Y Acad Sci*, *1012*, 51-64. https://doi.org/10.1196/annals.1306.005

Park, S. H., Park, T. E., Kim, Y. M., Kim, S. J., Baik, G. H., Kim, J. B., & Kim, D. J. (2009). Non-invasive model predicting clinically-significant portal hypertension in patients with advanced fibrosis. *J Gastroenterol Hepatol*, *24*(7), 1289-1293. https://doi.org/10.1111/j.1440-1746.2009.05904.x

Pedersen, K. J., Haange, S. B., Zizalova, K., Viehof, A., Clavel, T., Lenicek, M., Engelmann, B., Wick, L. Y., Schaap, F. G., Jehmlich, N., Rolle-Kampczyk, U., & von Bergen, M. (2022). Eggerthella lenta DSM 2243 Alleviates Bile Acid Stress Response in Clostridium ramosum and Anaerostipes caccae by Transformation of Bile Acids. *Microorganisms*, *10*(10). https://doi.org/10.3390/microorganisms10102025

Perreault, M., Bialek, A., Trottier, J., Verreault, M., Caron, P., Milkiewicz, P., & Barbier, O. (2013). Role of glucuronidation for hepatic detoxification and urinary elimination of toxic bile acids during biliary obstruction. *PLoS One*, *8*(11), e80994. https://doi.org/10.1371/journal.pone.0080994

Pettenkofer, M. J. V. (1844). Notiz ü eine bneue Rection auf galle und Zucker. *Liebig's Annual der chemie und Pharmacie52*, 90-96.

Philipp, B. (2011). Bacterial degradation of bile salts. *Appl Microbiol Biotechnol*, *89*(4), 903-915. https://doi.org/10.1007/s00253-010-2998-0

Philippe, M. A., Ruddell, R. G., & Ramm, G. A. (2007). Role of iron in hepatic fibrosis: one piece in the puzzle. *World J Gastroenterol*, *13*(35), 4746-4754. https://doi.org/10.3748/wjg.v13.i35.4746

Podda, M., Ghezzi, C., Battezzati, P. M., Bertolini, E., Crosignani, A., Petroni, M. L., & Zuin, M. (1989). Effect of different doses of ursodeoxycholic acid in chronic liver disease. *Dig Dis Sci*, *34*(12 Suppl), 59S-65S. https://doi.org/10.1007/BF01536665

Prasnicka, A., Lastuvkova, H., Alaei Faradonbeh, F., Cermanova, J., Hroch, M., Mokry, J., Dolezelova, E., Pavek, P., Zizalova, K., Vitek, L., Nachtigal, P., & Micuda, S. (2019). Iron overload reduces synthesis and elimination of bile acids in rat liver. *Sci Rep*, *9*(1), 9780. https://doi.org/10.1038/s41598-019-46150-7

Pyka, A. (2008). TLC of selected bile acids: Detection and separation. *Journal of Liquid Chromatography & Related Technologies*, *31*(9), 1373-1385. https://doi.org/10.1080/10826070802020028

Quinn, R. A., Melnik, A. V., Vrbanac, A., Fu, T., Patras, K. A., Christy, M. P., Bodai, Z., Belda-Ferre, P., Tripathi, A., Chung, L. K., Downes, M., Welch, R. D., Quinn, M., Humphrey, G., Panitchpakdi, M., Weldon, K. C., Aksenov, A., da Silva, R., Avila-Pacheco, J., . . . Dorrestein, P. C. (2020). Global chemical effects of the microbiome include new bile-acid conjugations. *Nature*, *579*(7797), 123-129. https://doi.org/10.1038/s41586-020-2047-9

Radominska-Pyrek, A., Zimniak, P., Irshaid, Y. M., Lester, R., Tephly, T. R., & St Pyrek, J. (1987). Glucuronidation of 6 alpha-hydroxy bile acids by human liver microsomes. *J Clin Invest*, *80*(1), 234-241. https://doi.org/10.1172/JCI113053

Ramirez-Perez, O., Cruz-Ramon, V., Chinchilla-Lopez, P., & Mendez-Sanchez, N. (2017). The Role of the Gut Microbiota in Bile Acid Metabolism. *Ann Hepatol*, *16 Suppl 1*, S21-S26. https://doi.org/10.5604/01.3001.0010.5672

Rembacz, K. P., Woudenberg, J., Hoekstra, M., Jonkers, E. Z., van den Heuvel, F. A., Buist-Homan, M., Woudenberg-Vrenken, T. E., Rohacova, J., Marin, M. L., Miranda, M. A., Moshage, H., Stellaard, F., & Faber, K. N. (2010). Unconjugated bile salts shuttle through hepatocyte peroxisomes for taurine conjugation. *Hepatology*, *52*(6), 2167-2176. https://doi.org/10.1002/hep.23954

Ridlon, J. M., Harris, S. C., Bhowmik, S., Kang, D. J., & Hylemon, P. B. (2016). Consequences of bile salt biotransformations by intestinal bacteria. *Gut Microbes*, *7*(1), 22-39. https://doi.org/10.1080/19490976.2015.1127483

Ridlon, J. M., Kang, D. J., & Hylemon, P. B. (2006). Bile salt biotransformations by human intestinal bacteria. *J Lipid Res*, *47*(2), 241-259. https://doi.org/10.1194/jlr.R500013-JLR200

Roda, A., & Fini, A. (1984). Effect of nuclear hydroxy substituents on aqueous solubility and acidic strength of bile acids. *Hepatology*, *4*(5 Suppl), 72S-76S. https://doi.org/10.1002/hep.1840040813

Rosenheim, & King, H. (1932). The chemistry of the sterols, bile acids, and other cyclic constituents of natural fats and oils. *Annual Review Biochemistry*(3), 87 – 110.

Russell, D. W. (2003). The enzymes, regulation, and genetics of bile acid synthesis. *Annu Rev Biochem*, *72*, 137-174. https://doi.org/10.1146/annurev.biochem.72.121801.161712

Sacquet, E., Parquet, M., Riottot, M., Raizman, A., Jarrige, P., Huguet, C., & Infante, R. (1983). Intestinal absorption, excretion, and biotransformation of hyodeoxycholic acid in man. *J Lipid Res*, *24*(5), 604-613. https://www.ncbi.nlm.nih.gov/pubmed/6875384

Salen, G. (1988). Clinical perspective on the treatment of gallstones with ursodeoxycholic acid. *J Clin Gastroenterol*, *10 Suppl 2*, S12-17. https://www.ncbi.nlm.nih.gov/pubmed/3062079

Sandberg, D. H., Sjoevall, J., Sjoevall, K., & Turner, D. A. (1965). Measurement of Human Serum Bile Acids by Gas-Liquid Chromatography. *J Lipid Res*, *6*, 182-192. https://www.ncbi.nlm.nih.gov/pubmed/14328425

Sarenac, T. M., & Mikov, M. (2018). Bile Acid Synthesis: From Nature to the Chemical Modification and Synthesis and Their Applications as Drugs and Nutrients. *Front Pharmacol*, *9*, 939. https://doi.org/10.3389/fphar.2018.00939

Setchell, K. D., Dumaswala, R., Colombo, C., & Ronchi, M. (1988). Hepatic bile acid metabolism during early development revealed from the analysis of human fetal gallbladder bile. *J Biol Chem*, *263*(32), 16637-16644. https://www.ncbi.nlm.nih.gov/pubmed/3182806

Sewell, R. B., Hoffman, N. E., Smallwood, R. A., & Cockbain, S. (1980). Bile acid structure and bile formation: a comparison of hydroxy and keto bile acids. *Am J Physiol*, *238*(1), G10-17. https://doi.org/10.1152/ajpgi.1980.238.1.G10

Sfakianos, M. K., Wilson, L., Sakalian, M., Falany, C. N., & Barnes, S. (2002). Conserved residues in the putative catalytic triad of human bile acid Coenzyme A:amino acid N-acyltransferase. *J Biol Chem*, *277*(49), 47270-47275. https://doi.org/10.1074/jbc.M207463200

Schubert, R., Jaroni, H., Schoelmerich, J., & Schmidt, K. H. (1983). Studies on the mechanism of bile salt-induced liposomal membrane damage. *Digestion*, *28*(3), 181-190. https://doi.org/10.1159/000198984

Simmonds, W. J., Korman, M. G., Go, V. L., & Hofmann, A. F. (1973). Radioimmunoassay of conjugated cholyl bile acids in serum. *Gastroenterology*, *65*(5), 705-711. https://www.ncbi.nlm.nih.gov/pubmed/4796644

Sjovall, J. (1953). On the separation of bile acids by partition chromatography. *Acta Physiol Scand*, *29*(2-3), 232-240. https://doi.org/10.1111/j.1748-1716.1953.tb01020.x

Sjovall, J. (1959). Dietary glycine and taurine on bile acid conjugation in man; bile acids and steroids 75. *Proc Soc Exp Biol Med*, *100*(4), 676-678. https://doi.org/10.3181/00379727-100-24741

Snoke, J. E., & Neurath, H. (1949). Structural requirements of specific substrates for carboxypeptidase. *J Biol Chem*, *181*(2), 789-802. https://www.ncbi.nlm.nih.gov/pubmed/15393798
Stiehl, A., Raedsch, R., Rudolph, G., Gundert-Remy, U., & Senn, M. (1985). Biliary and urinary excretion of sulfated, glucuronidated and tetrahydroxylated bile acids in cirrhotic patients. *Hepatology*, *5*(3), 492-495. https://doi.org/10.1002/hep.1840050325
Strecker, A. (1848). *Untersuchungen der ochsengalle*.
Styles, N. A., Falany, J. L., Barnes, S., & Falany, C. N. (2007). Quantification and regulation of the subcellular distribution of bile acid coenzyme A:amino acid N-acyltransferase activity in rat liver. *J Lipid Res*, *48*(6), 1305-1315. https://doi.org/10.1194/jlr.M600472-JLR200
Sullivan, J. L. (1996). Iron versus cholesterol--response to dissent by Weintraub et al. *J Clin Epidemiol*, *49*(12), 1359-1362. https://doi.org/10.1016/s0895-4356(96)00293-4
Sutherland, J. D., & Macdonald, I. A. (1982). The metabolism of primary, 7-oxo, and 7 beta-hydroxy bile acids by Clostridium absonum. *J Lipid Res*, *23*(5), 726-732. https://www.ncbi.nlm.nih.gov/pubmed/7119570
Tagliacozzi, D., Mozzi, A. F., Casetta, B., Bertucci, P., Bernardini, S., Di Ilio, C., Urbani, A., & Federici, G. (2003). Quantitative analysis of bile acids in human plasma by liquid chromatography-electrospray tandem mass spectrometry: a simple and rapid one-step method. *Clin Chem Lab Med*, *41*(12), 1633-1641. https://doi.org/10.1515/CCLM.2003.247
Tamesue, N., & Juniper, K., Jr. (1967). Concentrations of bile salts at the critical micellar concentration of human gall bladder bile. *Gastroenterology*, *52*(3), 473-479. https://www.ncbi.nlm.nih.gov/pubmed/6019966
Thomas, A., Guddat, S., Kohler, M., Krug, O., Schanzer, W., Petrou, M., & Thevis, M. (2010). Comprehensive plasma-screening for known and unknown substances in doping controls. *Rapid Commun Mass Spectrom*, *24*(8), 1124-1132. https://doi.org/10.1002/rcm.4492
Trefflich, I., Jabakhanji, A., Menzel, J., Blaut, M., Michalsen, A., Lampen, A., Abraham, K., & Weikert, C. (2020). Is a vegan or a vegetarian diet associated with the microbiota composition in the gut? Results of a new cross-sectional study and systematic review. *Crit Rev Food Sci Nutr*, *60*(17), 2990-3004. https://doi.org/10.1080/10408398.2019.1676697
Van Eldere, J., Celis, P., De Pauw, G., Lesaffre, E., & Eyssen, H. (1996). Tauroconjugation of cholic acid stimulates 7 alpha-dehydroxylation by fecal bacteria. *Appl Environ Microbiol*, *62*(2), 656-661. https://doi.org/10.1128/aem.62.2.656-661.1996
Vaz, F. M., & Ferdinandusse, S. (2017). Bile acid analysis in human disorders of bile acid biosynthesis. *Mol Aspects Med*, *56*, 10-24. https://doi.org/10.1016/j.mam.2017.03.003
Vitek, L., & Haluzik, M. (2016). The role of bile acids in metabolic regulation. *J Endocrinol*, *228*(3), R85-96. https://doi.org/10.1530/JOE-15-0469
Wang, Y., Peng, D., Zhu, Y., Xie, S., Pan, Y., Chen, D., Tao, Y., & Yuan, Z. (2019). Establishment of pressurized liquid extraction followed by HPLC-MS/MS method for the screening of adrenergic drugs, steroids, sedatives, colorants and antioxidants in swine feed. *J Sep Sci*, *42*(10), 1915-1929. https://doi.org/10.1002/jssc.201801001
Wieland, H. S., 0. (1924). *Z.. physiol. Chem*, *134*(276).
Wong, M. H., Oelkers, P., Craddock, A. L., & Dawson, P. A. (1994). Expression cloning and characterization of the hamster ileal sodium-dependent bile acid transporter. *J Biol Chem*, *269*(2), 1340-1347. https://www.ncbi.nlm.nih.gov/pubmed/8288599
Yang, T., Shu, T., Liu, G., Mei, H., Zhu, X., Huang, X., Zhang, L., & Jiang, Z. (2017). Quantitative profiling of 19 bile acids in rat plasma, liver, bile and different intestinal section contents to investigate bile acid homeostasis and the application of temporal variation of endogenous bile acids. *J Steroid Biochem Mol Biol*, *172*, 69-78. https://doi.org/10.1016/j.jsbmb.2017.05.015
Yeung, L. W., Taniyasu, S., Kannan, K., Xu, D. Z., Guruge, K. S., Lam, P. K., & Yamashita, N. (2009). An analytical method for the determination of perfluorinated compounds in whole blood using

acetonitrile and solid phase extraction methods. *J Chromatogr A*, *1216*(25), 4950-4956. https://doi.org/10.1016/j.chroma.2009.04.070

Zeisel, S. H. (2012). A brief history of choline. *Ann Nutr Metab*, *61*(3), 254-258. https://doi.org/10.1159/000343120

Zhao, X., Liu, Z., Sun, F., Yao, L., Yang, G., & Wang, K. (2022). Bile Acid Detection Techniques and Bile Acid-Related Diseases. *Front Physiol*, *13*, 826740. https://doi.org/10.3389/fphys.2022.826740

Zizalova, K., Novakova, B., Vecka, M., Petrtyl, J., Lanska, V., Pelinkova, K., Smid, V., Bruha, R., Vitek, L., & Lenicek, M. (2023). Serum concentration of taurochenodeoxycholic acid predicts clinically significant portal hypertension. *Liver Int*, *43*(4), 888-895. https://doi.org/10.1111/liv.15481

Zizalova, K., Vecka, M., Vitek, L., & Lenicek, M. (2020). Enzymatic methods may underestimate the total serum bile acid concentration. *PLoS One*, *15*(7), e0236372. https://doi.org/10.1371/journal.pone.0236372

Seznam zkratek

AlloCA	kyselina allocholová
ASBT	Apical sodium-dependent bile acid transporter
BAAT	Bile acid-CoA:amino-acid N-acyltransferasa
BAL	Bile acid CoA ligase
BSEP	Bile Salt Export Pump
BSH	Bile salt hydrolases
CA	kyselina cholová
CDCA	kyselina chenodeoxycholová
DCA	kyselina deoxycholová
GCA	kyselina glykocholová
GCDCA	kyselina glykochenodeoxycholová
GCDCA-3S	kyselina glykochenodeoxy-3sulfo-cholová
GDCA	kyselina glykodeoxycholová
GLCA	kyselina glykolithocholová
GUDCA	kyselina glykoursodeoxycholová
HCA	kyselina hyocholová
HDCA	kyselina hyodeoxycholová
HPLC	High-performance liquid chromatography
HSD	hydroxysteroiddehydrogenasa
LCA	kyselina lithocholová
LC-MS	kapalinová chromatografie s hmotnostní detekcí
LC-MS/MS	Kapalinová chromatografie s tandemovým hmotnostním detektorem
MDCA	kyselina murideoxycholová
NTCP	Na^+-taurocholate cotransporting polypeptide
OST	Organic solute transporter
PAPS	3´fosfoadenosin 5´fosfosulfát
TCA	kyselina taurocholová
TCDCA	kyselina taurochenodeoxycholová
TDCA	kyselina taurodeoxycholová
TLC	Chromatografie na tenké vrstvě
TLCA-3S	kyselina taurolitho-3sulfo-cholová
TUDCA	kyselina tauroursodeoxycholová
tα-MCA	kyselina tauro-α-muricholová
tβ-MCA	kyselina tauro-β-muricholová
UDCA	kyselina ursodeoxycholová
α-MCA	kyselina α-muricholová
β-MCA	kyselina β-muricholová
ω-MCA	kyselina ω-muricholová

Příloha 1

PLOS ONE

RESEARCH ARTICLE

Enzymatic methods may underestimate the total serum bile acid concentration

Kateřina Žižalová[1], Marek Vecka[1,2], Libor Vítek[1,2], Martin Leníček[1]*

1 Institute of Medical Biochemistry and Laboratory Diagnostics, 1st Faculty of Medicine, Charles University, Prague, Czech Republic, **2** 4th Department of Internal Medicine, 1st Faculty of Medicine, Charles University, Prague, Czech Republic

* martin.lenicek@lf1.cuni.cz

Abstract

Enzymatic assays based on bacterial 3α-hydroxysteroid dehydrogenase are the method of choice for quantification of total bile acids (BAs) in serum. Although non-specific, it is generally considered precise and robust. The aim of this study was to investigate how changes in the BA spectrum might affect the reliability of the method. We measured standard solutions of twenty-three human and murine BAs using a commercial enzymatic assay and compared the measured *vs*. expected concentrations. Additionally, total BA concentrations in rat and human cholestatic samples with an abnormal BA spectrum were measured using an enzymatic assay, and a more specific LC-MS/MS method. We observed a great variability in the response of individual BAs in the enzymatic assay. Relative signal intensities ranged from 100% in glycocholic acid (reference) to only 20% in α-muricholic acid. The enzymatic assay markedly underestimated the BA concentrations in both human and rat cholestatic sera when compared to the LC-MS/MS assay. Our study indicated that the performance of an enzymatic assay largely depends on the BA spectrum, and the total concentration of BAs can be markedly underestimated. Samples with an atypical BA spectrum (viz. in rodents) should preferably be measured by other methods.

Citation: Žižalová K, Vecka M, Vítek L, Leníček M (2020) Enzymatic methods may underestimate the total serum bile acid concentration. PLoS ONE 15(7): e0236372. https://doi.org/10.1371/journal.pone.0236372

Editor: Pavel Strnad, Medizinische Fakultat der RWTH Aachen, GERMANY

Received: April 3, 2020

Accepted: July 2, 2020

Published: July 24, 2020

Data Availability Statement: All relevant data are within the manuscript and its Supporting Information files.

Funding: This research was funded by grant GAUK 58217 given by the Charles University, Prague, Czech Republic.

Competing interests: The authors have declared that no competing interests exist.

Introduction

For decades, serum concentrations of bile acids (BAs) have been only considered a marginal marker in clinical chemistry, reserved predominantly for laboratory diagnosis of intrahepatic cholestasis of pregnancy as well as in several rare inherited cholestatic diseases [1]. With recent advances in our understanding of their versatile metabolic, regulatory, and signaling functions (for review see [2, 3]), BA determination has become indispensable in many clinical and experimental settings.

Due to its great simplicity and availability, enzymatic determination of BAs (described by Iwata *et al.* in 1964 [4]) has represented the predominant analytical method up to the present day. It is based on bacterial 3α-hydroxysteroid dehydrogenase (3α-HSD; EC 1.1.1.50) driven oxidation of the 3α-hydroxyl group; common for virtually all BAs found in the blood serum. Substantial differences in the physicochemical properties of BAs suggest that individual BAs

may vary in their reaction rates with 3α-HSD. Although an altered reaction rate may lead to a variable response, and consequently to an inaccurate quantification, only a few BAs so far have actually been tested [4, 5].

Therefore, using the standard enzymatic as well as the liquid chromatography-tandem mass spectrometry (LC-MS/MS) methods, in our current study we analyzed 23 commercially available 3α-hydroxy BAs to find out whether there were significant differences, which may affect the reliability of the enzymatic method of BA determination.

Materials and methods

Chemicals

Standards of cholic acid (CA), chenodeoxycholic acid (CDCA), glycocholic acid (GCA), deoxycholic acid (DCA), lithocholic acid (LCA), taurodeoxycholic acid (TDCA), glycodeoxycholic acid (GDCA), glycolithocholic acid (GLCA), glycoursodeoxycholic acid (GUDCA), hyocholic acid (HCA), taurocholic acid (TCA), and ursodeoxycholic acid (UDCA) were acquired from Sigma-Aldrich (St. Louis, MO, USA); the α-muricholic acid (α-MCA), glycochenodeoxycholic acid (GCDCA), allocholic acid (AlloCA), murideoxycholic acid (MDCA), β-muricholic acid (β-MCA), ω-muricholic acid (ω-MCA), tauro-α-muricholic acid (Tα-MCA), tauro-β-muricholic acid (Tβ-MCA), taurochenodeoxycholic acid (TCDCA), and tauroursodeoxycholic acid (TUDCA) were from Santa Cruz Biotechnology, Inc. (Dallas, TX, USA); and the hyodeoxycholic acid (HDCA) was from Supelco (Bellefonte, PA, USA). The deuterium labeled internal standards (d5-TCA, d5-GCA, d4-GCDCA, and d4-TCDCA) were purchased from Santa Cruz Biotechnology; the d4-CDCA, d4-LCA, d4-CA, d4-UDCA, d4-DCA together with ammonium acetate and formic acid (both LC-MS grade) as well as fetal bovine serum were from Sigma-Aldrich; the acetonitrile (LiChrosolv, isocratic grade) was from Merck, (Darmstadt, Germany); and the methanol (LC-MS grade) was from Biosolve BV (Valkenswaard, the Netherlands). A bile acids kit (450-A), for enzymatic determination of total BAs, was purchased from Trinity Biotech (Wicklow, Ireland).

Standards and sera

To prepare standards for an enzymatic assay, the fetal bovine serum (serves as a matrix) was spiked with a methanolic solution of the appropriate BA in order to reach final concentrations of 20, 50, or 100 μmol/L, and then sonicated for 10 min. The methanol content was always kept below 5%. Fetal bovine serum with 5% methanol was used as the blank. Six rat cholestatic sera (randomly chosen leftovers from our previous experimental *in vivo* study [6]) and six anonymous human cholestatic sera (anonymous leftovers of cholestatic sera, that were delivered to the clinical part of our laboratory for determination of total BAs concentration) served as samples with abnormal spectra of BAs. All sera were stored at -80˚C until analysis.

Enzymatic assays of BAs

In the first reaction, 3αHSD oxidizes BAs, forming equimolar quantity of NADH. In the subsequent reaction diaphorase oxidizes NADH to NAD with concomitant reduction of nitro blue tetrazolium salt to formazan, that is quantified spectrophotometrically. Samples or standards were processed in triplicates according to the manufacturer´s instructions, and measured using an Infinite M200 plate reader (Tecan, Mannedorf, Switzerland) set to 37˚C. Briefly, 50 μl of the sample was mixed with 125 μl of the test reagent and incubated for 5 min at 37˚C. The reaction was terminated by adding 25 μl of Stop reagent and absorbance was read at 530 nm after 5 min incubation. Blank reaction (lacking 3α-HSD) was prepared for each sample to

eliminate possible interferences. The results were either expressed as a concentration (calculated using the calibrator provided) or as a relative signal (absorbance of sample divided by absorbance of GCA at a given concentration). When needed, the incubation times were extended, as described in the Results section.

LC-MS/MS analysis

Upon addition of the deuterated internal standards and acetonitrile deproteination of serum, BA were quantified using LC-MS/MS as previously described [7]. The total BA concentration was obtained by summing up the concentrations of all the analyzed BAs.

Statistical analyses

Differences between total BA concentrations measured by LC-MS/MS vs enzymatically were tested using Wilcoxon signed-rank test. Reaction rates of individual BAs relative to GCA were evaluated using Mann-Whitney rank-sum test. Bonferroni correction was applied to counteract multiple testing (For clarity, p-values were corrected rather than the alpha value). Differences were considered statistically significant when the p-values were <0.05. Analyses were performed using Prism 8.0.1 software (GraphPad, San Diego, USA).

Results

Enzymatic determination of an individual BAs at the same concentration yielded considerably different responses. The relative signal intensities in major human BAs ranged from 100% in GCA (reference) to 60% in GCDCA. The differences were even more pronounced in minor BAs—the signal obtained from α-MCA, the "weakest" of tested BAs, reached just 20% of the reference ($p<0.0023$ for all comparisons, Fig 1).

Such marked differences, together with the fact that the enzymatic kit uses GCA as a calibrator, prompted us to test how the total BA concentration (determined enzymatically) would differ from reality in a serum sample with an abnormal spectrum of BAs. Therefore, we analyzed six cholestatic rat and six cholestatic human sera, both enzymatically as well as using LC-MS/MS. The enzymatic kit underestimated the total BA concentration by about 45% (range 18–74%) in humans, and by 60% (range 46–72%) in rats ($p = 0.031$ for both groups, Fig 2).

As the reaction rates for individual BAs can differ [8], we wondered whether the performance of the enzymatic method could be improved by prolonged incubation. Therefore, we incubated α-MCA for various periods of time in order to see if the signal reached the expected value. Although the signal markedly increased (almost threefold) when incubation was prolonged to 90 min (from the 5 min that is recommended by the manufacturer), it only reached just about half of the expected value (Fig 3).

Increasing the amount of enzyme (5 times) in the reaction mixture also did not improve the performance (S1 Fig).

Discussion

In the present study, we demonstrated the great variability of response during 3α-HSD mediated enzymatic determination of individual BAs. For major human BAs, the relative signals were within the range of 60–100%. The intensity of the signal decreased in the following order: cholic acid (CA) > deoxycholic acid (DCA) > lithocholic acid (LCA) > chenodeoxycholic acid (CDCA), which is similar to the results of previous studies [5, 8]. Free BAs tend to react faster than their glyco- or tauro-conjugated analogues, except for the most strongly reacting

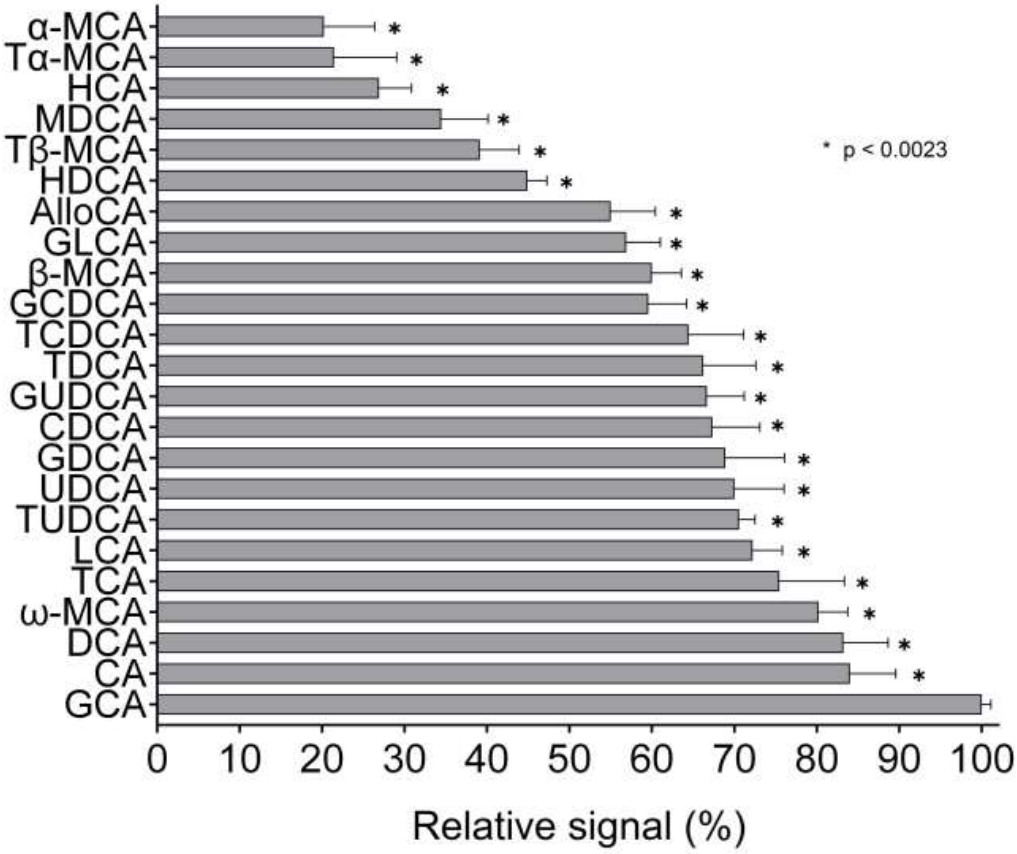

Fig 1. Relative signal intensities for individual BAs determined by an enzymatic method. Individual BAs were analyzed using an enzymatic kit, and the obtained signal was expressed as a % of the reference (GCA). Measurements were performed three times at three concentrations (20, 50, and 100 μmol/L)—each bar thus represents the average of nine values. All values differ significantly from reference: $p < 0.0023$ (original p-value of < 0.0001 was adjusted for 23 comparisons using Bonferroni correction).

https://doi.org/10.1371/journal.pone.0236372.g001

GCA. Importantly, we identified a group of poorly reacting BAs (mostly muricholic acids (MCAs) carrying hydroxyl group in position 6β), whose signal during enzymatic determination only reaches about 30% of what is expected. Enzymatic determination would therefore significantly underestimate the total concentration of BAs in samples rich in weakly reacting BAs (typically rodent sera). In fact, a severe underestimation was demonstrated in rat cholestatic sera, that contained about 40% of the slowest reacting BAs (MCAs, HDCA); while the fastest reacting GCA represented less than 10% of total BAs in most animals. In human cholestatic samples, the similarly severe underestimation was mostly due to abundant GCDCA or GUDCA (the later is likely present due to UDCA administration), that belong to intermediate/slow reactants (S2 Fig).

Although it has been described that prolonged incubation may completely compensate for the slower reaction rate of some BAs [8], we demonstrated that it was not sufficient for poorly reacting BAs. In the case of α-MCA, extending the incubation period from 5 to 90 min only

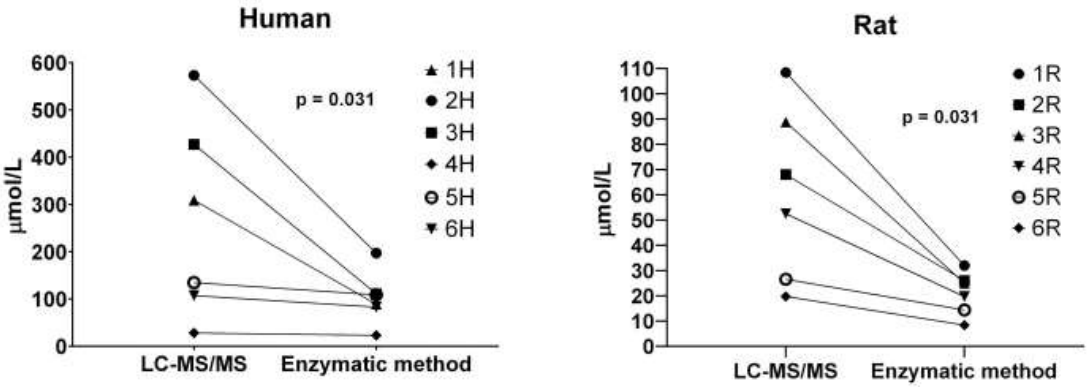

Fig 2. Enzymatic method underestimates total BA concentration in cholestatic serum samples with atypical BA spectra. Concentrations of total BAs in six cholestatic human sera and six cholestatic rat sera were determined using an enzymatic kit (triplicates) and LC-MS/MS (single measurement).

https://doi.org/10.1371/journal.pone.0236372.g002

increased the signal intensity from 20 to 50%. Further increase of the reaction time cannot be recommended, as the final reaction product is not stable, and the signal intensity decreases after about 60 min (see GCA, Fig 3).

Taken together, although enzymatic assays for measurement of total BA concentration are quite simple and straightforward, with good analytical performance [9], results depend greatly on the BA spectrum in the analyzed sample as well as on the composition of the calibrator.

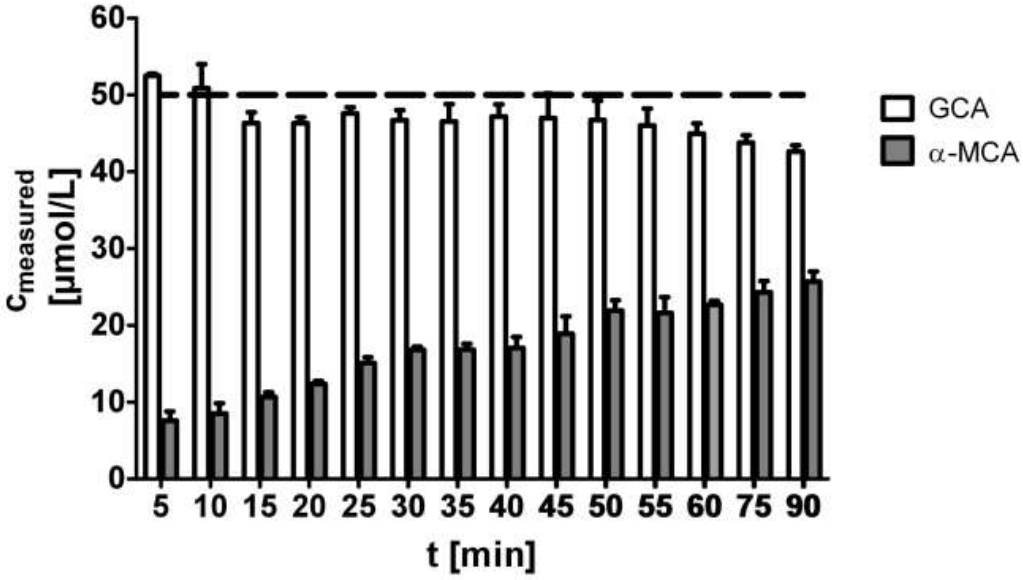

Fig 3. Prolonged incubation improves underestimation of poorly reacting BAs. Samples containing 50 µmol/L of either α-MCA or GCA were measured using an enzymatic kit. Incubation time varied from 5 min (recommended) up to 90 min. All measurements were done in triplicates; the dashed line represents the expected concentration.

https://doi.org/10.1371/journal.pone.0236372.g003

Commercially available calibrators typically contain strongly reacting BAs (GCA, CDCA, or TDCA) [9]. Therefore, the BA concentration in samples with an "atypical" spectrum of BAs will more-or-less be underestimated. Although such an atypical spectrum is mainly found in rodents, under pathological conditions (cholestasis [10, 11], exogenous BAs supplementation, small intestinal bacterial overgrowth [12], etc.) can be expected even in humans.

In conclusion, the performance of enzymatic assays for total BA determination in human serum seems to be appropriate for routine clinical use, where semiquantitative determination is generally sufficient. If the precise concentration is essential (mostly for research purposes), the results should be interpreted with care. In the rodent samples, enzymatic assays are far from reliable, and should be replaced by more precise analytical methods.

Supporting information

S1 Fig. Increased amount of enzyme partially improves underestimation of poorly reacting BAs. Samples containing 50 μmol/L of either α-MCA or GCA were measured using an enzymatic kit. Incubation time varied from 5 min (recommended) up to 90 min. The amount of enzyme was 5 times higher than recommended. All measurements were done in triplicates; the dashed line represents the expected concentration.
(TIF)

S2 Fig. BA spectra in cholestatic samples. Serum BA spectra (measured by LC-MS/MS) of the six cholestatic rats (a) and human patients (b) are provided. BA are grouped according to their reactivity with 3α-hydroxysteroid dehydrogenase. TLCA-S (taurolithocholic acid 3-sulfate) is presented as weakly reacting BA, although it does not react at all (due to the absence of 3α-hydroxy group). BA present in ≤2% are included in "other".
(JPG)

S1 Table. Basic characteristics of LC-MS/MS method.
(XLSX)

Author Contributions

Conceptualization: Martin Leníček.

Data curation: Kateřina Žížalová.

Methodology: Kateřina Žížalová.

Supervision: Marek Vecka, Martin Leníček.

Writing – original draft: Kateřina Žížalová, Martin Leníček.

Writing – review & editing: Marek Vecka, Libor Vítek.

References

1. European Association for the Study of the Liver. EASL Clinical Practice Guidelines: Management of cholestatic liver diseases. Journal of Hepatology. 2009; 51(2):237–67. https://doi.org/10.1016/j.jhep.2009.04.009 PMID: 19501929
2. Chiang JYL. Bile acid metabolism and signaling. Compr Physiol. 2013; 3(3):1191–212. https://doi.org/10.1002/cphy.c120023 PMID: 23897684.
3. Chiang JYL, Ferrell JM. Bile Acids as Metabolic Regulators and Nutrient Sensors. Annual Review of Nutrition. 2019; 39(1):175–200. https://doi.org/10.1146/annurev-nutr-082018-124344 PMID: 31018107.
4. Iwata T, Yamasaki K. Enzymatic Determination and Thin-layer Chromatography of Bile Acids in Blood. The Journal of Biochemistry. 1964; 56(5):424–31.

5. Mashige F, Tanaka N, Maki A, Kamei S, Yamanaka M. Direct spectrophotometry of total bile acids in serum. Clinical Chemistry. 1981; 27(8):1352. PMID: 6895053

6. Muchova L, Vanova K, Suk J, Micuda S, Dolezelova E, Fuksa L, et al. Protective effect of heme oxygenase induction in ethinylestradiol-induced cholestasis. Journal of cellular and molecular medicine. 2015; 19(5):924–33. Epub 2015/02/16. https://doi.org/10.1111/jcmm.12401 PMID: 25683492.

7. Prasnicka A, Cermanova J, Hroch M, Dolezelova E, Rozkydalova L, Smutny T, et al. Iron depletion induces hepatic secretion of biliary lipids and glutathione in rats. Biochimica et Biophysica Acta (BBA)—Molecular and Cell Biology of Lipids. 2017; 1862(12):1469–80. https://doi.org/10.1016/j.bbalip.2017.09.003.

8. Engert R, Turner MD. Problems in the measurement of bile acids with 3α-hydroxysteroid dehydrogenase. Analytical Biochemistry. 1973; 51(2):399–407. https://doi.org/10.1016/0003-2697(73)90493-4 PMID: 4349452

9. Danese E, Salvagno GL, Negrini D, Brocco G, Montagnana M, Lippi G. Analytical evaluation of three enzymatic assays for measuring total bile acids in plasma using a fully-automated clinical chemistry platform. PloS one. 2017; 12(6):e0179200–e. https://doi.org/10.1371/journal.pone.0179200 PMID: 28594875.

10. Trottier J, Bialek A, Caron P, Straka RJ, Milkiewicz P, Barbier O. Profiling Circulating and Urinary Bile Acids in Patients with Biliary Obstruction before and after Biliary Stenting. Plos One. 2011; 6(7).

11. Ye L, Liu SY, Wang M, Shao Y, Ding M. High-performance liquid chromatography-tandem mass spectrometry for the analysis of bile acid profiles in serum of women with intrahepatic cholestasis of pregnancy. Journal of Chromatography B-Analytical Technologies in the Biomedical and Life Sciences. 2007; 860(1):10–7.

12. Galloway D, Mezoff E, Zhang W, Byrd M, Cole C, Aban I, et al. Serum Unconjugated Bile Acids and Small Bowel Bacterial Overgrowth in Pediatric Intestinal Failure: A Pilot Study. Journal of Parenteral and Enteral Nutrition. 2019; 43(2):263–70. https://doi.org/10.1002/jpen.1316 PMID: 30035316

Příloha 2

www.nature.com/scientificreports

SCIENTIFIC REPORTS

OPEN

Iron overload reduces synthesis and elimination of bile acids in rat liver

Alena Prasnicka[1,4], Hana Lastuvkova[1], Fatemeh Alaei Faradonbeh[1], Jolana Cermanova[1], Milos Hroch[2], Jaroslav Mokry[3], Eva Dolezelova[4], Petr Pavek[5], Katerina Zizalova[6], Libor Vitek[6], Petr Nachtigal[4] & Stanislav Micuda[1]

Received: 25 October 2018
Accepted: 21 June 2019
Published online: 05 July 2019

Excessive iron accumulation in the liver, which accompanies certain genetic or metabolic diseases, impairs bile acids (BA) synthesis, but the influence of iron on the complex process of BA homeostasis is unknown. Thus, we evaluated the effect of iron overload (IO) on BA turnover in rats. Compared with control rats, IO (8 intraperitoneal doses of 100 mg/kg every other day) significantly decreased bile flow as a consequence of decreased biliary BA secretion. This decrease was associated with reduced expression of Cyp7a1, the rate limiting enzyme in the conversion of cholesterol to BA, and decreased expression of Bsep, the transporter responsible for BA efflux into bile. However, IO did not change net BA content in faeces in response to increased intestinal conversion of BA into hyodeoxycholic acid. In addition, IO increased plasma cholesterol concentrations, which corresponded with reduced Cyp7a1 expression and increased expression of Hmgcr, the rate-limiting enzyme in *de novo* cholesterol synthesis. In summary, this study describes the mechanisms impairing synthesis, biliary secretion and intestinal processing of BA during IO. Altered elimination pathways for BA and cholesterol may interfere with the pathophysiology of liver damage accompanying liver diseases with excessive iron deposition.

Bile production is an essential function of the liver and serves as an irreplaceable excretory pathway for elimination of lipophilic endo- and xenobiotics such as cholesterol, BA, bilirubin or drugs[1]. Moreover, as major components of bile, BA are required for micelle formation, intestinal fat digestion, regulation of bacterial growth, and immune response and production of regulatory mediators released to portal circulation such as fibroblast growth factor 19 or glucagon-like peptide 1. In addition, BA as the major metabolites of cholesterol, act as hormones by agonism at several receptors such as farnesoid X receptor (FXR), the G protein-coupled bile acid receptor 1 (TGR5), sphingosine-1-phosphate receptor 2, or pregnane X receptor (PXR), and regulate numerous liver functions including glucose and triglyceride metabolism[2]. Stimulation of these receptors demonstrates promising positive effects in liver diseases such as nonalcoholic steatohepatitis (NASH) or intrahepatic cholestasis[3]. On the other hand, BA accumulated during different forms of cholestasis may have a direct toxic effect on liver cells and tissues. Regulation of bile production and BA homeostasis are therefore key events in liver physiology and pathophysiology.

Iron is an essential trace element, in particular required to form haem for synthesis of haemoglobin, myoglobin or P450 enzymes. As a highly reactive molecule, iron is also involved in the cellular redox balance and generation of hydroxyl radicals which are necessary for regulation of several intracellular events including response to stressors or mitochondrial dysfunction[4]. Excessive concentration of iron in cells induces oxidative stress with peroxidative decomposition of polyunsaturated fatty acids in membrane phospholipids, thereby altering vital organelle integrity and cell function[5,6]. The metabolism of iron is therefore tightly regulated to prevent tissue damage. However, IO can occur in subjects with genetic disorders such as hereditary haemochromatosis and beta thalassaemia, or secondary to IO during blood transfusion and haemolysis[7,8]. Iron toxicity occurs especially in

[1]Department of Pharmacology, Charles University, Faculty of Medicine in Hradec Kralove, Hradec Kralove, Czech Republic. [2]Department of Medical Biochemistry, Charles University, Faculty of Medicine in Hradec Kralove, Hradec Kralove, Czech Republic. [3]Department of Histology and Embryology, Charles University, Faculty of Medicine in Hradec Kralove, Hradec Kralove, Czech Republic. [4]Department of Biological and Medical Sciences, Charles University, Faculty of Pharmacy in Hradec Kralove, Hradec Kralove, Czech Republic. [5]Department of Pharmacology and Toxicology, Charles University, Faculty of Pharmacy in Hradec Kralove, Hradec Kralove, Czech Republic. [6]Department of Medical Biochemistry and Laboratory Diagnostics, 1st Faculty of Medicine, Charles University, Prague, Czech Republic. Correspondence and requests for materials should be addressed to S.M. (email: micuda@lfhk.cuni.cz)

the liver, where the iron is mainly stored, leading to ongoing damage and finally to cirrhosis. Moreover, increased liver iron stores accompany common metabolic pathologies such as insulin resistance, type 2 diabetes mellitus, metabolic syndrome, and nonalcoholic fatty liver disease (NAFLD)[9]. It is of note, that these metabolic disorders produce marked changes in BA metabolism and could be treated by agonists of FXR receptor, which is the most important BA sensor[10]. However, the relationship between IO and BA liver homeostatic pathways has not been studied in depth.

Indeed, plasma concentrations of BA during IO have not been yet measured and only limited evidence suggests that biliary BA excretion may be reduced by dietary IO[5]. This observation may be related to IO-mediated reduction in the expression of cholesterol 7α-hydroxylase (Cyp7a1), the rate-limiting enzyme for conversion of cholesterol to BA in rats[5,11,12], although no association between liver iron concentration and Cyp7a1 was seen in this model of IO[13]. Reduction in Cyp7a1 may also explain increased serum cholesterol levels in iron-administered rats[5,14–17]. However, the effect of liver iron accumulation on other BA synthetic pathways and on biliary and faecal BA excretion is not known. Therefore, we postulated the hypothesis that iron accumulation in an organism markedly reduces elimination of BA.

In the present study we evaluated the effect of IO on the mechanisms responsible for BA homeostasis in rat liver and ileum. We showed that increased iron deposition in rat liver results in decreased bile formation due to reduced biliary BA secretion through downregulated Bsep and Mrp2 apical transporters. Plasma concentrations of BA were not significantly affected by IO because reduced biliary BA secretion was accompanied by reduced liver BA synthesis, intestinal BA processing, and increased basolateral output from hepatocytes and reduced uptake to hepatocytes.

Results

IO causes massive iron deposition in rat livers. To establish IO with significant iron liver accumulation in parenchymal and nonparenchymal cells, we used a validated rat model based on intraperitoneal (i.p.) administration of 8 doses (100 mg/kg per dose) of iron dextran-heptonic acid complex applied every other day[18]. This regimen resulted in massive iron liver deposition without significant hallmarks of hepatocellular or cholestatic injury as apparent from histological examination of haematoxylin-eosin (HE) and Prussian blue iron (PB) staining of liver sections (Fig. 1A). Massive iron deposition was apparent, especially in periportal zones of the liver acinus when compared with regions around the central vein as visualized by opalescent structures in HE staining and blue deposits in PB staining. This corresponds with previously reported data[8,19]. No apparent staining was present in the saline-administered animals. Liver weights were not changed by IO and were 13.5 ± 0.5 g in the saline-treated rats, and 14.2 ± 0.5 g in the IO rats. IO with excessive liver accumulation was further confirmed by increased plasma concentrations of iron and ferritin (Fig. 1C) and by increased liver mRNA expression of key iron metabolism associated genes such as hepcidin (*Hamp*), ferritin (*Ftl*), ferroportin (*Slc40a1*) and down regulation of transferrin receptor 1 (*Trfc*) (Fig. 1B). We also detected significantly reduced levels of iron-responsive element-binding protein 1 and iron-responsive element-binding protein 2 (IRP1 and IRP2) proteins (Fig. 1D), a markers of iron excess in the liver[20]. IRP1 and IRP2 were recently demonstrated as a positive regulator of *Cyp7a1* transcription[11]. These results demonstrated typical histological, biochemical and molecular hallmarks of significant iron deposition in the liver of treated animals.

IO causes mild liver injury and oxidative stress. Excessive iron deposition in the liver can induce oxidative liver injury[6]. To determine liver injury in our IO model, we analysed the plasma and livers for corresponding biomarkers. The harmful effect of IO on liver functions was demonstrated by a mild but significant increase in aspartate transaminase (AST) activity, and plasma cholesterol and bilirubin concentrations (Fig. 2A). Induction of oxidative stress in the liver of IO rats was confirmed by the increased presence of glutathione in its oxidized (GSSG) form (Fig. 2B), reduced GSH/GSSG ratio (Fig. 2B) and by increased protein expression of stress-response molecules, haem oxygenase 1 (Hmox1) and phosphorylated NF-κB p65 subunit (Fig. 2C). These changes did not trigger acute inflammatory response in the liver, as suggested by the absence of inflammatory cell accumulation in histology sections (Fig. 1A) and unchanged gene expression of tumour necrosis factor (*Tnfα*) and interleukin 6 (*Il6*) (Fig. 2D). On the other hand, deposited iron activated *Tgfβ1* production accompanied by increased expression of *Acta2* (encoding α-SMA protein) (Fig. 2D), a marker of activated hepatic stellate cells, which was also recently demonstrated[21].

Bile flow is reduced by IO in response to reduced biliary secretion of BA. Reduced biliary secretion of total BA during IO was reported previously in a single study[5]. To elaborate this finding, we performed a bile collection study with analysis of BA spectra and other major components of bile including BA-independent flow based mainly on biliary secretion of glutathione. IO caused significant reduction of net bile flow in rats (Fig. 3A), accompanied by decreased biliary secretion of BA. Individual BA were proportionally reduced in the presence of IO (Fig. 3B). Changes in biliary secretion of individual bile acids presents Supplementary Table 3. Biliary secretion of glutathione, cholesterol and phospholipids did not significantly differ between the control and IO rats (Fig. 3C). Similarly, concentrations of BA and their spectra in plasma and the concentration of cholesterol in liver were not changed by iron administration (Fig. 3D,E, Supplementary Table 3). Our data indicate that the reduction of bile production by IO reflected reduced biliary secretion of BA.

Impact of IO on liver expression of molecules responsible for BA and cholesterol turnover. In order to reveal the mechanisms responsible for changes in BA biliary kinetics, we analysed liver expression of transporting proteins and enzymes with crucial functions in cholesterol and BA uptake, secretion, and metabolism. Evaluating key genes in BA and cholesterol synthesis, IO significantly reduced mRNA expression of *Cyp7a1* and significantly increased gene expression of 3-hydroxy-3-methyl-glutaryl-coenzyme A reductase (*Hmgcr*)

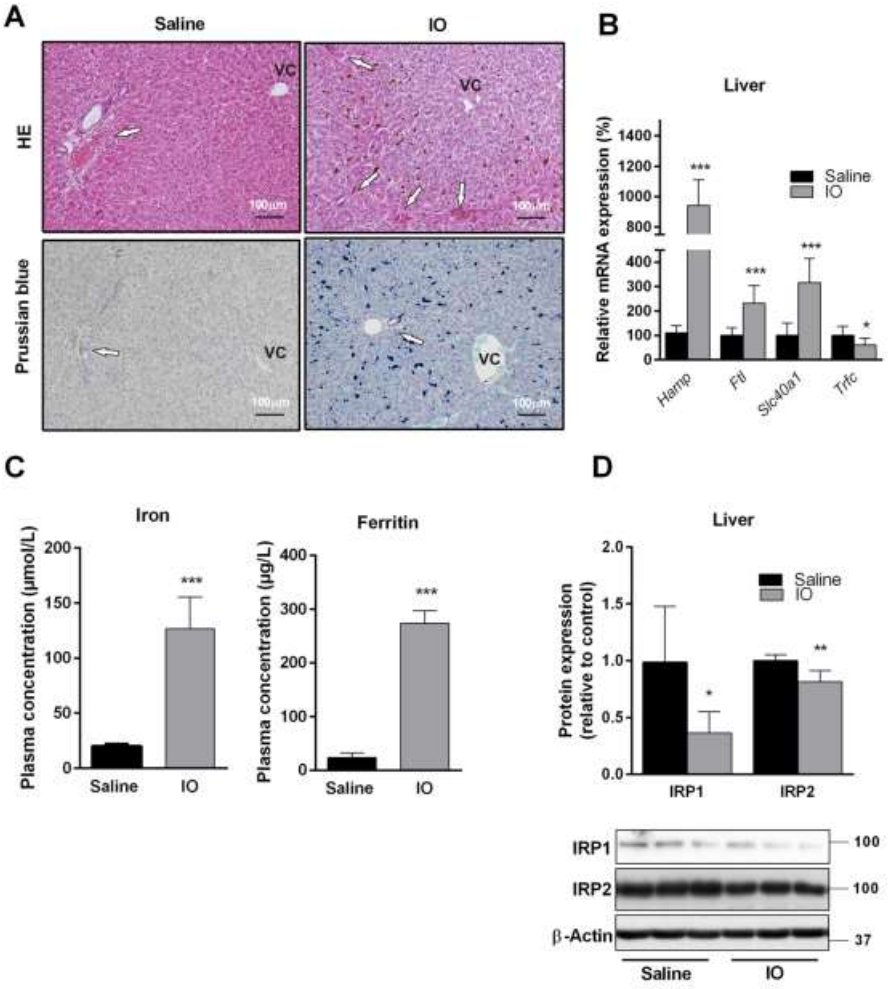

Figure 1. Excessive concentration of iron in IO rats administrated i.p. with 8 doses of gleptoferron every 2nd day. (**A**) Representative liver histology, stained with haematoxylin-eosin staining (HE) and Prussian blue. Arrows indicate periportal areas at the periphery of classical liver lobule; VC – vena centralis. Scale bar 100 µm. (**B**) mRNA liver expression of hepcidin (*Hamp*), ferritin (*Ftl*), ferroportin (*Slc40a1*) and transferrin receptor (*Trfc*) determined by real-time RT-PCR. (**C**) Concentration of iron and ferritin in plasma. (**D**) Liver protein content of IRP1 and IRP2 (iron-responsive element-binding protein 1 and 2) normalized to β-actin. Values are mean ± SD (n = 6 in each group). $*p < 0.05$, $**p < 0.01$, $***p < 0.001$ iron-treated vs. saline-treated rats.

(Fig. 4A). Of all apical and basolateral transporters, IO significantly increased mRNA expression of *Abcb1a/1b*, *Abcc3* and *Abcb4*, respectively (Fig. 4B). These transcriptional changes were followed by proportional changes in encoded proteins. We detected downregulation of Cyp7a1 (Fig. 4C) and up-regulation of Hmgcr, the rate-limiting enzyme for cholesterol synthesis (Fig. 4C), Mdr1 (Fig. 4D), the major apical transporter for biliary excretion lipophilic drugs, and Mrp3/Mrp4 (Fig. 4D), the basolateral efflux transporters for conjugated anionic compounds such as bilirubin glucuronides and BA. However, IO also down-regulated liver protein levels of Cyp8b1 enzyme for BA synthesis (Fig. 4C), Ntcp, an essential protein for uptake of BA from portal blood to hepatocytes (Fig. 4D). Increased expressions of Abcg8, an apical efflux transporter for cholesterol from liver to canaliculus, was not followed by a corresponding change in Abcg5, which may imply that the function of this heterodimer was not increased as also suggested by unchanged cholesterol biliary secretion (Fig. 3C). Previous studies described that Bsep, the rate limiting transporter for biliary BA secretion, and Mrp2, the rate-limiting transporter for anionic compounds including conjugates of BA and bilirubin, may be regulated post-transcriptionally by increased retrieval and degradation from the canalicular membrane[22]. Therefore, we performed immunohistochemical analysis in order to evaluate localization and expression of both proteins. Immunohistochemical staining in the

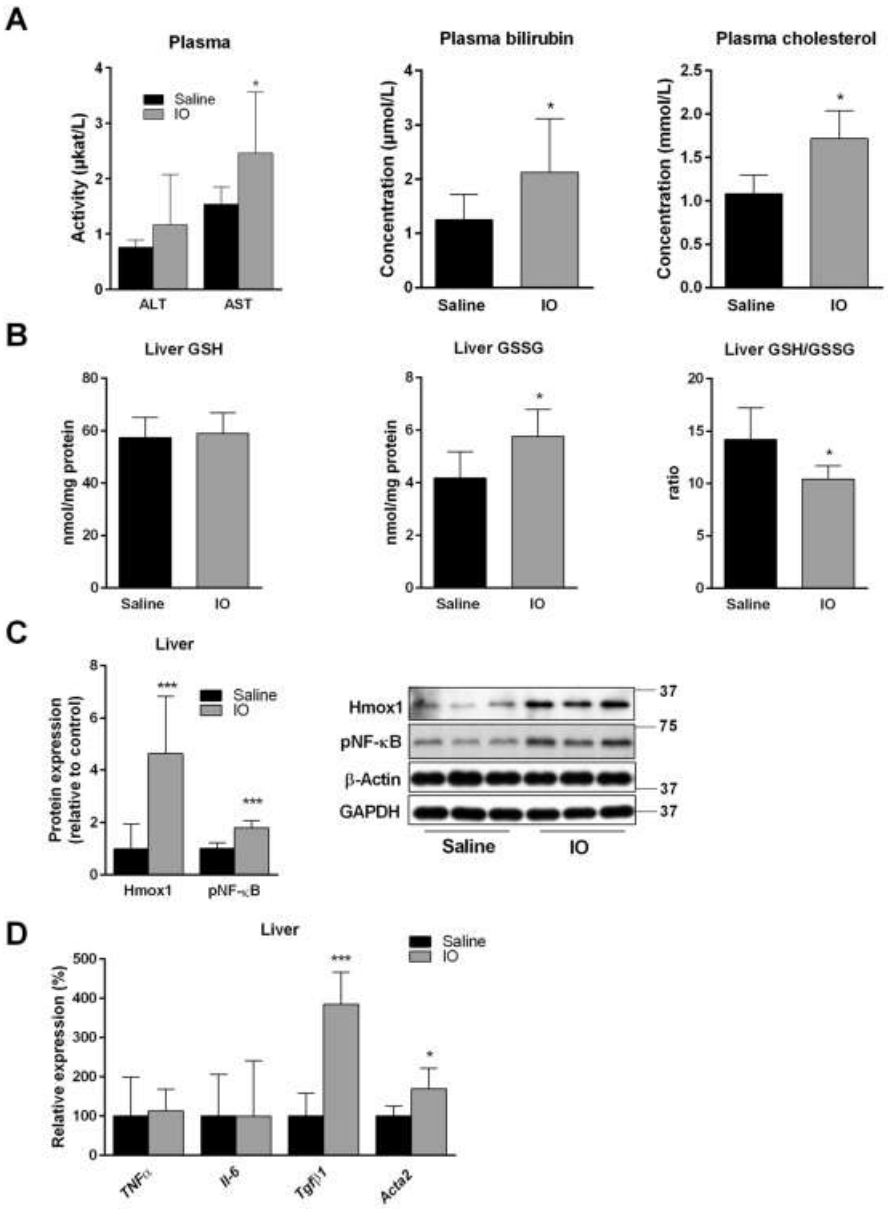

Figure 2. IO induced mild liver injury by activation of oxidative stress. (**A**) Activity and concentrations of ALT, AST, bilirubin, cholesterol in plasma. (**B**) Content of reduced and oxidized glutathione (GSSG) and GSH/GSSG ratio, determined by HPLC measurement. (**C**) Liver protein content of haem oxygenase (Hmox1) and phosphorylated NF-κB (p65) normalized to average of β-actin and Gapdh. (**D**) mRNA liver expressions of proinflammatory markers *TNFα*, *Il-6*, *Tgfβ1* and *Acta2* (encoding α-SMA protein) determined by real-time RT-PCR. Values are mean ± SD (n = 6 in each group). $*p < 0.05$, $**p < 0.01$, $***p < 0.001$ iron-treated vs. saline-treated rats.

liver showed strong Mrp2 expression in the canalicular membrane of hepatocytes in the control rats (Fig. 5A) as described in our previous paper[23]. On the contrary, Mrp2 expression was reduced in the IO rats (Fig. 5A). Similarly, Bsep expression was also detected in the canalicular membrane of hepatocytes in the control animals (Fig. 5A). However, Bsep staining was substantially weaker in the IO rats (Fig. 5A). Gene expressions of both

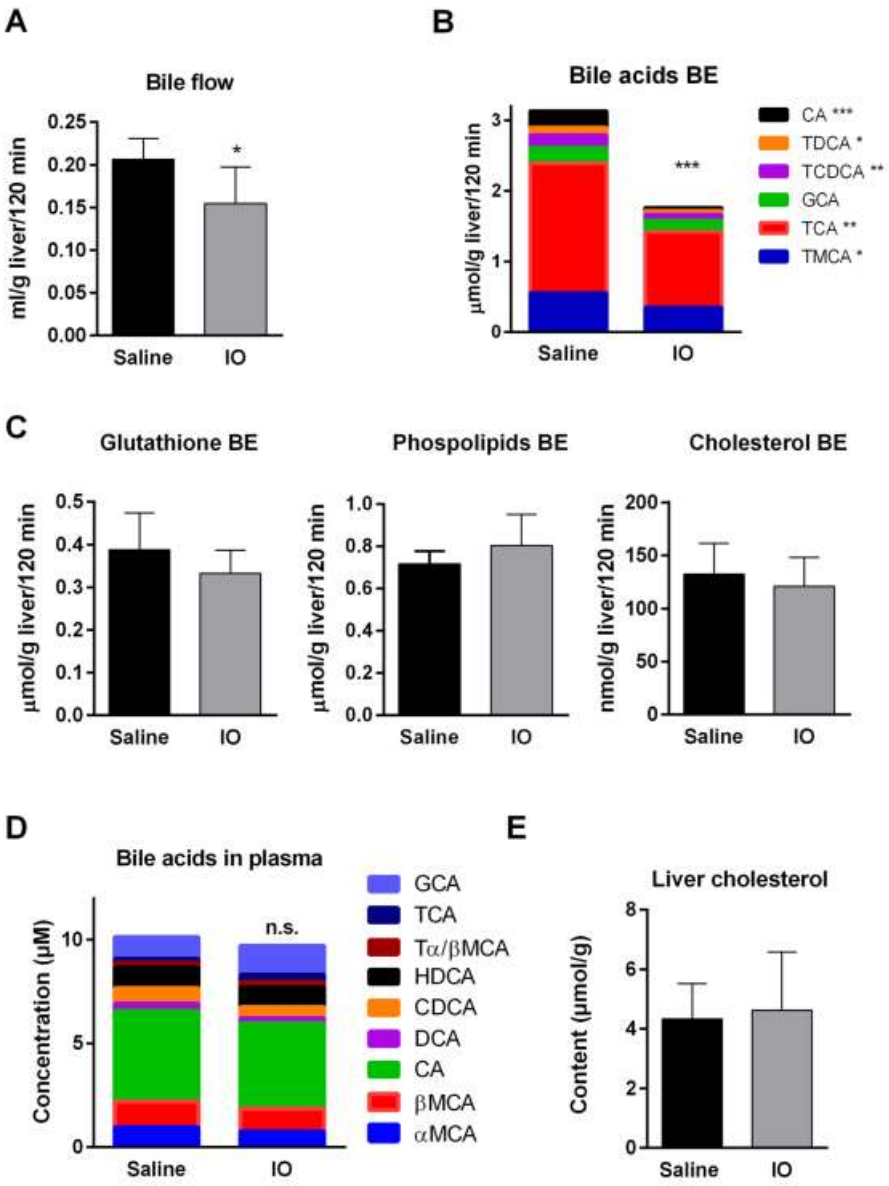

Figure 3. Bile flow was reduced in rats by IO in response to reduced biliary secretion of BA. (**A**) Rat bile duct was cannulated and bile was collected for 120 min. Then the bile flow was calculated from amount of collected bile to liver weight. (**B**,**D**) The concentrations of total and individual BAs in bile and plasma were measured by LC-MS analysis. (**C**,**E**) Biliary secretions of phospholipids, glutathione, cholesterol and hepatic content of cholesterol were determined by available commercial kits. Values are mean ± SD (n = 6 in each group). $^{*}p < 0.05$, $^{**}p < 0.01$, $^{***}p < 0.001$ iron-treated vs. saline-treated rats.

proteins were not changed by IO (Fig. 5B), while western blot analysis confirmed downregulation of both, Bsep and Mrp2 at protein levels (Fig. 5C). These data indicate significant posttranscriptional down-regulation of Bsep and Mrp2 by IO.

IO changes intestinal BA turnover. More than 90% of BA is reabsorbed from the ileum into portal blood, and subsequently reused by hepatocytes for secretion into the bile. In order to study intestinal turnover of BA, we analysed BA loss through faeces. BA were present in stool only in unconjugated form. In contrast to biliary

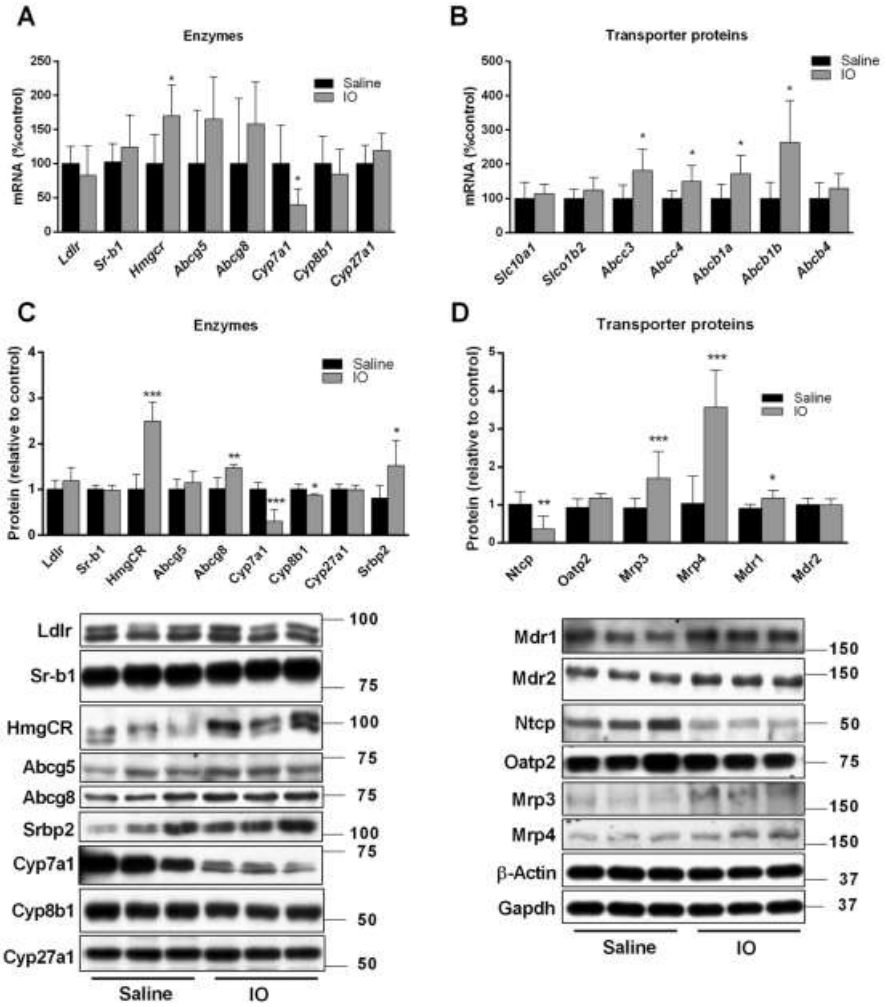

Figure 4. Impact of IO on liver mRNA and protein expression responsible for BA and cholesterol turnover. Isolated mRNAs (**A**,**B**), and proteins (**C**,**D**) from liver tissue were used to determine the expression of transporters and enzymes responsible for cholesterol and BAs homeostasis. The expression of these genes was analysed by a real-time RT-PCR system and proteins by western blot immunodetection. Values are mean ± SD (n = 6 in each group). $*p < 0.05$, $**p < 0.01$, $***p < 0.001$ iron-treated vs. saline-treated rats.

secretion, the net faecal excretion of BA was highly variable between individuals; therefore, the tendency for decreased net faecal excretion of BA in the IO rats failed to reach statistical significance (Fig. 6A, Supplementary Table 3). This suggests that potential hepatic retention of BA in response to reduced biliary secretion of BA was compensated for by their reduced ileum reabsorption. Western blot analysis did not confirm significant changes in protein expression of Asbt, and Ost α/β, the major transporters for BA reabsorption at apical and basolateral membranes of ileum enterocytes, respectively (Fig. 6B). We therefore focused on faecal content of individual BA. Liquid chromatography–mass spectrometry (LC-MS) analysis revealed that faecal BA loss was reduced for the majority of BA in the IO rats, with the exception of hyodeoxycholic acid (HDCA) (Fig. 6A). HDCA was present in significant amounts in four out of six IO rats, and produced such variability in net stool BA content. HDCA was absent in the faeces of all saline-administered rats. Interestingly, concentrations of HDCA in plasma from portal bloods were 12.4 ± 7.5 μM in control and 13.5 ± 5.3 μM in IO groups, respectively, and they were not statistically different (P = 0.77). This indicates that metabolic conversion of BA by gut microbiota may modify reduced biliary secretion of BA in IO rats.

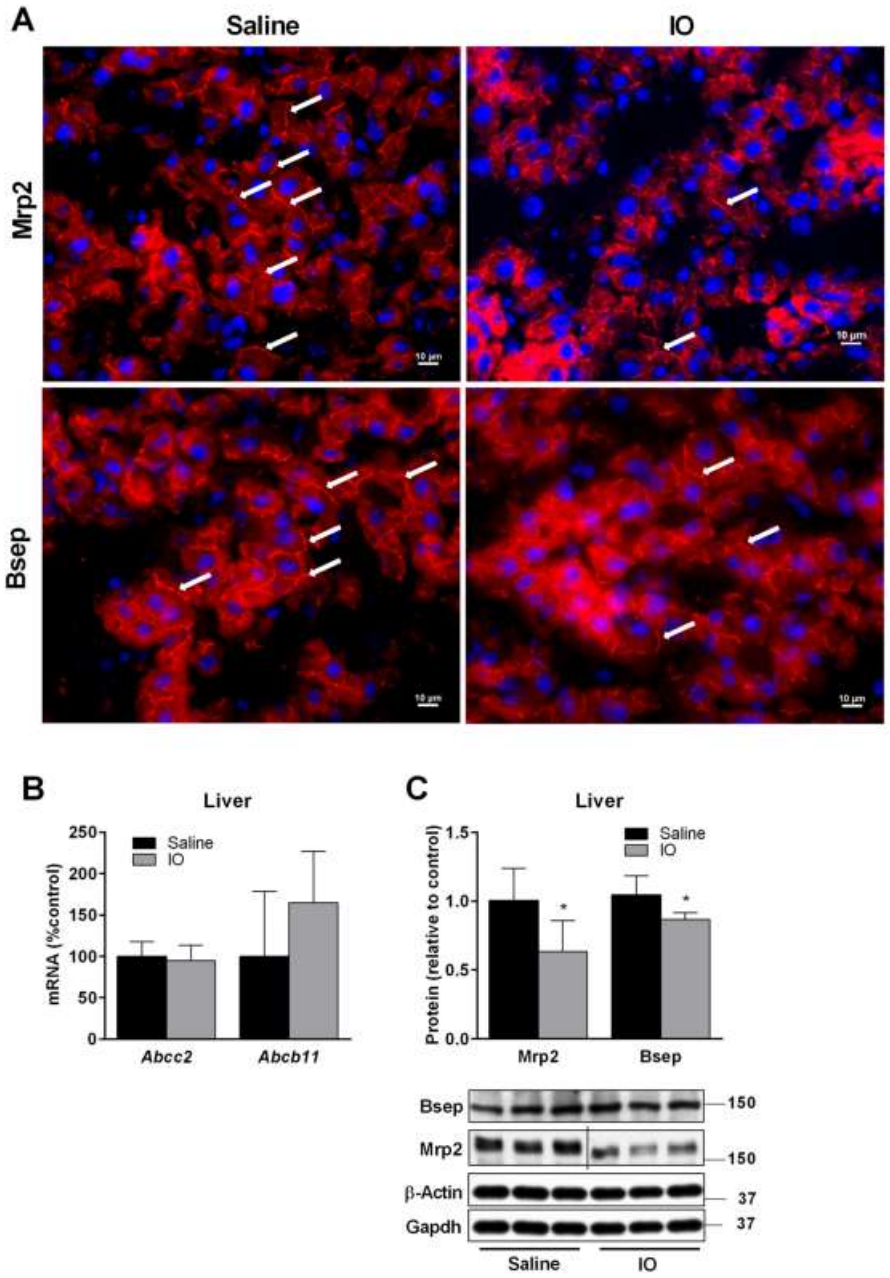

Figure 5. IO reduced posttranscriptionally the expression of Mrp2 and Bsep transporting proteins. (**A**) Immunohistochemical staining was used to detect Mrp2 and Bsep expression (red, white arrows) in the liver of saline and IO treated rats. Representative images of random fields are shown. Nuclei staining in blue (DAPI). Scale bar 10 µm. Isolated mRNA (**B**) and proteins (**C**) from liver tissue were used for evaluation of gene expression and protein levels. The expression of these genes was analysed by real-time RT-PCR system and proteins by western blot immunodetection. Values are mean ± SD (n = 6 in each group). $*p < 0.05$, $**p < 0.01$, $***p < 0.001$ iron-treated vs. saline-treated rats.

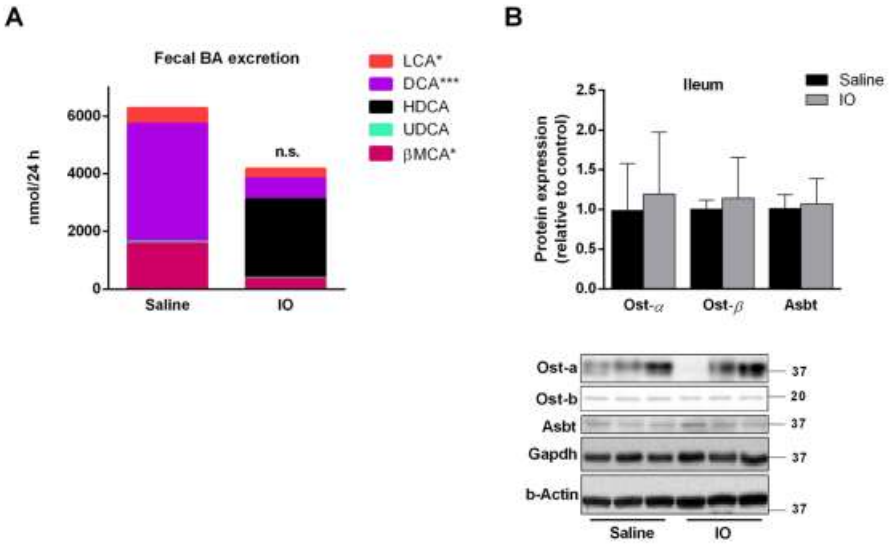

Figure 6. Iron overload changed intestinal BA turnover. (**A**) The BA were isolated from dried stool after 24 h collection. The concentrations of total and individual BA in bile and plasma were measured by LC-MS analysis. (**B**) Protein expression of major transporters for BA reabsorption in ileum was determined by western blot analysis and calculated to average of β-actin and Gapdh. Values are mean ± SD (n = 6 in each group). $*p < 0.05$, $**p < 0.01$, $***p < 0.001$ iron-treated vs. saline-treated rats.

Discussion

Alteration of cholesterol homeostasis by IO was reported by several studies, but the collected results indicate discrepancies between different models. While humans and mice[24] with genetically determined IO such as thalassaemia or hereditary haemochromatosis develop mostly reduced cholesterol plasma concentrations, rodent models based on iron administration usually develop increased plasma[5] or hepatic cholesterol[13] levels. Animal models based on excessive iron administration therefore better reflect hepatic iron deposition during dysmetabolic IO syndrome, the clinical syndrome detected in about one-third of patients with NAFLD or the metabolic syndrome, and characterized by iron liver deposition and elevated plasma cholesterol[25].

Research on molecular mechanisms explaining hypercholesterolaemia accompanying increased liver iron content has not yielded consistent results. Brunet *et al.*[5] demonstrated reduced hepatic activities of both Hmgcr and Cyp7a1 in dietary iron loaded rats in association with increased plasma and unchanged liver cholesterol levels, and reduced biliary excretion of BA and cholesterol. Reduced gene expression of *Cyp7a1* together with increased plasma cholesterol concentrations were also detected in $Hfe^{-/-}$ DBA/2 mice but not in $Hfe^{-/-}$ C57BL/6 mice[12]. In another study, dietary IO mice showed positive correlation between hepatic iron content and both mRNA expression of *Hmgcr* and hepatic cholesterol content, while no relationship was seen with Cyp7a1 or with plasma cholesterol concentration[13]. Indeed, the results of this study demonstrate important new information that excessive IO may even lead to a harmful combination of Cyp7a1 downregulation coupled with marked induction of Hmgcr. We speculate that discrepancies reported by available studies regarding IO-induced changes in both HMG-CoA reductase and Cyp7a1 are related to underlying pathology and different degree and localization of iron liver accumulation.

Liver Hmgcr is regulated by SREBP-2 transcription factor in response to reduced tissue cholesterol content[26]. Thus, unchanged liver cholesterol concentrations in our IO rats suggest another factor activating SREBP-2. Indeed, recently it has been described that SREBP-2 may be induced by reactive oxygen species (ROS)[27]. ROS production typically occurs during IO[6]. Reduced liver GSH/GSSG ratio and induced Hmox1 expression and NF-κB p65 phosphorylation confirmed marked oxidative stress in the IO rats. We therefore suggest that induction of liver ROS–SREBP-2 pathway is responsible for Hmgcr induction in IO rats. The absence of cholesterol accumulation in the liver together with its unchanged biliary excretion suggests that increased plasma cholesterol concentrations are related to its increased output from the liver to the bloodstream in response to increased synthesis by induced Hmgcr, and reduced metabolism to BA due to reduced Cyp7a1. The finding of induced Hmgcr also indicates potential therapeutic strategy by statins, the Hmgcr-blocking drugs which indeed showed beneficial effects in NASH, a syndrome associated with increased incidence of liver iron deposition[28].

The reduction of *Cyp7a1* gene expression in IO rats together with its recently detected induction during iron depletion[29] suggests that iron regulates Cyp7a1 expression by a transcriptional mechanism. Our recent study excluded involvement of major pathways regulating *Cyp7a1* transcription such as nuclear receptors (e.g. FXR or PXR) or Egf15-pERK/pJNK signalling in iron depletion-mediated induction of Cyp7a1[29]. On the other hand, Liang *et al.*[11] recently discovered that modulation of *Cyp7a1* mRNA by iron is executed by iron-regulating

proteins IRP1 and IRP2 in mice. In general, when cells are iron-deficient, IRPs bind to iron-responsive elements (IREs) in untranslated regions (UTRs) of target mRNAs such as divalent metal transporter 1 and transferrin receptor 1, and increase their expression by stabilizing the mRNAs, while IRPs binding to UTRs of ferritin or ferroportin 1 blocks the translation of these mRNAs. When iron is in excess, IRP1 acquires a 4Fe-4S cluster and creates an aconitase, while IRP2 undergoes degradation so their binding to UTRs generally declines[11,20]. Liang *et al.*[11] demonstrated that *Cyp7a1* has a non-canonical IRE structure in its 3′-UTR that can efficiently bind both IRP1 and IRP2 and increase transcription of this enzyme. Increased liver iron content reduces IRP1 and IRP2 and consequently reduces Cyp7a1 expression, while desferrioxamine, an iron chelator, has an inducing effect. Impairment of the IRE structure in the UTR of Cyp7a1 gene abolishes the modulating effect of iron. In the present study, reduced IRP2 expression and variable changes in liver FXR-SHP and FGF15-pJNK/pERK axes (data not shown) in IO rats imply iron-IRPs-Cyp7a1 regulation as a major mechanism of Cyp7a1 downregulation in IO rats.

Transporting proteins mediating hepatocyte uptake and biliary secretion of BA and bilirubin have not been previously studied in IO animals despite the evidence of reduced biliary BA secretion[5]. We demonstrate for the first time posttranscriptional down-regulation of Ntcp, Bsep and Mrp2 transporters for BA which resembles increased retrieval and degradation of these proteins during liver inflammation[22,30]. Data from immunohistochemistry indeed confirmed significantly reduced intensity and canalicular localization of both Bsep and Mrp2 in IO livers when compared with control rats. This pattern of regulation may correspond with significant oxidative stress induced by IO. In support, we detected upregulation of Mdr1, which is induced in the liver by binding of phosphorylated NF-κB to Mdr1 promotor[31]. These changes may, together with reduced BA synthesis, contribute to reduced biliary BA secretion in IO rats, and may modify biliary excretion of numerous compounds including drugs. Furthermore, reduced uptake of BA through reduced Ntcp, and their increased output to blood through induced Mrp4 may contribute to unchanged BA plasma concentrations and prevent intracellular BA accumulation due to impaired BA biliary excretion. Downregulation of apical Mrp2, and upregulation of basolateral Mrp3 transporters for bilirubin conjugates together with induced Hmox-1 may explain increased bilirubin plasma concentration in IO rats due to its increased synthesis and reversed transport to blood.

The impact of IO on faecal excretion of BA has been unknown to date. Despite reduced biliary BA secretion in the IO rats, the net BA output by stool remained statistically unaffected. Abst, and Osts, the major transporters for BA reuptake from the intestine, were not significantly changed by IO. In contrast, analysis of BA spectra in stool displayed marked but inter-individually variable intestinal conversion of BA into HDCA in the IO rats. A previous study showed inefficient absorption of HDCA from the intestinal tract in Wistar rats and proposed that HDCA formation might be an important mechanism for controlling the body cholesterol pools[32]. In our study, statistically unchanged concentrations of HDCA in the portal blood confirms limited capacity for HDCA intestinal reabsorption, which subsequently results in marked increase of HDCA in the stool of some IO animals. Therefore, we suggest that the marked but variable metabolism of BA into HDCA by intestinal bacteria[33] of the IO rats was the reason for statistically unchanged net stool BA excretion in comparison with saline-administered animals. Potential changes in gut microbiome composition caused by IO must be further studied. Moreover, we have detected for the first time a reduction of liver Cyp8b1, the crucial enzyme for neutral pathway of BA synthesis, in IO rats, and analysed BA spectra in these animals. Combined downregulation of Cyp8b1 and Cyp7a1 was associated with significantly reduced content of faecal DCA, the major representative of neutral pathway of BA synthesis, in IO rats. Moreover, we have detected formation of HDCA, the metabolite of muricholic acid, a typical product of the acidic pathway of BA synthesis.

In conclusion, our data showed that IO results in a complex effect on BA homeostasis combining reduced liver BA synthesis, biliary secretion and reabsorption in the intestine, with reduced uptake to hepatocytes and increased output from hepatocytes to the bloodstream. Complex changes in transporting proteins indicate possibly dysfunctional elimination of numerous substrates including drugs. We propose that these abnormalities developed in response to oxidative stress, and IRP2 repression produced by excessive liver iron deposition. IO markedly influenced faecal excretion of BA, and our data emphasize the necessity for simultaneous evaluation of biliary BA excretion together with their intestinal processing by transporters and the gut microbiome. The interaction between iron and intestinal bacterial colonization requires further study. Finally, we further elaborate the mechanisms responsible for increased plasma cholesterol and bilirubin concentrations accompanying IO, which may serve as a potential therapeutic target.

Methods

Animals. Male Wistar rats (200–250 g) obtained from Velaz (Prague) were used for the experimentation. The rats were fed a standard diet under controlled environmental conditions: 12-h light-dark cycle; temperature 22 ± 1 °C with free access to food and water. The rats were randomly divided into two groups (n = 6). The control group (saline) was administrated i.p. with physiological saline (1 ml/kg) and the IO group was administrated i.p. with 8 doses of gleptoferron (iron-dextran heptonic acid complex, 100 mg/kg) every other day as described previously[18]. Excessive iron accumulation in this model induces a marked increase in hepcidin production, thus significant suppression of ferroportin 1-mediated iron intestinal absorption can be expected[19]. Administration of the 7th dose was followed by placement of the rats into metabolic cages where the stool was collected for 24 h. Collected stools were dried for 72 h at room temperature and BA were isolated as described previously[34] with slight modifications. One day after the final i.p. dose, the animals were fasted overnight and the next day they were anaesthetized with sodium pentobarbital (50 mg/kg, i.p.). The common bile duct (for bile collection) and carotid artery (for plasma collection) were cannulated. The bile was collected in pre-weighted tubes for 120 min and a blood sample was taken in the middle of this period. Thereafter, samples from portal vein were taken and the animals were sacrificed by exsanguination through carotid artery, and the livers and ilea were harvested and weighed. Tissue samples, plasma, bile, and extracted stool were snap frozen in liquid nitrogen and stored at

−80 °C for future analysis. All animals received humane care in accordance with the guidelines set by the institutional Animal Use and Care Committee of Charles University, Faculty of Medicine in Hradec Kralove, Czech Republic. The protocol of the experiment was approved by the same committee (No. 18293/2016-2).

Analytical methods. Plasma AST/ALT activities and concentrations of iron, ferritin, cholesterol and bilirubin were measured by routine laboratory methods on a Cobas Integra 800 (Roche Diagnostics, Mannheim, Germany). Biliary concentrations of phospholipids were determined by Phosphatidylcholine Assay kit (Sigma-Aldrich, St.Louis, USA). Concentrations of reduced (GSH) and oxidized (GSSG) glutathione were analysed separately using the validated HPLC method with fluorescence detection as described previously[35]. The liver concentration of cholesterol was assayed by the commercial Cholesterol Assay Kit (Cayman Chemical, Michigan, USA) and the concentration of cholesterol in bile was measured by the commercial kit Cholesterol (Erba Lachema, Brno, Czech Republic). BA concentrations in plasma, bile and stool were measured using the LC-MS method described previously[29].

Quantitative real time RT-PCR. Gene expression analysis by mRNA quantification was performed by reverse transcription-polymerase chain reaction (qRT-PCR) on a 7500 HT Fast Real-Time PCR System (Applied Biosystems, Foster City, USA) as previously detailed[29]. The primers used for analysis are specified in Supplementary Table S1. Glyceraldehyde 3-phosphate dehydrogenase (Gapdh) gene was used as a reference for normalizing the data (Applied Biosystems, Foster City, USA).

Western blot. The procedure was performed as reported previously[29]. Briefly, liver lysates were prepared by homogenization in an ice-cold buffer (25 mM TRIS.HCl, pH = 7.6, 0.1% w/w TRITON-X), containing 0.5 µg/ml benzamidine, aprotinine, leptine and 10µl/ml phosphate inhibitors (Thermo Scientific Prague, Czech Republic), and supernatant prepared by centrifugation of the lysate was separated using SDS-PAGE. Proteins were blotted to PVDF membranes, which were then blocked for 1h with 5% non-fat dry milk in Tris-buffered saline containing 0.05% Tween 20, exposed to antibodies and chemiluminescent reagent, followed by quantification of bands on X-ray films or directly on membranes (Fusion Solo S, Vilber, France). Antibodies are described in the Supplementary Table S2. Equal loading of proteins onto the gel was confirmed by immunodetection of Gapdh and β-actin.

Histology. The livers were collected immediately after death, fixed in 10% neutral buffered formalin, embedded in paraffin, and cut to 4–5 µm thick sections. These were stained with haematoxylin-eosin for assessment of liver morphological changes and with Prussian blue for the presence of iron. Sections were assessed by the same person using a BX-51 light microscope (Olympus) at x100 of original magnification. Ten visual fields were analysed per liver section from each animal.

Immunohistochemistry of Mrp2 and Bsep. Five slides from each animal from each group were taken for immunohistochemical analysis. Serial cross-sections (7 µm) were cut on a cryostat and placed on gelatine-coated slides. Before antigen detection, the slides were incubated with anti-avidin and anti-biotin solutions (Vector Laboratories, USA). Thereafter, the slides were incubated with primary antibodies and after that biotinylated goat anti-rabbit secondary (Jackson ImmunoResearch, USA) (diluted 1:100 in BSA) and ExtraAvidin red fluorochrome CY3 (Sigma Chemical, USA) were used (diluted 1:300 in BSA) for the detection of either Mrp2 or Bsep. For nuclear counterstaining the blue-fluorescent DAPI nucleic acid stain (Invitrogen, Czech Republic) was used. Staining with nonimmune isotype-matched immunoglobulins assessed the specificity of the immunostaining. Primary antibodies included the following: mouse monoclonal antibody anti-Mrp2 (dilution 1:20, 1 h at RT), purchased from Enzo Life Sciences (USA), and rabbit polyclonal antibody anti-Bsep (dilution 1:50, 1 h at RT), purchased from Thermo Scientific (USA). Photo documentation and image digitizing from the microscope were performed with the Olympus AX 70, with a digital VDS Vosskühler (GmbH, Germany) with Image Analysis Software NIS (Laboratory Imaging, Czech Republic). Canalicular localization of Mrp2 was verified in our previous studies[23,29] using the same antibodies by co-localization with another canalicular protein, Zo-1.

Statistical analysis. Data are presented as mean ± SD. Differences between the groups were assessed by a two-tailed *t*-test assuming unequal variance. Six animals per group were analysed. Differences were considered significant at *P*-value less than 0.05. All analyses were performed using GraphPad Prism 6.0 software (San Diego, USA).

References

1. Boyer, J. L. Bile formation and secretion. *Comprehensive Physiology* **3**, 1035–1078, https://doi.org/10.1002/cphy.c120027 (2013).
2. Vitek, L. & Haluzik, M. The role of bile acids in metabolic regulation. *J Endocrinol* **228**, R85–96, https://doi.org/10.1530/joe-15-0469 (2016).
3. Halilbasic, E., Fuchs, C., Traussnigg, S. & Trauner, M. Farnesoid X Receptor Agonists and Other Bile Acid Signaling Strategies for Treatment of Liver Disease. *Digestive diseases* **34**, 580–588, https://doi.org/10.1159/000445268 (2016).
4. Zuo, L., Zhou, T., Pannell, B. K., Ziegler, A. C. & Best, T. M. Biological and physiological role of reactive oxygen species–the good, the bad and the ugly. *Acta physiologica* **214**, 329–348, https://doi.org/10.1111/apha.12515 (2015).
5. Brunet, S. *et al.* Dietary iron overload and induced lipid peroxidation are associated with impaired plasma lipid transport and hepatic sterol metabolism in rats. *Hepatology* **29**, 1809–1817, https://doi.org/10.1002/hep.510290612 (1999).
6. Philippe, M. A., Ruddell, R. G. & Ramm, G. A. Role of iron in hepatic fibrosis: one piece in the puzzle. *World J Gastroenterol* **13**, 4746–4754 (2007).
7. Fleming, R. E. & Ponka, P. Iron overload in human disease. *N Engl J Med* **366**, 348–359, https://doi.org/10.1056/NEJMra1004967 (2012).

8. Batts, K. P. Iron overload syndromes and the liver. *Mod Pathol* **20**(Suppl 1), S31–39, https://doi.org/10.1038/modpathol.3800715 (2007).
9. Aigner, E., Weiss, G. & Datz, C. Dysregulation of iron and copper homeostasis in nonalcoholic fatty liver. *World Journal of Hepatology* **7**, 177–188, https://doi.org/10.4254/wjh.v7.i2.177 (2015).
10. Neuschwander-Tetri, B. A. *et al*. Farnesoid X nuclear receptor ligand obeticholic acid for non-cirrhotic, non-alcoholic steatohepatitis (FLINT): a multicentre, randomised, placebo-controlled trial. *Lancet* **385**, 956–965, https://doi.org/10.1016/s0140-6736(14)61933-4 (2015).
11. Liang, H. *et al*. Effect of iron on cholesterol 7alpha-hydroxylase expression in alcohol-induced hepatic steatosis in mice. *J Lipid Res* **58**, 1548–1560, https://doi.org/10.1194/jlr.M074534 (2017).
12. Coppin, H. *et al*. Gene expression profiling of Hfe-/- liver and duodenum in mouse strains with differing susceptibilities to iron loading: identification of transcriptional regulatory targets of Hfe and potential hemochromatosis modifiers. *Genome Biol* **8**, R221, https://doi.org/10.1186/gb-2007-8-10-r221 (2007).
13. Graham, R. M. *et al*. Hepatic iron loading in mice increases cholesterol biosynthesis. *Hepatology* **52**, 462–471, https://doi.org/10.1002/hep.23712 (2010).
14. Silva, M. *et al*. Iron dextran increases hepatic oxidative stress and alters expression of genes related to lipid metabolism contributing to hyperlipidaemia in murine model. *BioMed research international* **2015**, 272617, https://doi.org/10.1155/2015/272617 (2015).
15. Cunnane, S. C. & McAdoo, K. R. Iron intake influences essential fatty acid and lipid composition of rat plasma and erythrocytes. *J Nutr* **117**, 1514–1519 (1987).
16. Dabbagh, A. J., Mannion, T., Lynch, S. M. & Frei, B. The effect of iron overload on rat plasma and liver oxidant status *in vivo*. *Biochem J* **300**(Pt 3), 799–803 (1994).
17. Bristow-Craig, H. E., Strain, J. J. & Welch, R. W. Iron status, blood lipids and endogenous antioxidants in response to dietary iron levels in male and female rats. *International journal for vitamin and nutrition research. Internationale Zeitschrift fur Vitamin- und Ernahrungsforschung. Journal international de vitaminologie et de nutrition* **64**, 324–329 (1994).
18. Najafzadeh, H., Jalali, M. R., Morovvati, H. & Tanavati, F. Comparison of the prophylactic effect of silymarin and deferoxamine on iron overload-induced hepatotoxicity in rat. *Journal of medical toxicology: official journal of the American College of Medical Toxicology* **6**, 22–26, https://doi.org/10.1007/s13181-010-0030-9 (2010).
19. Gulec, S., Anderson, G. J. & Collins, J. F. Mechanistic and regulatory aspects of intestinal iron absorption. *American Journal of Physiology-Gastrointestinal and Liver Physiology* **307**, G397–G409, https://doi.org/10.1152/ajpgi.00348.2013 (2014).
20. Anderson, C. P., Shen, M., Eisenstein, R. S. & Leibold, E. A. Mammalian iron metabolism and its control by iron regulatory proteins. *Biochim Biophys Acta* **1823**, 1468–1483, https://doi.org/10.1016/j.bbamcr.2012.05.010 (2012).
21. Mehta, K. J. *et al*. Iron Enhances Hepatic Fibrogenesis and Activates Transforming Growth Factor-beta Signaling in Murine Hepatic Stellate Cells. *Am J Med Sci* **355**, 183–190, https://doi.org/10.1016/j.amjms.2017.08.012 (2018).
22. Zinchuk, V., Zinchuk, O. & Okada, T. Experimental LPS-induced cholestasis alters subcellular distribution and affects colocalization of Mrp2 and Bsep proteins: a quantitative colocalization study. *Microsc Res Tech* **67**, 65–70, https://doi.org/10.1002/jemt.20184 (2005).
23. Cermanova, J. *et al*. Boldine enhances bile production in rats via osmotic and farnesoid X receptor dependent mechanisms. *Toxicol Appl Pharmacol* **285**, 12–22, https://doi.org/10.1016/j.taap.2015.03.004 (2015).
24. Padda, R. S. *et al*. A high-fat diet modulates iron metabolism but does not promote liver fibrosis in hemochromatotic Hjv(−)/(−) mice. *Am J Physiol Gastrointest Liver Physiol* **308**, G251–261, https://doi.org/10.1152/ajpgi.00137.2014 (2015).
25. Dongiovanni, P., Fracanzani, A. L., Fargion, S. & Valenti, L. Iron in fatty liver and in the metabolic syndrome: a promising therapeutic target. *J Hepatol* **55**, 920–932, https://doi.org/10.1016/j.jhep.2011.05.008 (2011).
26. Horton, J. D., Goldstein, J. L. & Brown, M. S. SREBPs: activators of the complete program of cholesterol and fatty acid synthesis in the liver. *J Clin Invest* **109**, 1125–1131, https://doi.org/10.1172/JCI15593 (2002).
27. Seo, K. & Shin, S. M. Induction of Lipin1 by ROS-Dependent SREBP-2 Activation. *Toxicological research* **33**, 219–224, https://doi.org/10.5487/tr.2017.33.3.219 (2017).
28. Dongiovanni, P. *et al*. Statin use and non-alcoholic steatohepatitis in at risk individuals. *J Hepatol* **63**, 705–712, https://doi.org/10.1016/j.jhep.2015.05.006 (2015).
29. Prasnicka, A. *et al*. Iron depletion induces hepatic secretion of biliary lipids and glutathione in rats. *Biochim Biophys Acta*, https://doi.org/10.1016/j.bbalip.2017.09.003 (2017).
30. Geier, A., Wagner, M., Dietrich, C. G. & Trauner, M. Principles of hepatic organic anion transporter regulation during cholestasis, inflammation and liver regeneration. *Biochim Biophys Acta* **1773**, 283–308, https://doi.org/10.1016/j.bbamcr.2006.04.014 (2007).
31. Nishanth, R. P. *et al*. C-Phycocyanin inhibits MDR1 through reactive oxygen species and cyclooxygenase-2 mediated pathways in human hepatocellular carcinoma cell line. *Eur J Pharmacol* **649**, 74–83, https://doi.org/10.1016/j.ejphar.2010.09.011 (2010).
32. Madsen, D. C., Chang, L. & Wostmann, B. ω-Muricholate: a tertiary bile acid of the Wistar rat. *Proc. Indiana Acad. Sci* **84**, 416–420 (1975).
33. Eyssen, H. J., De Pauw, G. & Van Eldere, J. Formation of hyodeoxycholic acid from muricholic acid and hyocholic acid by an unidentified gram-positive rod termed HDCA-1 isolated from rat intestinal microflora. *Appl Environ Microbiol* **65**, 3158–3163 (1999).
34. Yu, C. *et al*. Elevated cholesterol metabolism and bile acid synthesis in mice lacking membrane tyrosine kinase receptor FGFR4. *The Journal of biological chemistry* **275**, 15482–15489 (2000).
35. Hirsova, P. *et al*. Cholestatic effect of epigallocatechin gallate in rats is mediated via decreased expression of Mrp2. *Toxicology* **303**, 9–15, https://doi.org/10.1016/j.tox.2012.10.018 (2013).

Acknowledgements

We gratefully acknowledge the skilful technical assistance of Jitka Hajkova. This study was supported by grants from the Grant Agency of Charles University Progres Q40/05, SVV 260397/2017, and GAUK 5562/18, and by the ERDF-Project PERSONMED No. CZ.02.1.01/0.0/0.0/16_048/0007441.

Author Contributions

A.P., L.V. and S.M. analysed the data, and wrote the manuscript; A.P., H.L., F.F.A., J.C., E.D., P.P. and S.M. performed the *in vivo* experiments and all molecular analyses; J.M. performed the histology analyses; M.H. and K.Z. performed the LC-MS analyses; P.N. performed immunohistochemistry analyses. All authors participated in the revision and approved the final form of the manuscript.

Additional Information

Supplementary information accompanies this paper at https://doi.org/10.1038/s41598-019-46150-7.

Competing Interests: The authors declare no competing interests.

Příloha 3

microorganisms

MDPI

Article

Eggerthella lenta DSM 2243 Alleviates Bile Acid Stress Response in *Clostridium ramosum* and *Anaerostipes caccae* by Transformation of Bile Acids

Kristian Jensen Pedersen [1,†], Sven-Bastiaan Haange [1,†], Kateřina Žížalová [2], Alina Viehof [3], Thomas Clavel [3], Martin Leničček [2], Beatrice Engelmann [1], Lukas Y. Wick [4], Frank G. Schaap [5,6], Nico Jehmlich [1], Ulrike Rolle-Kampczyk [1] and Martin von Bergen [1,7,8,*]

1 Helmholtz-Centre for Environmental Research—UFZ GmbH, Department of Molecular Systems Biology, 04318 Leipzig, Germany
2 Institute of Medical Biochemistry and Laboratory Diagnostics, First Faculty of Medicine and General University Hospital in Prague, Charles University, Kateřinská 32, 12108 Prague, Czech Republic
3 Functional Microbiome Research Group, Institute of Medical Microbiology, RWTH University Hospital, 52074 Aachen, Germany
4 Helmholtz-Centre for Environmental Research—UFZ GmbH, Department of Environmental Microbiology, 04318 Leipzig, Germany
5 Department of Surgery, NUTRIM School of Nutrition and Translational Research in Metabolism, Maastricht University, 6229 Maastricht, The Netherlands
6 Department of General, Visceral and Transplant Surgery, University Hospital Aachen, 52074 Aachen, Germany
7 German Centre for Integrative Biodiversity Research (iDiv) Halle-Jena-Leipzig, Puschstraße 4, 04103 Leipzig, Germany
8 Institute of Biochemistry, Faculty of Biosciences, Pharmacy and Psychology, University of Leipzig, 04103 Leipzig, Germany
* Correspondence: martin.vonbergen@ufz.de
† These authors contributed equally to this work.

check for updates

Citation: Pedersen, K.J.; Haange, S.-B.; Žížalová, K.; Viehof, A.; Clavel, T.; Leničček, M.; Engelmann, B.; Wick, L.Y.; Schaap, F.G.; Jehmlich, N.; et al. *Eggerthella lenta* DSM 2243 Alleviates Bile Acid Stress Response in *Clostridium ramosum* and *Anaerostipes caccae* by Transformation of Bile Acids. *Microorganisms* **2022**, *10*, 2025. https://doi.org/10.3390/microorganisms10102025

Academic Editor: Harsharn Gill

Received: 28 July 2022
Accepted: 11 October 2022
Published: 13 October 2022

Publisher's Note: MDPI stays neutral with regard to jurisdictional claims in published maps and institutional affiliations.

Abstract: Bile acids are crucial for the uptake of dietary lipids and can shape the gut-microbiome composition. This latter function is associated with the toxicity of bile acids and can be modulated by bile acid modifying bacteria such as *Eggerthella lenta*, but the molecular details of the interaction of bacteria depending on bile acid modifications are not well understood. In order to unravel the molecular response to bile acids and their metabolites, we cultivated eight strains from a human intestinal microbiome model alone and in co-culture with *Eggerthella lenta* in the presence of cholic acid (CA) and deoxycholic acid (DCA). We observed growth inhibition of particularly gram-positive strains such as *Clostridium ramosum* and the gram-variable Anaerostipes cacae by CA and DCA stress. *C. ramosum* was alleviated through co-culturing with *Eggerthella lenta*. We approached effects on the membrane by zeta potential and genotoxic and metabolic effects by (meta)proteomic and metabolomic analyses. Co-culturing with *Eggerthella lenta* decreased both CA and DCA by the formation of oxidized and epimerized bile acids. *Eggerthella lenta* also produces microbial bile salt conjugates in a co-cultured species-specific manner. This study highlights how the interaction with other bacteria can influence the functionality of bacteria.

Keywords: gut microbiome interaction; bile acids; eggerthella lenta; hydroysteroid dehydrogenase; metaproteomics; metabolomics

1. Introduction

Over the past decades, it has become increasingly evident how crucial the gut microbiota is in health and disease. The gut microbiome protects from pathogens [1] and plays a major role in the synthesis of vitamins [2], as well as in the digestion of complex food components [3]. The metabolites from these processes function not only as nutrients, but

also as signaling molecules that can mediate the communication between gut and host. Bile acids are of particular interest in cross-communication due to their widespread systemic effects [4–7] and their capabilities to directly modulate gut-microbiome composition [8–10]. Their systemic effects are due to their ability to bind to nuclear receptors such as Farnesoid X receptor (FXR) and transmembrane receptors such a G protein-coupled bile acid receptor 1(TGR-5) [4,11,12]. The direct effect of bile acids shaping the microbiome can, for instance, be seen in the development of the microbiome in infant animals [13] as well as in defining the response of the microbiome of patients to the alterations in the gut topology after bariatric surgery [14]. It was also shown in mice that if bile flow is obstructed, it resulted in bacterial overgrowth and mucosal injury in the small intestine, which could be reverted in mice still expressing the FXR receptor, but not in ones lacking [5]. Bile acids are amphiphilic molecules and their toxicity towards bacteria is related to their hydrophobicity, and it is known that increasing hydrophobicity leads to increased toxicity [15–18]. Bile acids are synthesized in the liver from cholesterol via two biochemical pathways, which in humans result in cholic acid (CA) and chenodeoxycholic acid (CDCA), collectively termed primary bile acids [19]. In the liver, they are conjugated with either glycine or taurine and stored in the gallbladder until they are released into the duodenum upon stimulation [20]. In the small intestine, they facilitate the solubilization of lipids and lipid-soluble vitamins, and as they travel through the small intestine approximately 95% are actively reabsorbed across the distal small intestinal wall, in a process termed enterohepatic circulation, which functions as a negative feedback loop that regulates their own biosynthesis [21]. The remaining 5 % enter the large intestine where they primarily undergo extensive chemical modifications by bacteria [22]. Once primary bile acids have been modified by bacteria they are referred to as secondary bile acids, where 7α-dehydroxylation of CA and CDCA results in the more hydrophobic deoxycholic acid (DCA) and lithocholic acid (LCA) respectively. Physiological concentrations and compositions vary greatly through the body and also depend on external factors such as diet [23]. Generally, total bile acid concentration in the colon is between 200–1000 μM where DCA is estimated to be between 10–200 μM [24–26]. Some of the chemical modification that bile acids will undergo, whilst passing through the gastro-intestinal tract are deconjugation, dehydroxylation, oxidation, epimerization and, most recently, reconjugation [26,27]. The most widespread bile acid modification is the ability to deconjugate bile acids from the amino acid moieties, via microbial bile salt hydrolases (BSH) [28]. Dehydroxylation is a multistep pathway executed by enzymes that are encoded in the bile acid inducible (bai) operon, which is not common in commensal bacteria [29]. Strains that possess the bai operon are members of the Clostridium cluster XIVa [30,31]. Another widespread enzymatic function is dehydrogenation (oxidation) via hydroxysteroid dehydrogenases (HSDHs). HSDHs catalyze oxidation of the hydroxyl groups at the C-3, C-7 and C-12 position of the steroid core of bile acids [32–34]. Oxidation of the hydroxyl groups is stereospecific, since there are both α and β HSDHs. Hence a sequential oxidation and reduction of an OH group can result in epimerization at a given position [35]. Oxidation of the hydroxyl groups is of particular importance due to both the disruption of the amphiphilic structure of bile acids, but also since it hinders the possibility for dehydroxylation to occur [31]. *Eggerthella lenta* (*E. lenta*) (DSM 2243) is known to be a potent bile acid modifier expressing a 3, 7 and 12α HSDH [25,32], making it an interesting strain to co-cultivate with, to understand the significance of how these bile acid forms influence microbe–microbe interactions. It has recently been discovered that the gut microbiome is also capable of performing reconjugations of bile acids, forming bonds with amino acids other than glycine and taurine, which was a previously unknown mechanism. Initially, phenylalanocholic acid, tyrosocholic acid and leucocholic acid were discovered, with more than 50 different bile acid modifications currently identified in cultures of human fecal bacteria [26,36–38]. Structural differences in the cell envelopes of gram-negative and gram-positive strains influence how sensitive the bacteria are towards bile acids. Due to the differences in charge as well as gram-negatives possessing two cellular membranes, gram-positive bacteria are more sensitive towards bile acids [21,39,40]. Hence, with the

number of secondary bile acids increasing and novel bile acid modifying mechanisms being discovered, it is of growing importance to know specifically which strains are capable of performing such modifications, and also what the consequence of such modifications are both within and between bacteria. In this study, we aim to investigate what the molecular responses to bile acid stress are, and what the significance is of being co-cultivated with a known bile acid modifier using metabolomics and proteomics. In order to gain such insights, we cultivated strains from the simplified intestinal human microbiota extended (SIHUMIx) [41] and co-cultured the individual strains with *E. lenta*.

2. Materials and Methods

2.1. Bacterial Strains

The bacterial strains chosen for this study are from SIHUMIx, a model system of for the human intestinal microbiota [41], consisting of eight bacterial species *Anaerostipes caccae* (DSMZ 14662), *Bacteroides thetaiotaomicron* (DSMZ 2079), *Bifidobacterium longum* (NCC 2705), *Blautia producta* (DSMZ 2950), *Clostridium butyricum* (DSMZ 10702), *Clostridium ramosum* (DSMZ 1402), *Escherichia coli K-12* (MG1655), *Lactobacillus plantarum* (DSMZ 20174). The strain used for co-culturing was *Eggerthella lenta* (DSMZ 2243). Strains were cultivated as single strains in Yeast-Hemin-Brain-Heart-Infusion (BHI) medium under anaerobic conditions at 37 °C and 175 rpm shaking, maximum 72 h before bile acid stress assays were conducted. See Table S1 for BHI composition.

2.2. Bile Acid Stress Assay

At a maximum of 72 h before the assay(s) were conducted, strains were thawed individually in BHI media as described above. Shortly before inoculation, the type of anaerobic culture tubes (hungates) were supplemented with 600 µM CA (Sodium cholate hydrate, Sigma Aldrich, St. Louis, MO, USA) dissolved in H_2O or 200 µM DCA (Deoxycholic acid, Merck, Kenilworth, NJ, USA) dissolved in 70% EtOH and gassed with pure N_2. Strains were inoculated into the hungates in replicates of 6, with a start OD600 = 0.15 if grown as a single culture or 0.075 of each strain when co-cultured. Cultures were measured hourly on a Nanocolor® UV/VIS II, Macherey Nagel at 600 nm. After 6 h of growth, 2 mL bacteria cell suspension was centrifuged (3200× *g*; 10 min; 4 °C) supernatant and pellet were separated and both immediately frozen at −80 °C.

2.3. Bile Acid Measurements

For the bile acid determination, the Bile acid Kit from Biocrates (Innsbruck, Austria) was used. The exact description of the procedure can be found in [42]. All solvents and chemicals were of UPLC/MS grade. 10 µL of standards and internal standards mixture were pipetted onto the filter spots suspended in the wells of the 96-well filter plate. The filter plate was fixed on the top of a deep-well serving as a receiving plate for the extract (a combi-plate structure). In addition, quality controls were distributed on the plate. On the one hand, one QC each was measured with low, medium and high concentrations of the calibration range and additionally three further medium QC samples were distributed over the plate. A 7-point calibration curve (concentration range: 10 to 75,000 nmol/L bile acid specific) was used for calibration. Samples of 10 µL were pipetted on the spots of the kit plate, followed by nitrogen drying. Then, 100 µL methanol was added to the wells, and the combi-plate was shaken for 20 min. The combi-plate was centrifuged to elute the methanol extract into the lower receiving deep-well plate, which was then detached from the upper filter plate. After adding 60 µL Milli-Q water to the extracts, the samples were analyzed. 5 µL of each sample were injected using Acquity UPLC System (Waters) (UHPLC Column from Biocrates P.-No 91220052120868). Initial solvent was 65% A (solvent A: 100% H_2O, containing 10 mmol/L ammonium acetate), solvent B: 100% acetonitrile containing 10 mmol/L ammonium acetate and 0.1% formic acid (FA) at a flow rate of 0.5 mL/min at 50 °C. Gradient elution was performed using a Q-Trap 5500 mass spectrometer (Sciex). Mass spectrometric detection was employed with electrospray ionization in negative ion

mode (IS—4500 eV). Individual bile salts were monitored in MRM windows. Data was processed using Analyst 1.7.1. All peaks were visually inspected for correct integration including the internal standards using the quantification software from Analyst. AUC values were corrected for recovery of the assigned internal standard. Quadratic regression was used to calculate concentrations from standard curves. Afterwards, a further quality control was carried out using the Met IDQ software (version Oxygen) provided by the Biocrates company.

2.4. Zeta Potential Assay and Measurements

Strains were inoculated into hungates containing 10 mL BHI (pH = 7.01) in replicates of 3, with a start OD_{600} = 0.1 either with or without the bile acids already in the media. Once strains reached an OD600 = 1 they were centrifuged (970 g, 20 °C, 10 min) in the hungates, hereafter the supernatant was removed. The remaining pellet was washed with 10 mM KNO_3 (pH = 7), centrifuged as described before and washed again. After washing, pellets were resuspended in 500 µL of 10 mM KNO_3 and from this solution 50 µL were transferred into 10 mL of 10 mM KNO_3 and vortexed well. From this, 1 mL was used to fill up a capillary cell (DTS1070, Malvern Panalytical Ltd.) and measured at room temperature on the Zetasizer Ultra (Malvern Panalytical Ltd.) equipped with a He-Ne (633 nm) laser. The obtained data were analyzed with the ZS XPLORER (version 2.3.1.4) and then extracted into GraphPad Prism (version 9.4.0 for Windows, GraphPad Software, San Diego, California USA, www.graphpad.com.) Cell-free BHI controls supplemented with CA or DCA were also measured, but here ZP was = 0 (See Supplementary data). Cell cultures grown without bile acids were measured and used to calculate the ΔZP to either CA or DCA cultures.

2.5. Preparation of Proteomic Samples

Subsequently, 2 mL bacterial pellets were harvested at the end of the 6 h bile acid stress assay and resuspended in $CH_3OH/H_2O/CHCL_3$ (2:1:1, v:v:v). Following resuspension, samples were incubated on ice for 10 min and were then sonicated and centrifuged (1700× *g*; 10 min; 4 °C). Samples were then dried in a speed vac and resuspended in UT buffer (8 M Urea; 2 M thiourea). Protein concentration was determined on a NanoDrop 2000c (Thermo Scientific, Rockford, IL, USA) 4 µg of protein in UT-solution was filled with up to 20 µL with 20 mM ammonium bicarbonate followed by addition of 2 µL of 25 mM dithiothreitol solution for disulfide reduction and the samples were incubated via Thermoshaker (60 °C; 1 h; 1400 rpm). This was followed by alkylation, by adding 14 µL of 20 mM ammonium bicarbonate and 4 µL of 100 mM 2-iodoacetamide and incubation at 37 °C for 30 min at 1400 rpm. Overnight enzymatic digestion was performed with trypsin (Promega, Madison, WI, USA) at 37 °C. Extracted peptides were purified by SOLAµ (Thermo Scientific, Waltham, MA, USA) as per the manufacturer's recommendation. After evaporation peptides were resuspended in 20 µL 0.1% FA.

2.6. Proteomic Measurements

For each LC−MS run, 1 µg of peptides was injected into a Nano-HPLC (UltiMate3000, Dionex, Thermo Fisher Scientific, Waltham, MA, USA). Peptides were trapped for 3 min on a C18-reverse phase trapping column (Acclaim PepMap 100, 75 µm × 2 cm, particle size 3 µM, nanoViper, Thermo Fisher Scientific), followed by separation on a C_{18}-reverse phase analytical column (Acclaim PepMap100, 75 µm × 25 cm, particle size 3 µM, nanoViper, Thermo Fisher Scientific). A two-step gradient was used with A: 0.01% FA in H_2O and B: 80% ACN in H_2O and 0.01% FA in mobile phases. The first step of the gradient was 90 min, where B went from 4% to 30%, then 30 min where B went from 30% to 55%. This was followed by 30 min where B went from 55% back to 4%, with a flow rate of 300 nL/min and a column temperature of 35 °C. The eluted peptides were ionized by a nano ion source (Advion Triversa Nanomate, Ithaca, NY, USA) and detected via a Q Exactive HF-MS (Thermo Fisher Scientific) with the following settings: Scan range 150–2000 m/z, MS resolution 120,000, MS automatic gain control (AGC) target 3,000,000 ions, maximum

injection time for MS 80 ms, intensity threshold for MS/MS of 17,000 ions, dynamic exclusion 30 s, TopN = 20, isolation window 1.6 m/z, MS/MS resolution 15,000, MS/MS AGC target 50,000 ions, maximum injection time for MS/MS 120 ms. Mass spectrometric data processing was performed using Proteome Discoverer (v.2.5, Thermo Fischer Scientific, Waltham, MA, USA) with SequestHT search engine. The search settings were set to trypsin (Full), or Asp-N (Full), max. missed cleavage sites 2, precursor mass tolerance 10 ppm, and fragment mass tolerance 0.05 Da. Carbamidomethylation of cysteines was specified as a fixed modification. False discovery rates (FDR) were determined using Percolator. The searches against SequestHT were undertaken with a constructed proteome database containing the reference proteomes downloaded from Uniprot (www.uniprot.org, accessed on 10 Octorber 2022). Data from the searches were further processed as previously described [14]. Protein intensities were converted to relative abundances by dividing the intensity of the protein with the summed intensities of all proteins from the same species detected in the sample. Protein functions and pathway assignment were undertaken using Ghostkoala webapplication from KEGG [43]. Only pathways containing minimum five proteins and a minimum total coverage of 10% were selected for further analysis.

2.7. Untargeted Metabolomics Measurement

Prior to analysis, supernatants from the bile acid stress assay were mixed with five volumes of MeOH:ACN:H_2O in a 2:3:1 (v:v:v) ratio, sonicated for 5 min and centrifuged. 550 µL supernatant was then transferred and evaporated, before being resuspended in 100 µL 0.1% FA and 1% ACN in water. Samples measured in positive and negative ionization mode were further diluted 1:20 and 1:10, respectively. For measurement, 2 or 5 µL (positive and negative ionization, resp.) of each extract was injected onto a HPLC system coupled online with a 6546 UHD Accurate-Mass Q-TOF (Agilent Technologies). Metabolites were separated with an Agilent Zorbax Eclipse Plus C18 column (2.1 × 100 mm, 1.8 µm) equipped with a related pre-column (2.1 × 50 mm, 1.8 µm). The autosampler was kept at 5 °C and column oven was set to 45 °C. Separation was achieved using a binary solvent system of A (0.1% FA in water) and B (0.1% FA in ACN). The gradient was as follows: 0–5.5 min: 1% B; 5–20 min: 1–100% B; 20–22 min: 100% B; 22–22.5: 100–1% B; 22.5–25 min: 1% B. Metabolites were eluted at a constant flow rate of 0.3 mL/min. Eluted compounds were measured with the QTOF operated in centroid mode. Full scan data was generated with a scan range of 50–1000 m/z in positive and negative ionization mode. Out of the survey scan, the two most abundant precursor ions with charge state = 1 were subjected to fragmentation. The dynamic exclusion time after two acquired spectra was set to 0.1 min. Obtained spectral data (.d files) were imported into Progenesis QI software (Non-Linear Dynamics). Different ionization modes and microbial strains were analyzed separately. The adduct ions involved [M + H], [M + H − H_2O] and [M + H + Na] for positive mode and [M − H], [M − H_2O − H] and [M + FA − H] for negative mode. In a generic workflow, chromatogram were aligned using an automatically chosen reference chromatogram from the dataset. The following software-guided, peak-picking tool resulted in a data matrix, including the retention time, mass-to-charge ratio and corresponding normalized peak area. The subsequent automated database search based on a ChemSpider plug-in was used as identification method with *E. coli* metabolome database, fecal metabolome database and KEGG as resources. After exporting the results regarding compound measurement and putative identifications for all measured compounds, data was processed, as previously described [14].

2.8. Measurements of Keto and Iso Forms of Bile Acids/MSBCs

Bile acids and their oxidized forms were measured as previously described [44]. The data is semiquantitative since there were no standards available for all the different modifications at the time. Hence, the data is given as a percentage compared to the peak area of the parent bile acid. Furthermore, this lack of standards also refrains from distinguishing between the different keto and iso forms; hence, CA isoforms will be referred to as isoCA 1–3, and the single keto forms as monoketoCA 1–3. Likewise, keto forms of

DCA will be referred to as monoketoDCA 1–3. For measurement of microbial bile salt conjugates (MBSC)s, 50 µL of the medium was mixed with 10 µL of internal standard (d4GCDCA), deproteinized by three volumes of 2-propanol/acetonitrile (1:2), vortexed, and centrifuged at 13,000 g for 15 min at room temperature. The supernatant was dried at 65 °C under nitrogen, dissolved in 50 µL of 50% methanol and analyzed. Gradient for MBSC assay was slightly modified (methanol concentrations were as follows: 0–1 min 50%; 1.0–10.0 min 95 %; 10–14 min 95 %; 14–18 min 50%). Following in-house prepared standards were used: Leu-CDCA, Leu-CA, Phe-CDCA, Phe-CA, L-Tyr-CDCA, D-Tyr-CDCA, L-Tyr-CA, D-Tyr-CA, 3,7-diketo CA, 3,12-diketo DCA, 3,7,12-triketo CA. For qualitative use, standards of 3-ketoBA and 7-ketoBA were prepared from individual BA using either 3α-hydroxysteroid dehydrogenase (Reagent B: Bile acids kit 450-A, Trinity Biotech (Wicklow, Ireland) or 7α-hydroxysteroid dehydrogenase (in-house prepared recombinant HdhA from *E. coli* GC-10). CDCA conjugates (with Leucine, Phenylalanine and Tyrosine) were used to tune mass spectrometer parameters for detection of respective DCA derivatives. Media blanks containing either CA or DCA were averaged and subtracted from their respective categories within each strain.

2.9. Omics-Data Statistical Analysis

The statistics for proteomics and untargeted metabolomics were as previously described [14]. Principal component analyses (PCA) were conducted using the VEGAN package [45]. For single variables, Student's *t* test were preformed and where appropriate (number of tests > 20), *p*-values were corrected for multi-testing by the Benjamini–Hochberg method [46], and all other figures were constructed using the R package ggplots2 [47].

3. Results

3.1. Growth in the Presence of Bile Acids in Single Species Culture and Co-Cultures with E. Lenta

Growth curves from the bile acid stress experiments are displayed in Figure 1; the ranking is organized according to increased inhibition of growth caused by DCA. Amounts of 600 µM of CA and 200 µM DCA was selected since these are physiologically relevant concentrations encountered in the colon [19,24,48] and previous experiments suggested these concentrations to be fitting (Supplementary Figure S1). For growth curves of CA stress, see Supplementary Figure S2 and for growth data please, see Supplementary data.

When cultures were stressed with CA, there is no inhibition of growth in any strain; in the case of *E. lenta*, it even suggests that it grows slightly better. There are also no clear effects of co-culturing under CA stress, other than a slightly elevated final OD. When considering DCA stress, again *E. lenta* seems to feature an increased growth, whereas *A. caccae*, *B. longum*, *B. producta*, *C. butyricum* and *C. ramosum* are significantly inhibited. In the cases of *B. longum*, *B. producta*, *C. buturicum* and *C. ramosum* co-culturing seems to alleviate stress from DCA. These results suggest that the presence of *E. lenta* alleviates the bile acid toxicity, in particular for gram-positive strains, such as *C. ramosum*. For further analysis, *E. coli*, *A. caccae* and *C. ramosum* were selected as they showed a low, middle and pronounced stress response to DCA and co-culture. Furthermore, bile stress response in bacteria strongly depends on their type of membrane, where *E. coli* is gram- negative, *A. caccae* is gram-variable [49] and *C. ramosum* is gram-positive.

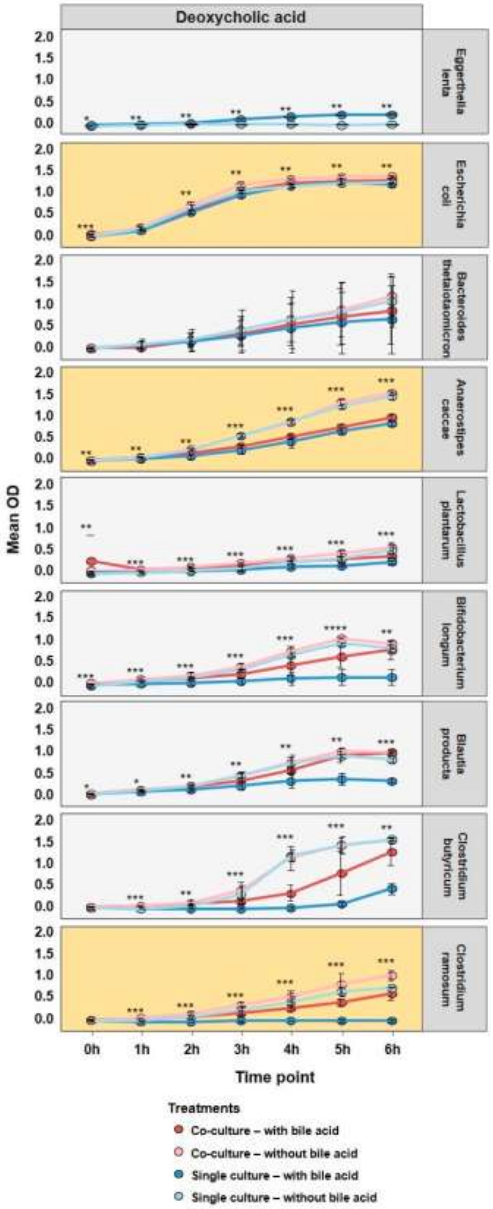

Figure 1. Growth of SIHUMIx species in single and co-culture with *E. lenta* with treatment 200 µM DCA. For each experiment, six replicates were analyzed and the line represents the mean. Strains are ranked according to increasing inhibition of growth when stressed with DCA. Error bars are standard deviations. Statistical significance was determined using ANOVA analysis, * $p < 0.05$, ** $p < 0.01$, *** $p < 0.005$, **** $p < 0.001$.

3.2. Concentrations of CA and DCA in Single Species Culture and Co-Cultures with E. lenta

In order to verify the concentrations of CA and DCA at the end of bile acid stress assays, supernatants from these cultures were measured and concentrations determined.

As seen in Figure 2, all single cultures are capable of transforming CA to a slight extent, but this significantly increases when co-cultured with *E. lenta*. On average single cultures of *E. coli* and *C. ramosum* the concentration decreased by 90.8 ± 43.3 µM and 65 ± 30.9 µM respectively, whereas co-cultures decreased concentrations by 281.2 ± 22.8 µM and 202 ± 22.9 µM. In the case of *E. coli*, the co-culture decreases the concentration more than *E. lenta* on its own. In the case of DCA the only single culture that could significantly decrease concentration was *E. coli* that on average decreased it by 20.3 ± 3.8 µM. In all other cases co-culturing significantly, decreased concentrations compared to their respective single culture, with an average of 61.5 ± 7.2 µM for *E. coli* co-cultures, 54.5 ± 7.7 µM for *A. caccae* co-cultures, and 64.7 ± 16.1 µM for *C. ramosum* co-cultures. Interestingly, single cultures of *E. lenta* outcompeted all co-cultures in decreasing DCA concentration, with an average decrease of 157.7 ± 5.4 µM.

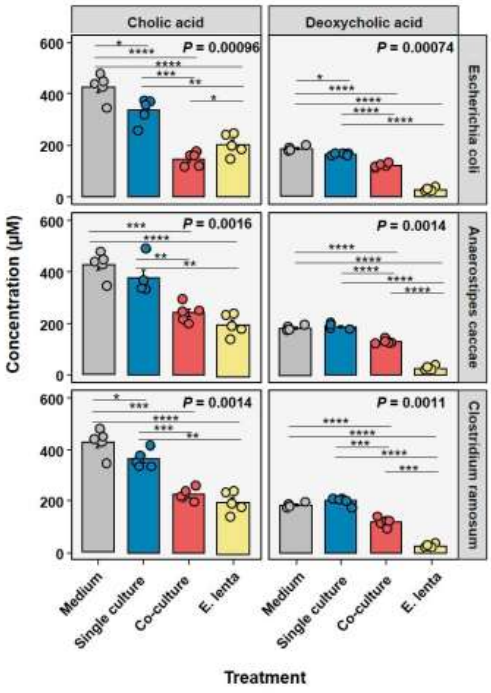

Figure 2. Determination of bile acid concentrations in single and co-culture after 6 h of incubation. For every sample, five replicates were measured and the bars represent the mean value. Group statistics were calculated by ANOVA with post-hoc pairwise Students *t*-test. (* $p < 0.05$, ** $p < 0.01$, *** $p < 0.001$ and **** $p < 0.0001$).

With the indication that bile acid concentrations decrease in particular in the presence of *E. lenta*, and the alleviation of growth inhibition, we investigated the membrane integrity. The remaining bile acids covered in the biocrates kit, can be seen in Supplementary Figure S3.

3.3. Assessment of Membrane Integrity by Zeta-Potential of E. coli, A. caccae, and C. ramosum in Single Species Culture and Co-Cultures with E. lenta

Zeta potential (ZP) measurements were performed to approach the effects of bile acids on the membrane. ZP is an electrochemical property that represents the potential at the shear plan of an electrical double layer encompassing a cell in an ionic solution. It provides critical information about cell-surface characteristics [50] and can reflect the physiological status of cells after, e.g., exposure to chemicals and nanoparticles [51,52]. Hence, ZP is being more frequently used to approach cell membrane integrity [53,54]. ZP values can be seen in Supplementary data and examples of full chromatograms of the ZP measurements can be seen in Supplementary Figure S4.

The change in ZP compared to their respective blanks of bacterial cultures stressed with CA or DCA can be seen in Figure 3. In this study, the average ZP for untreated cultures were found to be −51 (SD 0.81 +/−) and −54 (SD 01.14 +/−) mV for *E. coli* single and co-culture, −32 (SD 0.93 +/−) and −31 (SD 0.04 +/−) mV for *A. caccae* single and co-culture and −19 (SD 0.73 +/−) and −20 (SD 1.27 +/−) for *C. ramosum* single and co-culture (See Supplementary data). It can be observed that the gram-negative strain *E. coli* has the most negative ZP, the ZP of *A. caccae* the gram-variable is slightly less negative than *E. coli* and that the gram-positive strain *C. ramosum* has the least negative ZP. This is expected due to gram-negative bacteria possess the negatively charged LPS layer. As evident, neither bile acid nor co-culturing have any significant effect on either *E. coli* or *A. caccae.* When the single culture of *C. ramosum* is observed, it suggests that CA does not affect the ZP, whereas DCA on average decreases the ZP by −26 mV. Co-culturing reverts this decrease of ZP seen from single cultures to levels comparable with the blank.

Hence, *A. caccae* and *E. coli* show no significant changes in ZP from either bile acid, whereas *C. ramosum* again shows a clear protective effect when co-cultured. These results support the finding from the growth experiments that the presence of *E. lenta* alleviates bile acid toxicity for gram-positive bacteria in particular, and that *E. coli* and *A. caccae* seems unaffected on their membrane. This led us to conduct deeper functional investigations of the selected strains.

3.4. Proteomics Reveals Specific Responses to DCA Depending on Membrane Charecteristics and the Presence of E. lenta

The growth curves indicated that gram-positive strains are more susceptible to the effects of DCA than gram-negative species. Secondly, this growth inhibition can be alleviated in the presence of *E. lenta.* With respect to growth, there is only a slight effect detectable in the gram-variable *A. caccae*. After estimating the extent of membrane-associated effects by assessing the ZP, we wondered how the selected strains remodeled their structure and metabolism when stressed with CA and DCA and, therefore, analyzed the effects of co-culturing by (meta)proteomics (Figures 4 and 5). Pathways depicted on Figures 4 and 5 represent fold changes within the represented bacterium, where the direction of the change is color-coded, with red indicating an increase, blue indicating a decrease in the fold change in the co-culture. Pellets from the end of the bile acid stress assays were analyzed. The proteomic analysis yielded only very few, significantly altered, affected pathways in *E. coli* due to co-culturing, consistent with no effect on either growth or ZP. For *C. ramosum*, we detected 16 significantly altered pathways (Figure 4) and 55 for *A. caccae* (Figure 5). Only pathways containing a minimum of five proteins and a minimum total coverage of 10% were selected for further analysis. For relative species abundance and PCAs of proteomic data, please see Supplementary Figures S5 and S6.

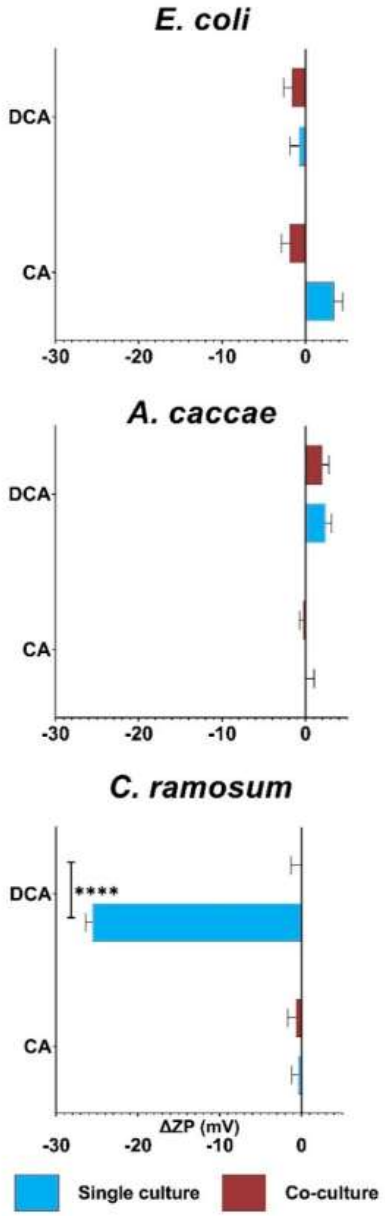

Figure 3. Relative change in zeta potential of cells in log phase exposed to bile acids. The change in ZP is compared to their respective blanks and is shown in mV. For all analyses, three replicates were analyzed and bars represent the mean value. Samples were harvested when OD_{600} = 1.0 Errors bars are standard deviations. Statistical significance was determined using a Student's *t*-test, **** $p < 0.001$.

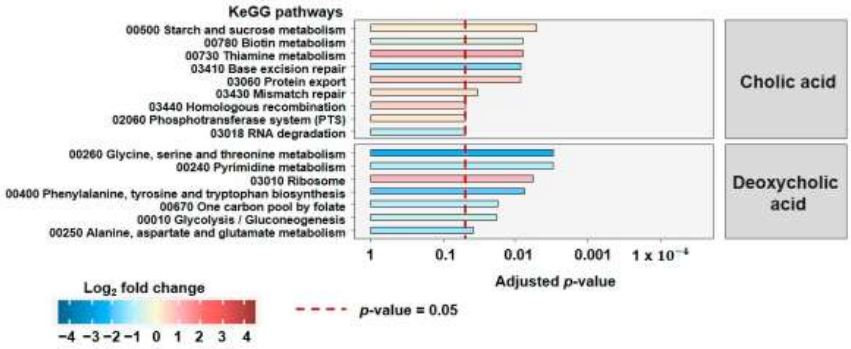

Figure 4. Molecular response of *C. ramosum* towards CA and DCA in co-culture with *E. lenta* vs. single culture. Depicted are the significantly altered KEGG metabolic pathways based on the relative abundance of proteins detected. The proteins stem from the bacterial pellet harvested from the end of the bile acid stress assays. The direction of the change is color-coded, red indicates an increase, blue a decrease in the fold change in the co-culture.

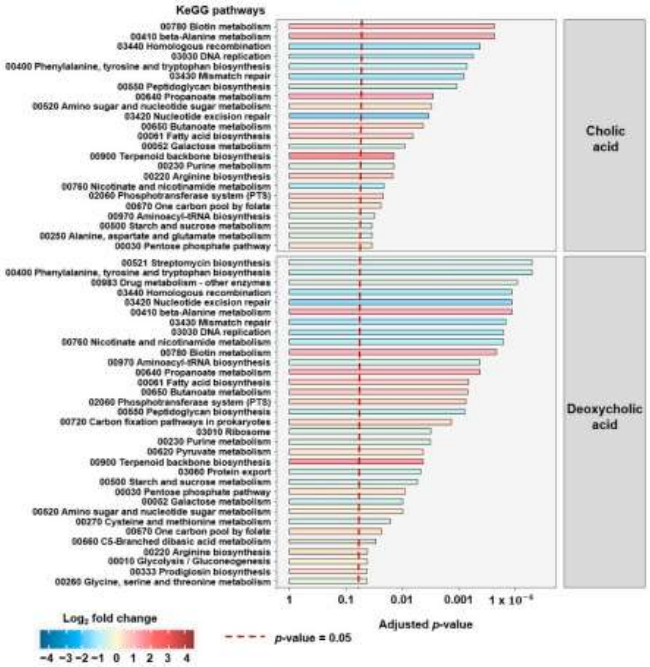

Figure 5. Molecular response of *A. caccae* towards CA and DCA in co-culture with *E. lenta* vs. single culture. Depicted are the significantly altered KEGG metabolic pathways based on the relative abundance of proteins detected. The proteins stem from the bacterial pellet harvested form the end of the bile acid stress assays. The direction of the change is color-coded, red indicates an increase, blue a decrease in the fold change in the co-culture.

Although there is a clear increase in growth in the presence of *E. lenta*, only a limited number of pathways are changed significantly in *C. ramosum*. For DCA the pathways of "glycine, serine and threonine metabolism", "phenylalanine, tyrosine and tryptophan metabolism", and "alanine, aspartate and glutamate metabolism" are downregulated in the co-culture. The same is true for the pathway of "Glycolysis" being down-regulated in the co-culture under DCA stress. The increased growth of *C. ramosum* in co-culture is reflected in the increase in the "ribosome pathway".

For CA, the decrease in the pathways "Base excision repair" and "RNA degradation" points to the alleviation of the genotoxic effects of bile acids in co-culture. The effects on the other pathways, except for induction of "thiamine metabolism" were not overly strong, and this is in line with the non-significant changes with respect to growth.

Interestingly, we found more affected pathways *A. caccae* (Figure 5), which showed a DCA-dependent but not a co-culture dependent effect in growth.

For both DCA and CA, we found a strong decrease for pathways such as "mismatch repair", "homologous recombination" and "nucleotide excision repair" that are linked to genotoxic effects that might be alleviated in the presence of *E. lenta*.

Even though we see only slight effects on growth, many pathways were elevated that are linked to increased growth such as carbon fixation, propanoate metabolism, butanoate metabolism, and fatty acid biosynthesis. In DCA, more pathways related to the synthesis of amino acids are affected. These results indicate that mechanisms related to growth are increased under these conditions, in combination with a decreased need to produce amino acids. The effect of co-culture, in the presence of both CA and DCA is especially strong on upregulated "Terpenoid backbone synthesis".

3.5. Metabolomics Reveals Metabolites Related to Altered Pathways Detected in Proteomics

The proteomic response to bile acid stress was validated by untargeted metabolic analyses of the supernatant from the end of the bile acid stress assays, in order to detect metabolites that potentially play a role in the interaction between the co-cultured species. The effects of CA and DCA in single and co-culture with *E. lenta* are depicted in Figure 6. For PCAs of these measurements, please see Supplementary Figure S7.

Similar to the proteomic results, the changes are least prominent in *E. coli*, more abundant in *C. ramosum* and strongest in *A. caccae*. Thus, we focus here on the effects in *C. ramosum* and *A. caccae*. A common feature for all co-cultures is the decrease of a metabolite, which might be L-Arginine (metabolite no 1). This could be related to an increased uptake by *E. lenta*, since it was reported that arginine leads to increased growth in *E. lenta* [55]. Another consistently decreased metabolite in co-cultures is metabolite no. 2, which we could putatively identify as 12α-Hydroxyamoorstatin, which is a rare metabolite but linked to the bile acid structure and thus is potentially indicating to an increased transformation of bile acids by *E. lenta*. In contrast, there is also one metabolite that is consistently increased in co-culture, which could be identified as L-ornithine (metabolite no. 3). L-Ornithine is involved in the synthesis of arginine and an increased uptake of arginine might result in a decrease of ornithine produced and secreted by *E. lenta*. Interestingly, we detected metabolites significantly altered in abundance between the co-culturing with *E. lenta* and single culturing for *A. caccae* and *C. ramosum*, which might be nucleosides. In both mentioned species, for DCA and for CA, we observed a significant increase in the co-culture of metabolite no. 6, which was putatively identify as inosine. Inosine is a degradation product of adenosine. We also observed a decrease in metabolite no. 7, which we putatively identified as adenine, a further degradation product of adenosine, in the co-culture of *C. ramosum* with DCA.

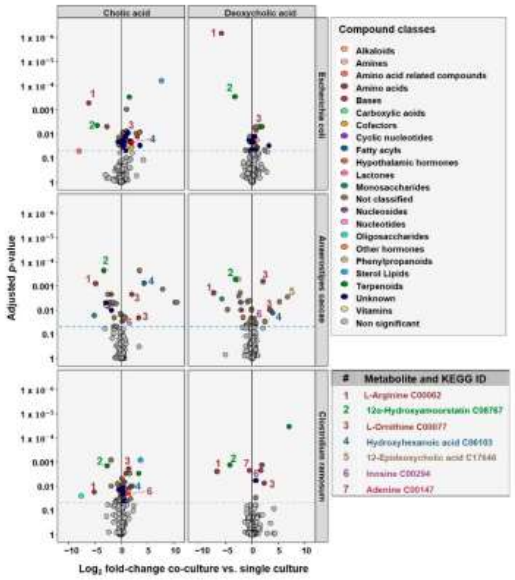

Figure 6. Change in relative abundance of metabolites detected in the medium as calculated by co-culture vs. single culture. Volcano Plot of metabolite Log_2 fold-change in metabolite abundances plotted against Benjamini–Hochberg adjusted *p*-values. Measurements are from the medium supernatants of cultures grown in the bile acid stress assays. Significant metabolites are color coded by compound class. Dashed blue line indicates $p = 0.05$.

In *A. caccae* metabolite no. 4, which was suggested to be 6-hydroxyhexanoic acid, was consistently elevated in co-cultures both in the presence of CA and DCA. 6-hydroxyhexanoic acid is part of the bacterial degradation pathway of bile acids [56]. Furthermore, metabolite no. 5, which is suspected to be 12-epideoxycholic acid, was seen to be elevated in *A. caccae* during co-culturing and DCA stress. 12-epideoxycholic acid is an epimer of the C-12 OH group of DCA.

3.6. Detection of Oxidized and Eperimized Bile Acids in Single Culture vs. Co-Culture

Based on the finding of elevated levels of 12-epideoxycholic in the supernatant of co-culture and the extended repertoire of bile acid modifying enzymes in *E. lenta* [25,32], we tested more comprehensively for bile acid oxidation and epimerization. Figure 7 shows semiquantitative abundances of the iso- (i.e., 3β epimers) and oxo (i.e., keto) forms of CA and DCA from the bile acid stress experiments depicted in Figure 1. The data is semiquantitative since there were no standards available at the time for all the different modifications; hence, the data is given as a%, compared to the peak of its original bile acid. For our definition of nomenclature, see Method section "2.8 Measurements of oxo and iso forms of bile acids/MSBCs". Keto/iso figure for all 8 SIHUMIx strains can be seen in Supplementary Figure S8.

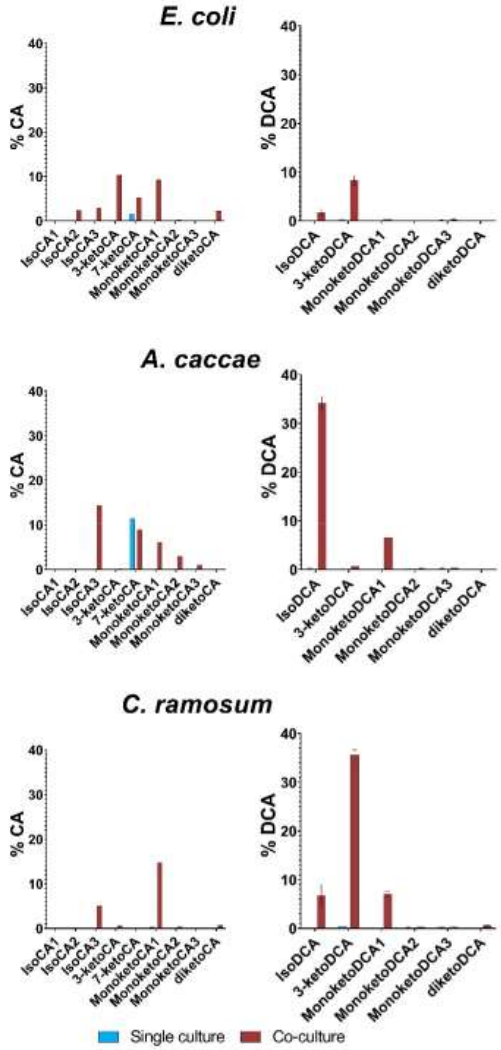

Figure 7. Epimerization and oxidization of CA and DCA in single and co-cultures. The bars represent the mean of three biological replicates and the abundances are ratios compared to the peaks of the original added bile acids due to lack of standard for the different iso and keto forms. Blue is single culture and red is co-culture.

When single cultures of *E. coli* are exposed to CA stress, only one modification is observed, namely 7-ketoCA. This is line with the fact that *E. coli* expresses a 7α-HSDH (WP_000483353.1, [57]). The corresponding co-culture shows a different pattern with signals for isoCA-2 and 3 as well as monoketoCA 1. 3-ketoCA and 7-ketoCA are also observed. Likewise, *A. caccae* single culture also only shows formation of 7-ketoCA, and indeed a 7α-HSDH homologue (WP_054335312.1, E value = 3×10^{-37}, identity 32.74%) was found by homology searching using NCBI's blastp tool against the 7α-HSDH described previously in *E. coli* (See Supplementary Table S2 for HSDH enzyme accession numbers). Co-culturing

again results in formation of isoCA 3 and monoketoCA 1–3. Single cultures of *C. ramosum* do not seem to form any iso or keto form of CA. Co-cultures have a different pattern in this case, with isoCA 3 and monoketoCA 1 being the dominant forms. Cultures in the presence of DCA show a more unambiguous trend, since no single culture produces any epimerized or oxidized form with an abundance exceeding 1%. For *E. coli* and *C. ramosum* co-cultures, 3-ketoDCA is readably observed, whereas *A. caccae* co-cultures seem more prone to form isoDCA. It is tempting to speculate that this iso form corresponds to 12-epideoxycholic acid identified in our metabolomic screen, although it cannot be ruled out that it concerns 3β-DCA. The latter would be in line with higher formation of especially 3-ketoDCA helps to explain the reduced toxicity as it potentially reaches 35% of DCA converted. This finding is accordance with the expression of 3α, 3β, 7α, and 12α HSDHs by *E. lenta* [25,32,58]. A novel 12β HSDH was also recently identified, completing the epi-bile acid pathway [59] where homology searching using blastp for this enzyme (WP_027099077.1) against *E. lenta* shows a candidate (WP_114518444.1, E value = 1×10^{-44}, 36.5% identity). Taken together, these results indicate that the oxidation and epimerization of bile acids is largely dependent on *E. lenta*, and provides a mechanistic framework for reduced bile acid toxicity, in particular, with DCA as a substrate. *E. coli* and *A. caccae* seem to be capable of forming 7-ketoCA on their own, but all other oxidized and epimerized forms are only formed when co-cultured with *E. lenta*. With these results indicating that *E. lenta* seems to be important in the formation of epimerized and oxidized forms of bile acids, we sought to investigate a recently discovered new class of bile acids, namely the MBSCs.

3.7. Detection of Microbial Bile Salt Conjugates in Single Culture vs. Co-Culture

MBSCs are a novel class of bile acids that are formed by microbial reconjugation of deconjugated/unconjugated bile acids with typically non-canonical amino acids, although host-resembling glycine conjugates can also be generated by microbes [27,36,37]. This novel reaction type was previously not suspected to be in the repertoire of bile acid modifications, but has opened the door to discovering new bile acids. Figure 8 shows the concentrations (nmol/L) of MBSCs from supernatant from the bacterial cultures. Due to the lack of a standard, DCA conjugates are to be considered semi-quantitative since their abundance is based on a *L*-Leu-CDCA standard. MBSC figure for all 8 SIHUMIx strains can be seen on Supplementary Figure S9. Media blanks containing either CA or DCA were averaged and subtracted from their respective categories within each strain.

Comparing *E. coli* single and co-cultures, statistically significant differences are seen for Leu-CA and Tyr-DCA. For Leu-CA, co-culturing increases the concentration, whereas the single culture seems to have a higher abundance of Tyr-DCA compared to co-culture (not detected). *A. caccae* cultures have no significant differences between single and co-culture, so *A. caccae* seems to be capable of producing detectable levels of most of the tested MBSCs by itself. For *C. ramosum*, Leu-CA is again significantly increased in the co-culture and Tyr-DCA is more abundant in the single culture. Leu-DCA and Phe-DCA are also significantly increased in the co-culture since there was no signal in the single cultures. Taken together, these results point towards the capacity of all strains to reconjugate bile acids with Leucine, Phenylalanine and Tyrosine, but that the presence of *E. lenta* in particular elevates levels of Leu-CA. These observations add the studied strains of *E. coli*, *A. caccae*, *C. ramosum* and *E. lenta* to the range of bacteria capable of non-canonical bile salt conjugation [37].

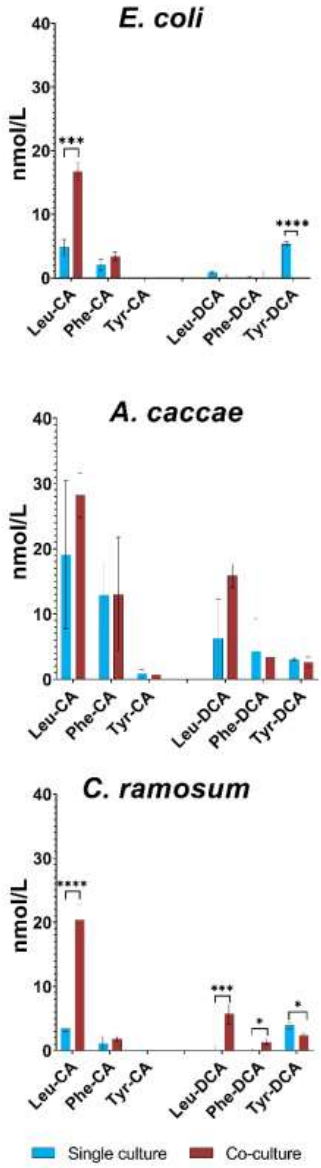

Figure 8. MBSCs produced in single and coculture. Bar charts showing the mean concentration from three biological replicates (nmol/L) of the MBSCs estimated from MS measurements of single and co-cultures. The left hand side of the graph shows the cultures stressed with CA and the right-hand side those treated with DCA. Blue colors are single cultures and red are co-cultures. Error bars are strandard deviation and statistical significance was determined using a two tailed Student's *t*-test, * $p < 0.05$, *** $p < 0.005$, **** $p < 0.001$.

4. Discussion

From the growth curves, it was seen that DCA inhibited growth for *A. caccae* and, in particular, *C. ramosum*, where co-culturing with *E. lenta* could alleviate some of this inhibition for *C. ramosum*, but not for *A. caccae*. This effect was also found to be bile acid specific with a stronger effect of the more hydrophobic DCA compared to CA. Bile acid sensitivity relates to the differences in cellular-envelope composition between gram-negative and gram-positive bacteria. [21]. The slight effect on *A. caccae* was interesting, since nothing was known about the bile acid sensitivity of gram-variable bacteria such as *A. caccae*. This species is described to be gram-positive in the lag phase and becoming more gram-negative during log phase [49]. Hence, it would be interesting to investigate how the proteome of *A. caccae* changes during cultivation, and investigate if there are certain transporters or other mechanisms to deal with bile acid stress. We did not see any response from bile acid stress in *E. coli* and it is also known that gram-negative strains are more bile acid resistant where *E. coli* is known for having mechanisms to cope with bile acid stress [21,60]. In regard to the experimental setup, the harvesting point could have been optimized for the individual stains, since they were all harvested after 6 h. This makes the intre-strain comparison less applicable; for instance, if selected strains are compared, it can be observed that *E. coli* has been in the stationary phase for approximately 4 h, whereas *A. caccae* and *C. ramosum* has just started to reach stationary phase. To gain insights into the specific molecular responses to bile acid stress, earlier time points should have been included as well. An interesting finding was that it seemed that *E. lenta* grew better under bile acid stress conditions. Normally, bacterial growth is inhibited by bile acids, but there are cases where certain strains grow better. *Akkermansia muciniphila* has previously been described to grow better under sodium deoxycholate conditions and actually be more inhibited by oxo-bile acids [61]. Via bile acid measurements, we suggested that co-culturing contributed to a significant decrease in concentration of both CA and DCA across all three strains. This speaks in favor of *E. lenta* being the main driver of bile acid transformations. It should, however, be considered that this decrease could also be caused by an uptake of bile acids into the cells or binding to the cell membranes or envelopes. Our results from ZP measurements indicated that *C. ramosum* had a shift towards a more negative ZP when stressed with DCA. Studies on the effects of antimicrobial peptides on *E. coli* suggest a correlation of ZP shifts towards neutral charge and increased permeability of cell membranes and decreased cell viability resp [53]. This difference could, however, be due to the difference in stressor exposure. For our bile acid assays, the bile acids were already in the media upon inoculation, whereas the antimicrobial peptide studies typically inject them at a certain point of growth. Other studies determined that bacteria exposed to bile acid stress caused drastic changes in cell morphology, having a shrunken appearance and displaying leakage. It could be hypothesized that the decrease in ZP here should be interpreted as a shrunken membrane that has been leaking [62]. Other studies also analyzed the effects of DCA on membrane integrity, but rather use markers such as DiBAC4 (bis-(1,3-dibutylbarbituric acid) trimethine oxonol), where it was also determined that DCA indeed is membrane disruptive in gram-positive bacteria [17]. The proteomic analyses also provide further hints for membrane disruption by the abundance pattern of the mevalonate pathway. This pathway leads to the production of farnesyl diphosphate, which is required for adding lipid anchors to protein-bound proteins and the pathway is downregulated in the co-culture. Bile acids cause genotoxicity and the DNA damage is reported to be caused by reactive oxygen species (ROS) [60]. Thus, our finding of downregulated proteins related to DNA repair in the co-culture seems to confirm that the membrane, indeed, is less permeable and hence leads to less damage to the DNA via ROS or other stressors. Beside the classical pathways for bile acid tolerance, we identified in *A. caccae* at least two more, namely, the terpenoid and the rhamnose pathway. Both became only detectable after in-detail scrutiny of other involved pathways. The strongly affected terpenoid pathway might be affected but the proteins detected in this study are the more generally related to it. Namely, the ACAT acetyl-CoA C-acetyltransferase [EC:2.3.1.9] and the dxs—1-deoxy-D-xylulose-5-phosphate

synthase [EC:2.2.1.7]. The more specific ones for the terpenoid backbone synthesis such as ispf 2-C-methyl-D-erythritol 2,4-cyclodiphosphate synthase [EC:4.6.1.12], the FDPS—farnesyl diphosphate synthase [EC:2.5.1.1 2.5.1.10] and the GGPS1—geranylgeranyl diphosphate synthase [EC:2.5.1.1 2.5.1.10 2.5.1.29]. The decreased abundance in the presence in *E. lenta* indicates that the lipid anchored proteins are of specific importance when the bile stress on the membrane is more pronounced and after reduced membrane stress the abundance is downregulated. Another putative resilience mechanism was found within the proteins that led to the detection of the Streptomycin und Carbapenem pathway. Since these antibiotics are known to be synthesized by fungi, we checked the involved proteins identified in this study in more detail. It turned out that three out of the three proteins, namely, inrfbA (glucose-1-phosphate thymidylyltransferase [EC:2.7.7.24]), rfbB (dTDP-glucose 4,6-dehydratase [EC:4.2.1.46]) and rfbC (dTDP-4-dehydrorhamnose 3,5-epimerase [EC:5.1.3.13]), are also part of the biosynthesis of rhamnose, a deoxysugar critical for membrane integrity. The last one, proA (glutamate-5-semialdehyde dehydrogenase [EC:1.2.1.41] that leads to the production of L-proline is also an upregulated metabolite for both CA and DCA stress. When considering the results from untargeted metabolomics, we, in particular, putatively identified upregulated metabolites that were related to nucleotide metabolism, namely inosine and adenine, in particular for *A. caccae* and *C. ramousm*. These finding are somewhat in contrast to what can be observed in the literature. Studies in the gram-positive strain *Ruminococcus bromii* suggests that metabolites related to carbohydrate and nucleotide metabolism to be downregulated during stress with DCA and LCA [17]. However, metabolites were detected in intracellularly and it could, hence, be hypothesized that both are true, although strains and methodologies are different so such comparisons should be undertaken cautiously. 12-epideoxycholic acid is a metabolite of DCA as a consequence of sequential oxidation and epimerization via 12α and 12β HSDH, and this metabolite was upregulated in *A. caccae* co-cultures. Additionally, we do see a high formation of isoDCA from the measurements of oxidized and epimerized bile acids, but we could not say which isoform it was. It could be hypothesized that with 12-epideoxycholic acid being an upregulated metabolite, and given that we do detect isoDCA in *A. caccae* co-cultures, that this isoform indeed is 12-epideoxycholic acid. Since this metabolite is only significantly detected in *A. caccae* it could be expected that some combination of 12α and 12β HSDH is present in this co-culture. Both *A. caccae* and *E. lenta* carry high scoring homologues to the recently annotated 12β HSDH, so determining whether one or both carry such an enzyme remains to be studied [59]. The increased levels of inosine and adenine stem from the degradation of adenosine, which was also reduced in co-cultures. The reduced levels of adenosine in co-culture can be interpreted as an indication of less genotoxicity in co-cultures, since these metabolites relates to the "Purine metabolism" pathway. There have also been investigations into how *Clostridiodies difficile* (*C. difficile*) responds to bile acid stress using proteomics and scanning electron microscopy (SEM). These investigations revealed that CA induced changes in different pathways compared to CDCA, DCA and LCA. Furthermore, it was also suggested that pathways related to butyrate fermentation and Stickland fermentation of leucine were affected, as well as changes in morphology, such as loss of flagella [63]. If these observations are considered in the context of our findings, there is some overlap when considering changes in metabolic pathways and how bile acid response is specific to the bile acid. The formation of oxidized and epimerized forms of CA and DCA helps explain the reduced toxicity seen in strains such as *C. ramosum*. What drives bile acid toxicity is their amphiphilic nature and their hydrophobicity, and it has previously been described that iso forms of bile acids are less toxic [25,64]. The formation of 3-ketoDCA could, thereby, help explain the differences seen in both growth and ZP of *C. ramosum*, since our data also suggests that *E. lenta* rather rapidly forms the keto and iso forms. We could detect them after only 6 h of growth, whereas other studies have used 24 or 48 h [32,37,59]. Oxidized and epimerized bile acids are less likely to undergo dehydroxylation [32] and performing these transformations may, thereby, further help bacteria reduce stress from bile acids, both via formation of less toxic species and inhibition of formation or more toxic

ones such as DCA and LCA. Specifically, what the influence of oxidized and epimerized bile acids are remains to be elucidated, but it has been suggested that isoDCA increased Foxp3 by acting on dendritic cells to diminish their immunostimulatory properties, with 3-oxoDCA exhibiting similar effects but to a lesser extent [65]. 3-ketoLCA has also been shown to be a potent agonist for the Vitamin D Receptor [66]. It was only recently that MBSCs were discovered and this finding (revolutionized the bile acid community since it) brought light a new mode of action by the gut microbiota, namely re-conjugating bile acids with novel amino acid residues [36]. Unconjugated bile acids are more toxic compared to their conjugated counterparts [22,67]. Hence, the formation of MBSCs could be expected to reduce toxicity. In our study we detect MBSCs in all cultures, see Supplementary Figure S9), where in particular Leu-CA seems to increase when co-cultured with *E. lenta*. However, in our analyses the concentration of MBSCs in the medium supernatant is mostly in the 5–40 nM range even though the starting concentration was 600 µM for CA. With such concentrations of MBSCs, it is not likely to reduce toxicity significantly. It remains to be determined whether *E. lenta* facilitates formation of MBSCs or produces them by itself and exactly by which means bacteria re-conjugate bile acids. The in vivo implications of MBSCs remain to be elucidated, both locally and systematically.

5. Conclusions

In summary, our study reaffirms that a bacterium's response to bile acid stress depends greatly on both the membrane organization of the bacteria and the hydrophobicity of the bile acid. Co-culturing with *E. lenta* alleviated bile acid stress by modifying bile acids into their oxidized and epimerized forms, which in particular was beneficial for *C. ramosum*. An interesting finding was growth behavior and ZP of the gram-variable strain *A. caccae* did not seem to benefit from co-culturing; however, proteomic and metabolomic investigations did indeed produce pronounced effects. The effects of co-culturing with *E. lenta* is strain specific, as reflected in the differences in proteomic and metabolomic analyses between strains. We found that *E. lenta* is, indeed, a potent bile acid modifier, quickly forming oxidized and epimerized forms of CA and DCA. Surprisingly, all strains from the SIHUMIx model system seem capable of forming the novel MBSCs. Overall, our study highlights the importance of conducting in depth molecular investigations, in order to gain insights that are not immediately apparent. We conclude that the presence of potent bile acid modifiers has a relevant impact on the microbe–microbe interaction and potentially, also, on the microbiome-host interaction.

Supplementary Materials: The following supporting information can be downloaded at: https://www.mdpi.com/article/10.3390/microorganisms10102025/s1. Figure S1: Screening of bile acid concentrations in *B. producta* and *B. thermiotaomicron*; Figure S2: Growth curves of SIHUMIx strains when stressed with cholic acid; Figure S3: Additional analyzed bile acids covered in the biocrates bile acid kit from bile acid stress assays; Figure S4: Examples of zeta potential chromatograms; Figure S5: Quality check of proteomic measurements; Figure S6: Principal component analysis of proteomic data; Figure S7: Principal component analysis of untargeted metabolomics data; Figure S8: Oxidized and epimerized bile acids in SIHUMIx cultures; Figure S9: Microbial bile salt conjugations in SIHUMIx cultures; Table S1: YH-BHI media composition: Table S2: Accession numbers of hydroxysteroid dehydrogenase enzymes.

Author Contributions: Conceptualization, K.J.P.; Data curation, K.J.P., S.-B.H., B.E. and U.R.-K.; Formal analysis, K.J.P, S.-B.H., K.Ž., B.E. and U.R.-K.; Funding acquisition, T.C. and M.v.B.; Investigation, K.J.P., M.L., F.G.S. and N.J.; Methodology, S.-B.H., K.Ž., M.L., L.Y.W., F.G.S., N.J. and U.R.-K.; Project administration, K.J.P. and M.v.B.; Resources, K.Ž., M.L., A.V., T.C., F.G.S., N.J., U.R.-K. and M.v.B.; Software, S.-B.H.; Supervision, M.L., N.J., U.R.-K. and M.v.B.; Validation, S.-B.H., B.E. and U.R.-K.; Visualization, K.J.P., S.-B.H. and B.E.; Writing—original draft, K.J.P., S.-B.H. and M.v.B.; Writing—review & editing, K.J.P., S.-B.H., M.L., B.E., L.Y.W., F.G.S., N.J., U.R.-K. and M.v.B. All authors have read and agreed to the published version of the manuscript.

Funding: K.J.P., T.C. and M.v.B. are grateful for funding by the DFG, German Research Foundation—Project-ID 403224013–SFB 1382. U.R.-K., S.-B.H. and N.J. are grateful for funding of the UFZ for the ProMetheus platform for proteomics and metabolomics. The work presented in this article is supported by the Novo Nordisk Foundation grant NNF21OC0066551.

Institutional Review Board Statement: Not applicable.

Informed Consent Statement: Not applicable.

Data Availability Statement: The mass spectrometry proteomics data have been deposited to the ProteomeXchange Consortium via the PRIDE [68] partner repository with the dataset identifier PXD035496. Remaining data can be found in the Supplementary data file (https://zenodo.org/record/7193128#.Y0e9XxrP1aS, accessed on 10 Octorber 2022).

Acknowledgments: We thank Nicole Bock and Olivia Pleßow for excellent technical assistance. M.v.B. and K.J.P. are grateful for funding by the DFG, German Research Foundation—Project-ID 403224013–SFB 1382. The work presented in this article is supported by Novo Nordisk Foundation grant NNF21OC0066551. M.v.B., B.E., U.R.-K., and N.J. are grateful for funding of the UFZ for the ProMetheus platform for proteomics and metabolomics. We also thank Arno Classen and Carsten Bolm for the supplying us with the standards for MBSC measurements (Institute of Organic Chemistry, RWTH Aachen University, Professor-Pirlet-Str. 1, 52056 Aachen, Germany). We would also like to thank the late Milan Jirsa for supplying us with standards for oxidized bile acids (Charles University, Prague).

Conflicts of Interest: The authors declare no conflict of interest.

References

1. Wu, H.J.; Wu, E. The Role of Gut Microbiota in Immune Homeostasis and Autoimmunity. *Gut Microbes* **2012**, *3*, 4–14. [CrossRef]
2. Magnúsdóttir, S.; Ravcheev, D.; De Crécy-Lagard, V.; Thiele, I. Systematic Genome Assessment of B-Vitamin Biosynthesis Suggests Cooperation among Gut Microbes. *Front. Genet.* **2015**, *6*, 148. [CrossRef]
3. Koh, A.; De Vadder, F.; Kovatcheva-Datchary, P.; Bäckhed, F. From Dietary Fiber to Host Physiology: Short-Chain Fatty Acids as Key Bacterial Metabolites. *Cell* **2016**, *165*, 1332–1345. [CrossRef]
4. Wahlström, A.; Sayin, S.I.; Marschall, H.U.; Bäckhed, F. Intestinal Crosstalk between Bile Acids and Microbiota and Its Impact on Host Metabolism. *Cell Metab.* **2016**, *24*, 41–50. [CrossRef]
5. Inagaki, T.; Moschetta, A.; Lee, Y.K.; Peng, L.; Zhao, G.; Downes, M.; Yu, R.T.; Shelton, J.M.; Richardson, J.A.; Repa, J.J.; et al. Regulation of Antibacterial Defense in the Small Intestine by the Nuclear Bile Acid Receptor. *Proc. Natl. Acad. Sci. USA* **2006**, *103*, 3920–3925. [CrossRef]
6. Gomez-Ospina, N.; Potter, C.J.; Xiao, R.; Manickam, K.; Kim, M.S.; Kim, K.H.; Shneider, B.L.; Picarsic, J.L.; Jacobson, T.A.; Zhang, J.; et al. Mutations in the Nuclear Bile Acid Receptor FXR Cause Progressive Familial Intrahepatic Cholestasis. *Nat. Commun.* **2016**, *7*, 10713. [CrossRef]
7. Pols, T.W.H.; Noriega, L.G.; Nomura, M.; Auwerx, J.; Schoonjans, K. The Bile Acid Membrane Receptor TGR5: A Valuable Metabolic Target. *Dig. Dis.* **2011**, *29*, 37–44. [CrossRef]
8. Albalak, A.; Zeidel, M.L.; Zucker, S.D.; Jackson, A.A.; Donovan, J.M. Effects of Submicellar Bile Salt Concentrations on Biological Membrane Permeability to Low Molecular Weight Non-Ionic Solutes. *Biochemistry* **1996**, *35*, 7936–7945. [CrossRef]
9. Islam, K.B.M.S.; Fukiya, S.; Hagio, M.; Fujii, N.; Ishizuka, S.; Ooka, T.; Ogura, Y.; Hayashi, T.; Yokota, A. Bile Acid Is a Host Factor That Regulates the Composition of the Cecal Microbiota in Rats. *Gastroenterology* **2011**, *141*, 1773–1781. [CrossRef]
10. Kakiyama, G.; Pandak, W.M.; Gillevet, P.M.; Hylemon, P.B.; Heuman, D.M.; Daita, K.; Takei, H.; Muto, A.; Nittono, H.; Ridlon, J.M.; et al. Modulation of the Fecal Bile Acid Profile by Gut Microbiota in Cirrhosis. *J. Hepatol.* **2013**, *58*, 949–955. [CrossRef]
11. Ridlon, J.M.; Kang, D.J.; Hylemon, P.B.; Bajaj, J.S. Bile Acids and the Gut Microbiome. *Curr. Opin. Gastroenterol.* **2014**, *30*, 332–338. [CrossRef]
12. Chiang, J.Y.L. Bile Acid Metabolism and Signaling. *Compr. Physiol.* **2013**, *3*, 1191–1212. [CrossRef]
13. van Best, N.; Rolle-Kampczyk, U.; Schaap, F.G.; Basic, M.; Olde Damink, S.W.M.; Bleich, A.; Savelkoul, P.H.M.; von Bergen, M.; Penders, J.; Hornef, M.W. Bile Acids Drive the Newborn's Gut Microbiota Maturation. *Nat. Commun.* **2020**, *11*, 3692. [CrossRef]
14. Haange, S.B.; Jehmlich, N.; Krügel, U.; Hintschich, C.; Wehrmann, D.; Hankir, M.; Seyfried, F.; Froment, J.; Hübschmann, T.; Müller, S.; et al. Gastric Bypass Surgery in a Rat Model Alters the Community Structure and Functional Composition of the Intestinal Microbiota Independently of Weight Loss. *Microbiome* **2020**, *8*, 13. [CrossRef]
15. Van Velkinburgh, J.C.; Gunn, J.S. PhoP-PhoQ-Regulated Loci Are Required for Enhanced Bile Resistance in *Salmonella* spp. *Infect. Immun.* **1999**, *67*, 1614–1622. [CrossRef]
16. Urdaneta, V.; Casadesús, J. Interactions between Bacteria and Bile Salts in the Gastrointestinal and Hepatobiliary Tracts. *Front. Med.* **2017**, *4*, 163. [CrossRef]

17. Tian, Y.; Gui, W.; Koo, I.; Smith, P.B.; Allman, E.L.; Nichols, R.G.; Rimal, B.; Cai, J.; Liu, Q.; Patterson, A.D. The Microbiome Modulating Activity of Bile Acids. *Gut Microbes* **2020**, *11*, 979–996. [CrossRef]
18. Schubert, K.; Olde Damink, S.W.M.; von Bergen, M.; Schaap, F.G. Interactions between Bile Salts, Gut Microbiota, and Hepatic Innate Immunity. *Immunol. Rev.* **2017**, *279*, 23–35. [CrossRef]
19. Di Ciaula, A.; Garruti, G.; Baccetto, R.L.; Molina-Molina, E.; Bonfrate, L.; Wang, D.Q.H.; Portincasa, P. Bile Acid Physiology. *Ann. Hepatol.* **2017**, *16*, s4–s14. [CrossRef]
20. Li, T.; Chiang, J.Y.L. Bile Acid Signaling in Metabolic Disease and Drug Therapy. *Pharmacol. Rev.* **2014**, *66*, 948–983. [CrossRef]
21. Begley, M.; Gahan, C.G.M.; Hill, C. The Interaction between Bacteria and Bile. *FEMS Microbiol. Rev.* **2005**, *29*, 625–651. [CrossRef]
22. De Aguiar Vallim, T.Q.; Tarling, E.J.; Edwards, P.A. Pleiotropic Roles of Bile Acids in Metabolism. *Cell Metab.* **2013**, *17*, 657–669. [CrossRef]
23. Trefflich, I.; Marschall, H.U.; Di Giuseppe, R.; Ståhlman, M.; Michalsen, A.; Lampen, A.; Abraham, K.; Weikert, C. Associations between Dietary Patterns and Bile Acids—Results from a Cross-Sectional Study in Vegans and Omnivores. *Nutrients* **2020**, *12*, 47. [CrossRef]
24. Keating, N.; Mroz, M.S.; Scharl, M.M.; Marsh, C.; Ferguson, G.; Hofmann, A.F.; Keely, S.J. Physiological Concentrations of Bile Acids Down-Regulate Agonist Induced Secretion in Colonic Epithelial Cells. *J. Cell Mol. Med.* **2009**, *13*, 2293–2303. [CrossRef]
25. Devlin, A.S.; Fischbach, M.A. A Biosynthetic Pathway for a Prominent Class of Microbiota-Derived Bile Acids. *Nat. Chem. Biol.* **2015**, *11*, 685–690. [CrossRef]
26. Ridlon, J.M.; Harris, S.C.; Bhowmik, S.; Kang, D.J.; Hylemon, P.B. Consequences of Bile Salt Biotransformations by Intestinal Bacteria. *Gut Microbes* **2016**, *7*, 22–39. [CrossRef]
27. Ay, Ü.; Leníček, M.; Classen, A.; Olde Damink, S.W.M.; Bolm, C.; Schaap, F.G. New Kids on the Block: Bile Salt Conjugates of Microbial Origin. *Metabolites* **2022**, *12*, 176. [CrossRef]
28. Tanaka, H.; Doesburg, K.; Iwasaki, T.; Mierau, I. Screening of Lactic Acid Bacteria for Bile Salt Hydrolase Activity. *J. Dairy Sci.* **1999**, *82*, 2530–2535. [CrossRef]
29. Vital, M.; Rud, T.; Rath, S.; Pieper, D.H.; Schlüter, D. Diversity of Bacteria Exhibiting Bile Acid-Inducible 7α-Dehydroxylation Genes in the Human Gut. *Comput. Struct. Biotechnol. J.* **2019**, *17*, 1016–1019. [CrossRef]
30. Marion, S.; Studer, N.; Desharnais, L.; Menin, L.; Escrig, S.; Meibom, A.; Hapfelmeier, S.; Bernier-Latmani, R. In Vitro and in Vivo Characterization of Clostridium Scindens Bile Acid Transformations. *Gut Microbes* **2019**, *10*, 481–503. [CrossRef]
31. Wells, J.E.; Berr, F.; Thomas, L.A.; Dowling, R.H.; Hylemon, P.B. Isolation and Characterization of Cholic Acid 7α-Dehydroxylating Fecal Bacteria from Cholesterol Gallstone Patients. *J. Hepatol.* **2000**, *32*, 4–10. [CrossRef]
32. Harris, S.C.; Devendran, S.; Méndez- García, C.; Mythen, S.M.; Wright, C.L.; Fields, C.J.; Hernandez, A.G.; Cann, I.; Hylemon, P.B.; Ridlon, J.M. Bile Acid Oxidation by Eggerthella Lenta Strains C592 and DSM 2243 T. *Gut Microbes* **2018**, *9*, 523–539. [CrossRef] [PubMed]
33. Doden, H.; Sallam, L.A.; Devendran, S.; Ly, L.; Doden, G.; Daniel, S.L.; Alves, J.M.P.; Ridlon, J.M. Metabolism of Oxo-Bile Acids and Characterization of Recombinant 12α- Hydroxysteroid Dehydrogenases from Bile Acid 7α-Dehydroxylating Human Gut Bacteria. *Appl. Environ. Microbiol.* **2018**, *84*, e00235-18. [CrossRef] [PubMed]
34. Macdonald, I.A.; Meier, E.C.; Mahony, D.E.; Costain, G.A. 3α-, 7α- And 12α-Hydroxysteroid Dehydrogenase Activities from Clostridium Perfringens. *Biochim. Biophys. Acta (BBA)/Lipids Lipid Metab.* **1976**, *450*, 142–153. [CrossRef]
35. Lee, J.Y.; Arai, H.; Nakamura, Y.; Fukiya, S.; Wada, M.; Yokota, A. Contribution of the 7β-Hydroxysteroid Dehydrogenase from Ruminococcus Gnavus N53 to Ursodeoxycholic Acid Formation in the Human Colon. *J. Lipid Res.* **2013**, *54*, 3062–3069. [CrossRef]
36. Quinn, R.A.; Melnik, A.V.; Vrbanac, A.; Fu, T.; Patras, K.A.; Christy, M.P.; Bodai, Z.; Belda-Ferre, P.; Tripathi, A.; Chung, L.K.; et al. Global Chemical Effects of the Microbiome Include New Bile-Acid Conjugations. *Nature* **2020**, *579*, 123–129. [CrossRef]
37. Lucas, L.N.; Barrett, K.; Kerby, R.L.; Zhang, Q.; Cattaneo, L.E.; Stevenson, D.; Rey, F.E.; Amador-Noguez, D. Dominant Bacterial Phyla from the Human Gut Show Widespread Ability To Transform and Conjugate Bile Acids. *mSystems* **2021**, *6*, e00805-21. [CrossRef]
38. Setchell, K.D.R.; Lawson, A.M.; Tanida, N.; Sjovall, J. General Methods for the Analysis of Metabolic Profiles of Bile Acids and Related Compounds in Feces. *J. Lipid Res.* **1983**, *24*, 1085–1100. [CrossRef]
39. Hyronimus, B.; Le Marrec, C.; Hadj Sassi, A.; Deschamps, A. Acid and Bile Tolerance of Spore-Forming Lactic Acid Bacteria. *Int. J. Food Microbiol.* **2000**, *61*, 193–197. [CrossRef]
40. Jacobsen, C.N.; Nielsen, V.R.; Hayford, A.E.; Møller, P.L.; Michaelsen, K.F.; Pærregaard, A.; Sandström, B.; Tvede, M.; Jakobsen, M. Screening of Probiotic Activities of Forty-Seven Strains of Lactobacillus Spp. by in Vitro Techniques and Evaluation of the Colonization Ability of Five Selected Strains in Humans. *Appl. Environ. Microbiol.* **1999**, *65*, 4949–4956. [CrossRef]
41. Becker, N.; Kunath, J.; Loh, G.; Blaut, M. Human Intestinal Microbiota: Characterization of a Simplified and Stable Gnotobiotic Rat Model. *Gut Microbes* **2011**, *2*, 25–33. [CrossRef] [PubMed]
42. Pham, H.T.; Amhard, K.; Asad, Y.J.; Deng, L.; Felder, T.K.; St John-Williams, L.; Kaever, V.; Leadley, M.; Mitro, N.; Muccio, S.; et al. Inter-Laboratory Robustness of Next-Generation Bile Acid Study in Mice and Humans: International Ring Trial Involving 12 Laboratories. *J. Appl. Lab. Med.* **2016**, *1*, 129–142. [CrossRef] [PubMed]
43. Kanehisa, M.; Sato, Y.; Morishima, K. BlastKOALA and GhostKOALA: KEGG Tools for Functional Characterization of Genome and Metagenome Sequences. *J. Mol. Biol.* **2016**, *428*, 726–731. [CrossRef] [PubMed]

44. Prasnicka, A.; Cermanova, J.; Hroch, M.; Dolezelova, E.; Rozkydalova, L.; Smutny, T.; Carazo, A.; Chladek, J.; Lenicek, M.; Nachtigal, P.; et al. Iron Depletion Induces Hepatic Secretion of Biliary Lipids and Glutathione in Rats. *Biochim. Biophys. Acta—Mol. Cell Biol. Lipids* **2017**, *1862*, 1469–1480. [CrossRef]
45. Dixon, P. Computer Program Review VEGAN, a Package of R Functions for Community Ecology. *J. Veg. Sci.* **2003**, *14*, 927–930. [CrossRef]
46. Benjamini, Y.; Hochberg, Y. Controlling the False Discovery Rate: A Practical and Powerful Approach to Multiple Testing. *J. R. Stat. Soc. Ser. B (Methodol.)* **1995**, *57*, 289–300.
47. Wickham, H. Ggplot2. *Wiley Interdiscip. Rev. Comput. Stat.* **2011**, *3*, 180–185. [CrossRef]
48. Hamilton, J.P.; Xie, G.; Raufman, J.P.; Hogan, S.; Griffin, T.L.; Packard, C.A.; Chatfield, D.A.; Hagey, L.R.; Steinbach, J.H.; Hofmann, A.F. Human Cecal Bile Acids: Concentration and Spectrum. *Am. J. Physiol.—Gastrointest. Liver Physiol.* **2007**, *293*, 256–263. [CrossRef]
49. Schwiertz, A.; Hold, G.L.; Duncan, S.H.; Gruhl, B.; Collins, M.D.; Lawson, P.A.; Flint, H.J.; Blaut, M. Anaerostipes Caccae Gen. Nov., Sp. Nov., a New Saccharolytic, Acetate-Utilising, Butyrate-Producing Bacterium from Human Faeces. *Syst. Appl. Microbiol.* **2002**, *25*, 46–51. [CrossRef]
50. Tokumasu, F.; Ostera, G.R.; Amaratunga, C.; Fairhurst, R.M. Modifications in Erythrocyte Membrane Zeta Potential by Plasmodium Falciparum Infection. *Exp. Parasitol.* **2012**, *131*, 245–251. [CrossRef]
51. Baumgarten, T.; Sperling, S.; Seifert, J.; von Bergen, M.; Steiniger, F.; Wick, L.Y.; Heipieper, H.J. Membrane Vesicle Formation as a Multiple-Stress Response Mechanism Enhances Pseudomonas Putida DOT-T1E Cell Surface Hydrophobicity and Biofilm Formation. *Appl. Environ. Microbiol.* **2012**, *78*, 6217–6224. [CrossRef] [PubMed]
52. Baumgarten, T.; Vazquez, J.; Bastisch, C.; Veron, W.; Feuilloley, M.G.J.; Nietzsche, S.; Wick, L.Y.; Heipieper, H.J. Alkanols and Chlorophenols Cause Different Physiological Adaptive Responses on the Level of Cell Surface Properties and Membrane Vesicle Formation in Pseudomonas Putida DOT-T1E. *Appl. Microbiol. Biotechnol.* **2012**, *93*, 837–845. [CrossRef] [PubMed]
53. Arakha, M.; Saleem, M.; Mallick, B.C.; Jha, S. The Effects of Interfacial Potential on Antimicrobial Propensity of ZnO Nanoparticle. *Sci. Rep.* **2015**, *5*, 9578. [CrossRef] [PubMed]
54. Oh, J.K.; Yegin, Y.; Yang, F.; Zhang, M.; Li, J.; Huang, S.; Verkhoturov, S.V.; Schweikert, E.A.; Perez-Lewis, K.; Scholar, E.A.; et al. The Influence of Surface Chemistry on the Kinetics and Thermodynamics of Bacterial Adhesion. *Sci. Rep.* **2018**, *8*, 17247. [CrossRef]
55. Haiser, H.J.; Gootenberg, D.B.; Chatman, K.; Sirasani, G.; Balskus, E.P.; Turnbaugh, P.J. Predicting and Manipulating Cardiac Drug Inactivation by the Human Gut Bacterium Eggerthella Lenta. *Science* **2013**, *341*, 295–298. [CrossRef]
56. Hayakawa, S.; Fujiwara, T. Microbiological Degradation of Bile Acids. Further Degradation of a Cholic Acid Metabolite Containing the Hexahydroindane Nucleus by Corynebacterium Equi. *Biochem. J.* **1977**, *162*, 387–397. [CrossRef]
57. Tanaka, N.; Nonaka, T.; Tanabe, T.; Yoshimoto, T.; Tsuru, D.; Mitsui, Y. Crystal Structures of the Binary and Ternary Complexes of 7α-Hydroxysteroid Dehydrogenase from Escherichia Coli. *Biochemistry* **1996**, *35*, 7715–7730. [CrossRef]
58. Hirano, S.; Masuda, N. Transformation of Bile Acids by Eubacterium Lentum. *Appl. Environ. Microbiol.* **1981**, *42*, 912–915. [CrossRef]
59. Doden, H.L.; Wolf, P.G.; Gaskins, H.R.; Anantharaman, K.; Alves, J.M.P.; Ridlon, J.M. Completion of the Gut Microbial Epi-Bile Acid Pathway. *Gut Microbes* **2021**, *13*, 1907271. [CrossRef]
60. Bernstein, C.; Bernstein, H.; Payne, C.M.; Beard, S.E.; Schneider, J. Bile Salt Activation of Stress Response Promoters in Escherichia Coli. *Curr. Microbiol.* **1999**, *39*, 68–72. [CrossRef]
61. Hagi, T.; Geerlings, S.Y.; Nijsse, B.; Belzer, C. The Effect of Bile Acids on the Growth and Global Gene Expression Profiles in Akkermansia Muciniphila. *Appl. Microbiol. Biotechnol.* **2020**, *104*, 10641–10653. [CrossRef] [PubMed]
62. Leverrier, P.; Dimova, D.; Pichereau, V.; Auffray, Y.; Boyaval, P.; Jan, G. Susceptibility and Adaptive Response to Bile Salts in Propionibacterium Freudenreichii: Physiological and Proteomic Anlysis. *Appl. Environ. Microbiol.* **2003**, *69*, 3809–3818. [CrossRef] [PubMed]
63. Sievers, S.; Metzendorf, N.G.; Dittmann, S.; Troitzsch, D.; Gast, V.; Tröger, S.M.; Wolff, C.; Zühlke, D.; Hirschfeld, C.; Schlüter, R.; et al. Differential View on the Bile Acid Stress Response of Clostridioides Difficile. *Front. Microbiol.* **2019**, *10*, 258. [CrossRef] [PubMed]
64. Sutherland, J.D.; Macdonald, I.A. The Metabolism of Primary, 7-Oxo, and 7β-Hydroxy Bile Acids by Clostridium Absonum. *J. Lipid Res.* **1982**, *23*, 726–732. [CrossRef]
65. Campbell, C.; McKenney, P.T.; Konstantinovsky, D.; Isaeva, O.I.; Schizas, M.; Verter, J.; Mai, C.; Jin, W.B.; Guo, C.J.; Violante, S.; et al. Bacterial Metabolism of Bile Acids Promotes Generation of Peripheral Regulatory T Cells. *Nature* **2020**, *581*, 475–479. [CrossRef] [PubMed]
66. Makishima, M.; Lu, T.T.; Xie, W.; Whitfield, G.K.; Domoto, H.; Evans, R.M.; Haussler, M.R.; Mangelsdorf, D.J. Vitamin D Receptor as an Intestinal Bile Acid Sensor. *Science* **2002**, *296*, 1313–1316. [CrossRef]
67. Heuman, D.M. Quantitative Estimation of the Hydrophilic-Hydrophobic Balance of Mixed Bile Salt Solutions. *J. Lipid Res.* **1989**, *30*, 719–730. [CrossRef]
68. Perez-Riverol, Y.; Bai, J.; Bandla, C.; García-Seisdedos, D.; Hewapathirana, S.; Kamatchinathan, S.; Kundu, D.J.; Prakash, A.; Frericks-Zipper, A.; Eisenacher, M.; et al. The PRIDE Database Resources in 2022: A Hub for Mass Spectrometry-Based Proteomics Evidences. *Nucleic Acids Res.* **2022**, *50*, D543–D552. [CrossRef]

Příloha 4

Journal of Chromatography B, 1033–1034 (2016) 317–320

Contents lists available at ScienceDirect

Journal of Chromatography B

journal homepage: www.elsevier.com/locate/chromb

Short communication

Comparison of simple extraction procedures in liquid chromatography–mass spectrometry based determination of serum 7α-hydroxy-4-cholesten-3-one, a surrogate marker of bile acid synthesis

Martin Leníček[a,*,1], Marek Vecka[a,b,1], Kateřina Žížalová[a], Libor Vítek[a,b]

[a] Institute of Medical Biochemistry and Laboratory Diagnostics, 1st Faculty of Medicine, Charles University in Prague, Kateřinská 32, 12108 Prague, Czech Republic
[b] 4th Department of Internal Medicine, 1st Faculty of Medicine, Charles University in Prague, Kateřinská 32, 12108 Prague, Czech Republic

ARTICLE INFO

Article history:
Received 19 April 2016
Received in revised form 29 August 2016
Accepted 31 August 2016
Available online 31 August 2016

Keywords:
7α-Hydroxy-4-cholesten-3-one
Bile acids
Cholesterol 7α-hydroxylase
Mass spectrometry

ABSTRACT

The serum concentration of 7α-hydroxy-4-cholesten-3-one (C4), a marker of cholesterol 7α-hydroxylase activity, has recently become an attractive diagnostic tool for researchers interested in cholesterol and bile acid metabolism. The rapidly increasing demand of C4 measurement led to the development of various fast, mostly mass spectrometry-based analytical methods. Our aim was to compare four simple (i.e., not requiring solid phase extraction) extraction procedures (two "one-phase", and two "two-phase") in terms of basic analytical performance and their labouriousness. All methods exhibited comparable extraction recoveries (ranging from 88 to 97%) and intra-assay precision (variation coefficients below 10%), and failed in the removal of phospholipids. Although marked differences were observed in desalting and deproteination, all methods can be considered satisfactory. Simple acetonitrile precipitation can be recommended if a fast extraction and minimal hands-on time is preferred; while two-phase ammonium sulphate:acetonitrile extraction should be chosen when maximal deproteination is required.

1. Introduction

Cholesterol 7α-hydroxylase (CYP7A1, EC 1.14.13.17) initiates the neutral (classic) pathway of bile acid (BA) biosynthesis, which also represents an important pathway for cholesterol elimination. As conversion of cholesterol to 7α-hydroxycholesterol (catalyzed by CYP7A1) is the rate-limiting step in this pathway and is under negative feedback regulation of BA, determination of CYP7A1 activity may not only serve as a marker of cholesterol homeostasis, but also that of BA synthesis and/or malabsorption. The fact that a liver biopsy is needed for direct determination of CYP7A1 disqualifies this parameter from clinical use in humans, and surrogate markers are being used instead. Serum concentrations of 7α-hydroxy-4-cholesten-3-one (C4, BA synthesis intermediate) were shown to reflect CYP7A1 activity almost three decades ago [1]. Since then, a wide variety of analytical methods for C4 determination have been proposed. With the rapid expansion of mass spectrometry (MS) instrumentation into clinical laboratories, traditional high-performance liquid chromatography with UV detection is being replaced by liquid chromatography–mass spectrometry (LC–MS) based methods. These offer higher sensitivity and specificity, allowing less thorough sample purification – solid phase extraction, an essential step in former sample preparation, is now often omitted. However, the simplified preparation of the sample might be redeemed by shortening of the column's (and other hardware) lifetime, signal suppression/enhancement, and other adverse effects. During development of the analytical method, an acceptable compromise between simplicity of sample preparation and its purity needs to be found. In this work, we compared the performance of four simple serum purification procedures suitable for C4 determination, taking into account the efficacy of removing the main contaminants (proteins, anorganic salts, and phospholipids), extraction recovery, and importantly, the ease of the entire procedure. Those methods requiring solid phase extraction, or any kind of derivatization, were not considered.

Abbreviations: au, arbitrary units; BA, bile acid(s); C4, 7α-hydroxy-4-cholesten-3-one; CYP7A1, cholesterol 7α-hydroxylase; IS, internal standard; LC–MS, liquid chromatography–mass spectrometry; MS, mass spectrometry.

* Corresponding author.
E-mail address: martin.lenicek@lf1.cuni.cz (M. Leníček).
[1] These authors contributed equally to this work.

http://dx.doi.org/10.1016/j.jchromb.2016.08.046
1570-0232/

2. Materials and methods

2.1. Serum samples

A large pool of anonymous serum leftovers (from over 50 individuals, referred to the Department of Medical Biochemistry and Laboratory Diagnostics for determination of serum BA levels) were collected ("low C4" sample). A "high C4" sample was created by spiking the "low C4" with synthetic C4 (in methanol, final methanol concentration below 0.1%); with mixtures of "high C4" and "low C4" in various ratios used for the preparation of all of the other sera.

2.2. Chemicals

C4 (7α-hydroxy-4-cholesten-3-one) was obtained from Steraloids (Newport, RI, USA); deuterium-labeled C4 (d7-7α-hydroxy-4-cholesten-3-one, internal standard (IS)) was purchased from Santa Cruz Biotechnology (Dallas, TX, USA); acetic acid, chloroform, methanol, sodium chloride, and ammonium sulfate (all analytical grade) came from Penta (Prague, Czech Republic); ammonium acetate (LC–MS grade), and *tert*-butyl methyl ether (analytical grade) from Sigma-Aldrich (St. Louis, MO, USA); acetonitrile (LiChrosolv, isocratic grade) was obtained from Merck (Darmstadt, Germany); methanol (LC–MS grade) from Biosolve BV (Valkenswaard, The Netherlands); diethylether (HPLC grade), and heptane (Chromapur grade) from Chromservis (Prague, Czech Republic); and iodine (resublimed) came from Lachema (Prague, Czech Republic).

2.3. Extraction procedures

Sample purifications were performed according to the relevant publications with slight modifications; reagent volumes were scaled up or down to process 100 μL of serum. Method "A" [2]: 100 μL of serum and 40 μL of IS were mixed with 320 μL of acetonitrile, vortexed for 1 min, centrifuged for 15 min at 13000g, after which the supernatant was collected. Method "B" [3]: 100 μL of serum and 40 μL of IS were mixed with 2 mL of methanol:*tert*-butyl methyl ether:chloroform mixture (1.33:1:1 by vol), vortexed for 1 min, incubated 30 min at room temperature, vortexed again, and then centrifuged for 10 min at 3000g; the supernatant was then collected. Method "C" [4]: 100 μL of serum and 40 μL of IS were mixed with 500 μL of chloroform:methanol mixture (2:1 by vol), vortexed for 1 min, and centrifuged for 3 min at 3000g. The upper phase was discarded, 200 μL of 125 mM NaCl in 50% methanol was added to the remainder, vortexed, and centrifuged as previously. The lower phase was collected. Method "D" [5]: 100 μL of serum and 40 μL of IS were mixed with 350 μL of water, 1 mL of acetonitrile and 1 mL of ammonium sulfate (400 g/L), vortexed for 1 min, incubated for 30 min, and centrifuged for 25 min at 2100g at 4 °C (rotor brakes were disabled). The upper phase was evaporated at 45 °C under a gentle stream of nitrogen, resuspended in 200 μL of methanol, vortexed, and incubated for 10 min. Finally, the sample was centrifuged for 2 min at 11,000g, and the supernatant was collected. Isolated samples from all methods were dried at 60 °C under nitrogen, resuspended in 80 μL of 75% methanol, and 20 μL were analysed using LC–MS.

2.4. LC–MS analysis

The sample was separated on a HPLC system (Dionex Ultimate 3000, Dionex Softron GmbH, Germany) equipped with a Hypersil GOLD column (150 × 2.1 mm, 3 μm, Thermo Scientific, USA) and SecurityGuard column (Phenomenex, USA). The mobile phase consisted of water, methanol, and ammonium acetate; flow rate was 0.3 mL/min, with the column chamber set to 40 °C. While ammonium acetate concentration at all times was kept at 0.1% (w/v), methanol concentrations (v/v) were as follows: 1–8 min 82–90%; 8–10 min 90%; 10–12 min 99%; 12–17 min 82%. To reduce contamination of the detector, the HPLC flow was allowed to the detector from 5 to 10.5 min only. C4 was detected in a triple quadrupole mass spectrometer (TSQ Quantum Access Max with H-ESI II probe, Thermo Fisher Scientific, Inc., USA) operating in SRM mode. The heated HESI-II probe for MS detector was run under the following conditions: spray voltage +3000 V, vaporizer temperature 350 °C, sheath gas 38 arbitrary units (au), auxiliary valve flow 8 au, ion sweep gas pressure 1.2 au, capillary temperature 320 °C. Tube lens voltage was set at 92 V, with the skimmer offset voltage not used. The tuning of MS/MS transitions was performed by the combined infusion of C4 (10 mg/L in the mobile phase, 20 μL/min) and the mobile phase (400 μL/min); collision gas (Ar) pressure was set to 1.5 mTorr. Monitored transitions (collision energy) were as follows: C4 [401.4 → 177.3 (25 V); 401.4 → 383.6 (18 V)], IS [408.4 → 177.3 (25 V); 408.4 → 390.6 (18 V)]. When needed, the elution of phospholipids was monitored as *m/z* 184 → 184 (7 V) and *m/z* 104 → 104 (7 V) [6].

2.5. Efficacy of deproteination and desalting

One hundred μL of serum were processed (using the methods in Section 2.3, above). For protein determination, final evaporates were dissolved in 100 μL of phosphate-buffered saline (overnight at 4 °C) and measured using DC Protein Assay (Bio-Rad, Hercules, CA, USA) according to the manufacturer's instructions. For salt content determination, evaporates were dissolved in distilled water, and conductivity was measured using a conductivity flow cell (Bio-

Table 1
Analytical performance of various extraction methods.

	Residual proteins (%)[a]	Residual conductivity (%)[a]	Extraction recovery (%)[b]	Intra-assay precision (as CV)[c]
A	0.27 ± 0.02	89.8 ± 3.8	96 ± 5	6.3% 7.2% 3.3%
B	1.02 ± 0.07	85.5 ± 1.8	97 ± 13	2.1% 2.5% 7.0%
C	0.26 ± 0.10	0.8 ± 0.6	90 ± 7	7.8% 7.2% 9.3%
D	0.08 ± 0.02	23.9 ± 0.9	88 ± 7	7.5% 1.2% 4.8%

[a] Performed in triplicates.
[b] Performed using six different serum samples (C4 levels within 16–200 μg/L).
[c] Analysis in pentaplicates on three C4 levels (28, 120, and 228 μg/L).

Logic LP System, Bio-Rad, Hercules, CA, USA). All analyses were performed in triplicate and expressed as a % of the initial content in the original serum sample.

2.6. Phospholipid analysis

To assess possible differences in phospholipids removal, semi-quantitative analysis of the phospholipids was employed. A total of ten samples purified by all extraction methods were analysed. Samples were dissolved in 40 μL of toluene:methanol mixture (9:1 by vol), separated using thin layer chromatography [stationary phase: 20 × 20 cm TLC silica gel 60 plates (Merck KGaA, Darmstadt, Germany); mobile phase: heptane-diethylether-acetic acid (85:15:1 by volume)], detected using iodine sublimation, and visually inspected. A representative chromatogram is shown in the Supplementary Figure.

2.7. Imprecision, extraction recovery

Intra-assay imprecision (calculated as the coefficient of variance) was based upon 5 measurements of three different serum samples (with C4 concentrations of 28, 120, and 228 μg/L). To estimate extraction recovery, 100 μL of sample was spiked with 3 ng of C4, either before or after extraction. It was calculated as: $[C4]_{sample\,spiked\,before\,extraction}/[C4]_{sample\,spiked\,after\,extraction}$, using six different serum samples (C4 concentration ranging from 16 to 200 μg/L).

2.8. Estimated time requirement

Total and "hands-on" time needed for processing one sample was estimated by two independent researchers familiar with all methods. Their estimates were then averaged.

3. Results and discussion

All methods proved satisfactory performance in the most important sample purification step – deproteination; residual protein content was reduced below (or to) 1% of the initial protein load (Table 1). Even though all methods were satisfactory, some of them were more efficient than the others. Method "D", due to protein precipitation in the presence of ammonium sulfate, proved to be by far the best in this respect – approximately 3 times more potent than methods "A" or "C", and over ten times better then method "B".

Phospholipid content was not sufficiently reduced by any extraction procedure (Supplementary Figure) and possible C4 signal suppression (which can affect accuracy even with the use of isotopically labeled IS [7]) should be prevented by sufficient spatial separation. A methanol based mobile phase (rather than acetonitrile based) and a higher column temperature would favour early phospholipid elution [6]. In our case, most of phospholipids were eluted before C4 (Fig. 1).

Not surprisingly, the efficacy of desalting (estimated as conductivity) was superior in the "two-phase purification" methods ("D" and "C", were capable of removing about three quarters, and almost all of the salts, respectively), when compared to "one-phase" purification methods ("A" and "B", removing less than one quarter of the salts) (Table 1).

On the contrary, one-phase extraction methods exhibited slightly better extraction recoveries (Table 1). However, the extraction recovery of even the least efficient method ("D", 88%) can be considered as sufficient. Intra-assay precision was always below 10% at all of the C4 levels tested, which seems to be acceptable taking into account the fact that inter-injection precision (repeated injection of the same sample) was 3.1%.

The total estimated time of purification varied from 24 min (method "C") to 102 min (method "D"). The estimated "hands-on"

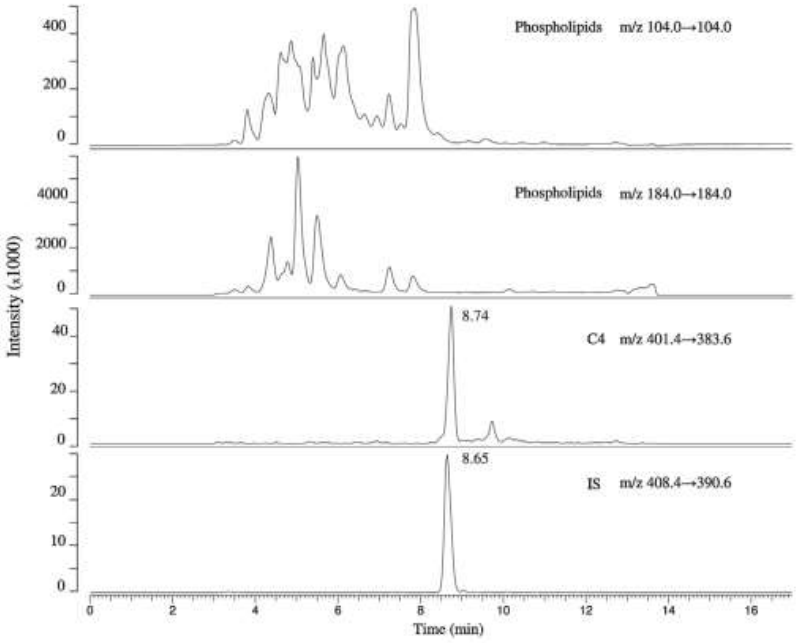

Fig. 1. Elution of phospholipids during a typical run.
The vast majority of phospholipids (top panels) are eluted before C4 and IS (bottom panels). Sample was purified using method "A". For better mapping of the elution profile, flow was allowed to the detector from 3 to 13 min (in a typical C4 analysis we monitor only 5–10.5 min).

time (much more important, as it increases with the number of samples) is 2 min with method "A", while the other methods are more laborious (5 min for methods "B" and "D", and 7 min for "C"). It should be noted that these are only estimates, and that significant person to person variability should be expected.

Taken together, no evident superiority was found for any of the tested methods. All of the methods proved to be sufficiently reliable, and a researcher needs to consider the finest details when choosing the preferred procedure. In the most common situation, when C4 is to be measured in the plasma/serum sample, a smart method by Camilleri et al. ("D") [5] should be considered due to analytical performance – specifically excellent deproteination. However, certain laboriousness and time consumption represent a clear handicap over simpler "one-phase extraction" methods. Acetonitrile precipitation (referred here as method "A") combines very good analytical performance with excellent simplicity, and thus can be suggested as a method of choice for everyday use (methanol deproteination, in principle equal to acetonitrile precipitation, was not tested here as it should yield samples with a higher phospholipid content [8]). Additionally, this extraction method proved to be reliable for quantification of BA [2], which offers a great advantage, since the C4 and a BA spectrum are often studied together. The method by Pellegrino et al. [3] ("B"), exhibiting superior recovery of all lipid classes, would be useful specifically in studies focused on an analysis of the global serum lipidome, where lipid substances other than C4 are not considered as contaminants.

When C4 is to be measured in matrices with high salt content (e.g., NaBr solutions after lipoprotein ultracentrifugation), in abundant samples with very low C4 concentration, or other "complicated" fluids (e.g., bile), the chloroform:methanol extraction ("C"), seems to be the method of choice due to the almost perfect desalting and the ease of C4 concentrating into chloroform. For the most complex matrices (e.g., tissue homogenates or cell cultures), more thorough purification might be required. In such samples, a combined chloroform:methanol and solid phase extraction [4] gives reliable results (data not shown). In rare low C4 samples, one would want to turn to more laborious methods, where derivatization ensures very high sensitivity [9].

To conclude, simple acetonitrile precipitation ("A") appears to be the most appropriate procedure for C4 determination in serum (ammonium sulfate:acetonitrile extraction ("D") being the close second), while methanol:*tert*-butyl methyl ether:chloroform extraction ("B") is not the method of choice.

Acknowledgement

This work was supported by grant RVO-VFN64165 from the Czech Ministry of Health.

Appendix A. Supplementary data

Supplementary data associated with this article can be found, in the online version, at http://dx.doi.org/10.1016/j.jchromb.2016.08.046.

References

[1] M. Axelson, A. Aly, J. Sjovall, FEBS Lett. 239 (1988) 324–328.
[2] D. Tagliacozzi, A.F. Mozzi, B. Casetta, P. Bertucci, S. Bernardini, C. Di Ilio, A. Urbani, G. Federici, Clin. Chem. Lab. Med. 41 (2003) 1633–1641.
[3] R.M. Pellegrino, A. Di Veroli, A. Valeri, L. Goracci, G. Cruciani, Anal. Bioanal. Chem. 406 (2014) 7937–7948.
[4] M. Lenicek, M. Juklova, J. Zelenka, J. Kovar, M. Lukas, M. Bortlik, L. Vitek, Clin. Chem. 54 (2008) 1087–1088.
[5] M. Camilleri, A. Nadeau, W.J. Tremaine, J. Lamsam, D. Burton, S. Odunsi, S. Sweetser, R. Singh, Neurogastroenterol. Motil. 21 (2009) 734–743.
[6] J.L. Little, M.F. Wempe, C.M. Buchanan, J. Chromatogr. B—Anal. Technol. Biomed. Life Sci. 833 (2006) 219–230.
[7] S. Wang, M. Cyronak, E. Yang, J. Pharm. Biomed. Anal. 43 (2007) 701–707.
[8] E. Chambers, D.M. Wagrowski-Diehl, Z.L. Lu, J.R. Mazzeo, J. Chromatogr. B—Anal. Technol. Biomed. Life Sci. 852 (2007) 22–34.
[9] A. Honda, K. Yamashita, M. Numazawa, T. Ikegami, M. Doy, Y. Matsuzaki, H. Miyazaki, J. Lipid Res. 48 (2007) 458–464.

Příloha 5

Received: 19 July 2022 | Revised: 16 November 2022 | Accepted: 18 November 2022

DOI: 10.1111/liv.15481

ORIGINAL ARTICLE

Liver INTERNATIONAL WILEY

Serum concentration of taurochenodeoxycholic acid predicts clinically significant portal hypertension

Kateřina Žížalová[1] | Barbora Nováková[1,2] | Marek Vecka[1,2] | Jaromír Petrtýl[2] | Věra Lánská[3] | Květa Pelinková[1] | Václav Šmíd[2] | Radan Brůha[2] | Libor Vítek[1,2] | Martin Leníček[1]

[1]Institute of Medical Biochemistry and Laboratory Diagnostics, First Faculty of Medicine and General University Hospital in Prague, Charles University, Prague, Czech Republic

[2]4th Department of Internal Medicine, First Faculty of Medicine and General University Hospital in Prague, Charles University, Prague, Czech Republic

[3]Institute for Clinical and Experimental Medicine, Prague, Czech Republic

Correspondence
Martin Leníček, Institute of Medical Biochemistry and Laboratory Diagnostics, First Faculty of Medicine and General University Hospital in Prague, Charles University, Kateřinská 32, Prague 12108, Czech Republic.
Email: martin.lenicek@lf1.cuni.cz

Funding information
Czech Society of Hepatology; Ministerstvo Zdravotnictví České Republiky

Handling Editor: Luca Valenti

Abstract

Background & Aims: Severity of portal hypertension is usually quantified by measuring the hepatic venous pressure gradient (HVPG). However, due to its invasiveness, alternative markers are being sought. Bile acids (BA), being synthesized, metabolized, and transported by the liver, seem to have the potential to serve as endogenous markers. The aim of the present study was to determine whether serum BA reflect the severity of portal hypertension.

Methods: We correlated serum concentrations of individual BA with portal pressure (as HVPG) in an exploratory cohort of 21 cirrhotic patients with portal hypertension. The predictive potential of selected candidates was then confirmed in an independent validation cohort ($n = 214$). Additionally, nine previously published noninvasive markers were added to the stepwise logistic regression model to identify the most relevant ones, which were eventually used to create a prognostic index of portal hypertension.

Results: Serum levels of taurochenodeoxycholic acid (TCDCA) significantly correlated with HVPG and showed a high potential to predict clinically significant portal hypertension (HVPG ≥ 10mm Hg: AUROC = 0.97 ± 0.06). This was confirmed in the validation cohort (AUROC = 0.96 ± 0.01). The predictive index (constructed based on AST/ALT, spleen diameter, and TCDCA concentration) was able to distinguish clinically significant portal hypertension with 95% sensitivity and 76% specificity.

Conclusions: TCDCA seems to be a promising noninvasive marker of clinically significant portal hypertension. Its predictive potential may be further enhanced when it is combined with both the AST/ALT ratio and spleen diameter.

KEYWORDS
bile acids, cirrhosis, noninvasive markers, portal hypertension, taurochenodeoxycholic acid

Abbreviations: ALT, alanine aminotransferase; AST, aspartate aminotransferase; AUROC, area under the ROC; BA, bile acid(s); CA, cholic acid; CDCA, chenodeoxycholic acid; GCDCA, glycochenodeoxycholic acid; HVPG, hepatic venous pressure gradient; ROC, receiver operator characteristic; TCDCA, taurochenodeoxycholic acid.

1 | INTRODUCTION

Portal hypertension is one of the main consequences of cirrhosis and is responsible for its most severe complications. The severity of portal hypertension is useful as both a diagnostic and as a prognostic tool, with important therapeutic implications.[1] Although measurement of the porto-systemic gradient by catheterization of the hepatic veins (hepatic venous pressure gradient, HVPG) is considered the gold standard,[2,3] this minimally invasive procedure is only available in specialized centers. Therefore, noninvasive surrogate marker(s) of portal pressure are in the spotlight of current research. Bile acids (BA) are synthesized in the liver, conjugated with either glycine or taurine and sent to duodenum as a crucial component of bile. In the distal ileum, conjugated BA are effectively resorbed, while a small fraction of BA that spills over into the colon is deconjugated and may be further modified and partially resorbed. Resorbed BA return to the liver via portal vein for re-conjugation and re-secretion. For more detailed information about BA, we refer the reader to one of the many review articles available, eg. Refs. [4,5].

Portal hypertension leads to the formation of porto-systemic collaterals, and diverts portal blood from the liver to the systemic circulation.[6] If the amount of blood that bypasses the liver through these shunts was proportional to the portal pressure, analytes with a high first-pass effect should markedly increase in the systemic blood; thus reflecting the portal pressure. BA, endogenous compounds that undergo efficient enterohepatic circulation,[7] appear to be logical candidates. Moreover, some BA were described as vasoactive molecules in animals three decades ago.[8,9] Recently, BA have been confirmed as an important factor in the pathophysiology of the dynamic component of portal hypertension in both animal models and in humans.[10] Therefore, the aim of our work was to find out whether the serum concentrations of some BA may reflect the portal pressure, and could be used as a surrogate marker of portal hypertension.

Lay summary

To identify a noninvasive surrogate marker of portal hypertension, we correlated HVPG values with serum concentrations of individual BA in an exploratory cohort of 21 cirrhotic patients. We demonstrated that the serum concentration of TCDCA can predict clinically significant portal hypertension (HVPG ≥ 10 mm Hg) in cirrhotic patients with high sensitivity. This was further confirmed in an independent validation cohort of 214 cirrhotic patients. The predictive power of TCDCA may be further improved by its combination with the AST/ALT ratio and spleen diameter.

2 | MATERIALS AND METHODS

2.1 | Study subjects

In the present study, we investigated cirrhotic patients with portal hypertension, who underwent HVPG measurement at the 4th Department of Internal Medicine, First Faculty of Medicine and General University Hospital in Prague. Most of the subjects were already included in our previous study.[11] The blood samples from the portal vein were collected during simultaneous hepatic vein catheterization and transjugular liver biopsy when the right branch of the portal vein was punctured. Peripheral blood samples were taken at the same time as the invasive procedure. Serum/plasma samples were stored at −80°C until needed. The study was approved (No. 126/16) by the Ethics Committee of the General University Hospital in Prague, and all patients gave their written informed consent.

2.2 | Portal pressure measurement

The portal pressure was measured during hepatic vein catheterization (as the HVPG) using the classical wedge technique.[12] Briefly, after an overnight fast, the patient was given local anaesthesia, and a 7F catheter introducer was placed in the right jugular vein using the Seldinger technique. HVPG was calculated as the difference between the wedged hepatic venous pressure and the free hepatic venous pressure that was measured with a 7F balloon-tipped catheter (B. Braun Melsungen AG, Melsungen, Germany).

2.3 | Ultrasonography of the spleen

All patients had undergone a standard abdominal ultrasound with a Siemens Acuson S2000 ultrasound system with a 6C1 HD convex ultrasound probe (Siemens, Munich, Germany). The spleen was measured along its maximal longitudinal plane, placing its hilum at the center of the image during recording of the maximum spleen diameter.

2.4 | Biochemical analyses

Upon addition of a mix of nine deuterium-labelled internal standards and acetonitrile deproteination, the BA were quantified using liquid chromatography–tandem mass spectrometry, as previously described.[13] The following BA standards were used: cholic acid (CA), chenodeoxycholic acid (CDCA), glycocholic acid, deoxycholic acid, lithocholic acid, taurodeoxycholic acid, glycodeoxycholic acid, glycolithocholic acid, glycoursodeoxycholic acid, hyocholic acid, taurocholic acid, taurolithocholic acid 3-sulfate, and ursodeoxycholic acid (all from Sigma-Aldrich, St. Louis, MO, USA); the α-muricholic acid, glycochenodeoxycholic acid (GCDCA), allocholic acid, murideoxycholic acid, β-muricholic acid, ω-muricholic acid, tauro-α-muricholic acid, tauro-β-muricholic acid, taurochenodeoxycholic acid (TCDCA), and tauroursodeoxycholic acid were from Santa Cruz Biotechnology, Inc. (Dallas, TX, USA); and the hyodeoxycholic acid was from Supelco

(Bellefonte, PA, USA). Some of the deuterium-labelled standards (d5-taurocholic acid, d5-glycocholic acid, d4-GCDCA, and d4-TCDCA) were obtained from Santa Cruz Biotechnology Inc. (Dallas, TX, USA); and others (d4-chenodeoxycholic acid, d4-lithocholic acid, d4-CA, d4-ursodeoxycholic acid, and d4-deoxycholic acid) were from Sigma-Aldrich (St. Louis, MO, USA). The osteopontin was quantified using a Human Osteopontin Quantikine ELISA kit (R&D Systems, Minneapolis, MN, USA) according to the manufacturer's instructions. Other biochemical parameters: hyaluronic acid (Hyaluronic Acid LT Assay, Fujifilm, Wako Chemicals Europe), creatinine (Creatinine Jaffé Gen.2), bilirubin (Bilirubin Total Gen.3), aspartate aminotransferase (AST, ASTPM), alanine aminotransferase (ALT, ALTPM), albumin (ALB2) (all obtained from Roche Diagnostics, Risch-Rotkreuz, Switzerland) were measured using an automatic Cobas 8000 analyser.

2.5 | Statistical analyses

To determine the relationship between variables, the Spearman correlation coefficient was used. The Mann–Whitney or Wilcoxon test was used for comparison of continuous variables of independent or dependent samples respectively. Fisher exact test was used for discrete variables of independent samples. The Bonferroni correction was used to compensate for multiple comparisons. For easier interpretation, the individual *p*-values were corrected rather than the significance threshold. Stepwise (forward) logistic regression was used to find the relevant predictors for portal pressure above 10 mm Hg. Based on their β estimates, formula for "portal hypertension index" was constructed. Analyses were performed using either Prism 8.0.1 software (GraphPad, San Diego, CA, USA) or JMP 15.2.0, 2019 (SAS Institute Inc., Cary, NC, USA). Receiver operator characteristic (ROC) analyses were performed using a web based calculator.[14] *p*-values $< .05$ were considered as significant throughout the study.

3 | RESULTS

3.1 | Baseline clinical characteristics of patients

A total of 487 cirrhotic patients underwent the HVPG procedure at our department between 2007 and 2020. After exclusion of patients undergoing ursodeoxycholic acid therapy, those with incomplete clinical data, hepatocellular cancer, or cholangiocarcinoma, 255 patients were available for analysis. Most of the patients were men (65%), median age 58 years (interquartile range 48–64) with ethylic aetiology (72%). The indication for portal vein catheterization was either to assess the severity of portal hypertension (78%) or to perform simultaneous transjugular liver biopsy and hemodynamic evaluation of portal hypertension (22%). Exploratory cohort consisted of patients ($n = 21$) from whom both portal and systemic (taken from the vena cava) blood samples were available, while patients from whom only peripheral blood samples were available (i.e., lacking portal blood sample, $n = 214$; 20 patients with aetiology of cirrhosis other than ethylic, hepatitis B, C or NASH were excluded) formed the validation cohort. See Table 1 and Figure 1 for basic description of both cohorts and the study flowchart, respectively.

3.2 | BA differences in the portal and peripheral blood

In an effort to identify the BA with the greatest first-pass effect (a promising candidate marker for portal hypertension), we measured 23 BA species in the portal and peripheral serum from our exploratory cohort. The mean uptake of individual BA species was only 11% ± 0.44 and was virtually independent of the number of hydroxyl groups or its conjugation status (Figure 2, Table 2).

3.3 | GCDCA and TCDCA predict HVPG

As the previous analysis did not reveal a clear candidate, we tested the correlation between the HVPG values and the concentrations of individual BA in our exploratory cohort. Eight rare BA (detectable in less than 50% of the patients) were not considered, while the remaining 15 BA species were further analysed. Of these, GCDCA and TCDCA correlated significantly with HVPG (Table S1, Figure S1). We used ROC analysis to assess their potential to predict clinically relevant HVPG values (10, 16, and 20 mm Hg, reflecting: clinically significant portal hypertension,[15,16] a risk of massive bleeding, and a risk of potentially fatal variceal bleeding, respectively).[2,3] The portal pressure of 12 mm Hg (as a risk factor for variceal bleeding) could not be tested, as none of the patients in our exploratory cohort were within the HVPG 10–12 mm Hg range (Table 1). Both BA showed a high predictive potential to identify patients with HVPG ≥ 10 mm Hg. The area under the ROC curve (AUROC) was 0.97 ± 0.06 and 0.96 ± 0.07 for TCDCA and GCDCA, respectively (Figure 3). The predictions for other portal pressure thresholds were weaker. The AUROCs for TCDCA and GCDCA were as follows: 0.78 ± 0.1 and 0.75 ± 0.11 for 16 mm Hg; and 0.92 ± 0.08 and 0.66 ± 0.11 for 20 mm Hg, respectively. In order to confirm the ability of TCDCA and GCDCA to identify patients with HVPG ≥ 10 mm Hg, we repeated the ROC analysis in the independent validation cohort of 214 subjects. Both BA proved to be strong predictors: the AUROCs for TCDCA and GCDCA were 0.96 ± 0.01 and 0.92 ± 0.03, respectively (Figures 3 and 4).

3.4 | TCDCA versus other non-invasive markers

We had wondered whether the predictive potential of BA could be strengthened by combining them with other previously described non-invasive markers. Therefore, we correlated the HVPG values in our validation cohort with serum albumin,[17] hyaluronic acid,[18] bilirubin,[19] AST/ALT ratio,[20] creatinine,[21] osteopontin,[11] and

TABLE 1 Basic characteristics of exploratory and validation cohorts

		Exploratory cohort (*n* = 21)	Validation cohort (*n* = 214)
Age	[years]	51 (47–56)	58 (49–64)
Men		18 (88%)	147 (68%)
HVPG	[mm Hg]	15 (12–19)	16 (12–20)
HVPG distribution			
<10 mm Hg		5 (24%)	32 (15%)
10–11 mm Hg		0 (0%)	19 (9%)
12–15 mm Hg		7 (33%)	52 (24%)
16–19 mm Hg		5 (24%)	52 (24%)
≥20 mm Hg		4 (19%)	59 (28%)
Child-Pugh score			
A		4 (19%)	108 (50%)[a]
B		4 (19%)	67 (31%)[a]
C		6 (29%)	31 (14%)[a]
Unknown		7 (33%)	8 (4%)
Aetiology of cirrhosis			
Ethylic		15 (70%)	169 (79%)
HCV		1 (5%)	20 (9.3%)
NASH		1 (5%)	20 (9.3%)
HBV		2 (10%)	5 (2.3%)
AIH		1 (5%)	–
Porphyria		1 (5%)	–
Albumin	[g/L]	28 (25–36.1)	35.4 (29.8–40)
ALT	[μkat/L]	0.5 (0.33–0.66)	0.57 (0.4–0.84)[b]
AST	[μkat/L]	0.78 (0.68–1.12)	0.83 (0.6–1.26)[b]
AST/ALT	[–]	1.89 (1.5–2.2)	1.45 (1.1–2)[b]
Bilirubin	[μmol/L]	39.8 (21.9–66.6)	25.3 (14.1–43.6)[a,b]
Creatinine	[μmol/L]	79.5 (56.3–88)	78.5 (65–93)[b]
Hyaluronic acid	[μg/L]	–	177.6 (77.6–452.3)[b]
Osteopontin	[μg/L]	–	102.1 (67–170.7)[b]
Spleen diameter	[mm]	–	135 (120–150)[b]

Abbreviations: ALT, alanine aminotransferase; AST, aspartate aminotransferase; HBV, hepatitis B; HCV, hepatitis C; HVPG, hepatic venous pressure gradient; NASH, non-alcoholic steatohepatitis.

[a]No significant differences between cohorts were observed except for bilirubin and Child-Pugh score, which were higher in the exploratory cohort (uncorrected $p = .025$ (Mann–Whitney) and $p = .014$ (Fisher exact), respectively).

[b]Some clinical data are not available in the validation cohort. The number of cases is as follows: albumin ($n = 193$); ALT, AST, ALT/AST ($n = 196$); bilirubin ($n = 195$); creatinine ($n = 194$); hyaluronic acid ($n = 172$); spleen diameter ($n = 190$). Data presented as median (interquartile range) or *n* (%).

measurement of the spleen diameter (42 patients with incomplete data were excluded, Figure 1). Apart from creatinine and AST, all the parameters correlated significantly with the degree of portal hypertension (Table 3). From the parameters described above, the most important predictors of clinically significant portal hypertension (HVPG ≥ 10 mm Hg) were selected using stepwise logistic regression analysis based on their *p*-values (Table S2). Subsequently, the "portal hypertension index" was created from the β estimates of these three parameters: AST/ALT, spleen diameter, and TCDCA (Table S3). The ROC analysis was used to set up the threshold with a high sensitivity and an acceptable specificity. As a result, HVPG above 10 mm Hg can be expected in a patient if:

$$\frac{\text{Spleen diameter[mm]}}{42} + 2.3 \times \frac{\text{AST}}{\text{ALT}} + 0.6 \times \text{TCDCA}[\mu\text{mol/L}] \geq 6$$

In this setting, the sensitivity was 95%, and the specificity was 76% (AUROC = 0.93 ± 0.04).

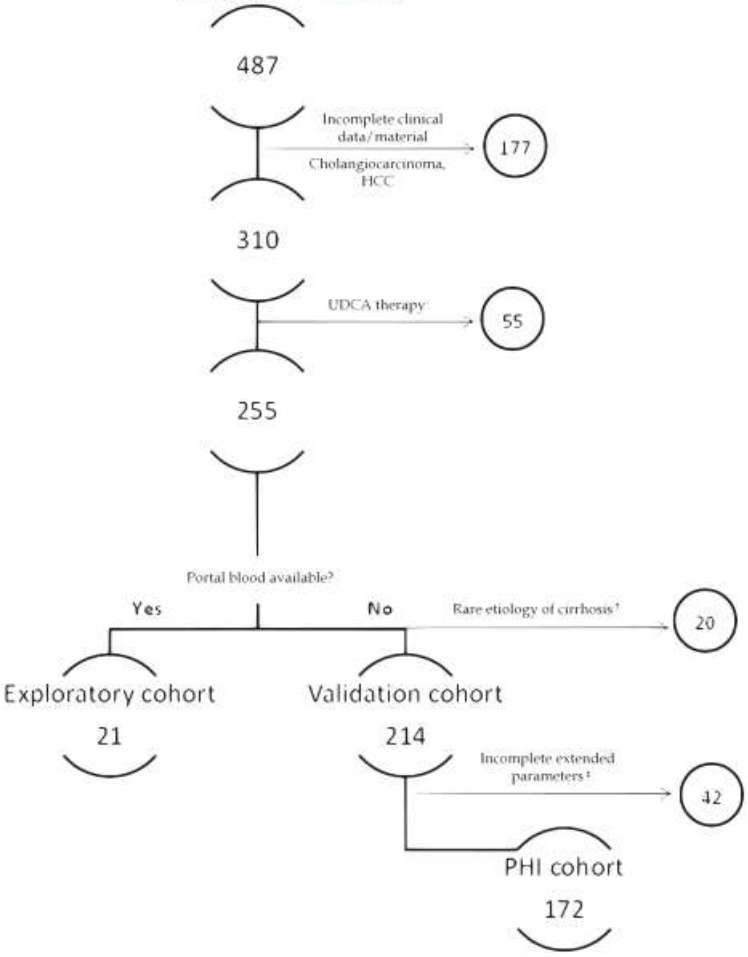

FIGURE 1 Study flowchart. †To reduce heterogeneity of the validation cohort, patients with rare or unclear aetiology of cirrhosis were excluded. Rare etiologies include: autoimmune hepatitis, Wilson's disease, porphyria, amyloidosis, cardiac cirrhosis, congenital fibrosis, drug induced liver injury, hemochromatosis, primary biliary cholangitis, and primary sclerosing cholangitis. ‡Extended parameters were those needed for PHI calculation. HCC-hepatocellular carcinoma; PHI-portal hypertension index; UDCA-ursodeoxycholic acid.

4 | DISCUSSION

In the present study we analysed the relationship between serum concentrations of individual BA species and the portal pressure in patients with cirrhotic portal hypertension. We found that GCDCA and TCDCA correlated significantly with the portal pressure (as measured by HVPG); in fact, even better than most of the previously described non-invasive markers of portal hypertension (Tables 3 and S1). Importantly, the serum levels of both BA showed a surprisingly strong predictive power for clinically significant portal hypertension (HVPG ≥ 10 mm Hg), with AUROC values above 0.9, which was also confirmed in the validation cohort. This seems to be in agreement with the results of Hayashi et al.,[22] who demonstrated a considerable level for prediction of portal hypertension of 200 mm H_2O (being roughly equivalent to 15 mm Hg) by total serum BA, determined enzymatically. By combining TCDCA, spleen diameter, and the AST/ALT ratio we created a "portal hypertension index" that can indicate clinically significant portal hypertension with a high sensitivity and an acceptable specificity, as well (95% and 76% respectively). Why does serum TCDCA increase along with portal hypertension more than other BA? In theory, in patients with liver disorders leading to decreased biliary BA secretion, one would expect a relative increase in the primary over secondary BA (especially their conjugates); for example, as observed in patients with cirrhosis or non-alcoholic fatty liver disease.[23,24] Our results (at least partially) fulfil such an expectation (Table 1). In fact, conjugates of both primary BA (CA and CDCA) correlated with portal hypertension in our exploratory cohort; although the correlation of those derived from CA was weaker and did not pass the strict Bonferroni correction. Still, the observed CA:CDCA ratio was approximately 1:3, which is in striking contrast to the normal ratio of about 3:1.[25] Although the relative excess of CDCA over CA derivatives seem to be a common feature of liver cirrhosis (fibrosis)[25-28] as well as non-alcoholic fatty liver disease,[24] the mechanism behind this remains somewhat enigmatic. As the differences in the first pass effect of individual BA were minimal in our cohort (surprisingly, the liver uptake of all BA having been much lower than expected), with either enhanced renal excretion or suppressed synthesis of CA likely being involved. The renal excretion

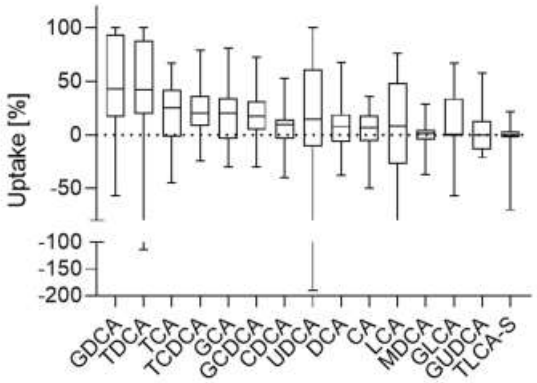

FIGURE 2 Hepatic uptake of individual BA. The uptake was determined as the relative decrease in the concentration of individual BA in the vena cava compared to portal blood. Data (from the entire exploratory cohort, $n = 21$) are presented as the median, interquartile range (box), and minimum-maximum (whiskers). Only BA that were at least detectable in 50% of the patients were analysed. BA, bile acid(s); CA, cholic acid; CDCA, chenodeoxycholic acid; DCA, deoxycholic acid; GCA, glycocholic acid; GCDCA, glycochenodeoxycholic acid; GDCA, glycodeoxycholic acid; GLCA, glycolithocholic acid; GUDCA, glycoursodeoxycholic acid; LCA, lithocholic acid; MDCA, murideoxycholic acid; TCA, taurocholic acid; TCDCA, taurochenodeoxycholic acid; TDCA, taurodeoxycholic acid; TLCA-S, taurolithocholic acid 3-sulfate; UDCA, ursodeoxycholic acid.

TABLE 2 BA spectrum in exploratory cohort

	Portal vein [μmol/L] ($n = 21$)	V. cava [μmol/L] ($n = 21$)
CA	0.2 (0.2–0.5)	0.2 (0.1–0.5)
CDCA	0.6 (0.2–1.3)	0.6 (0.2–1.2)
DCA	0.3 (0.1–0.6)	0.2 (0.1–0.6)
GCA	3.2 (1.8–5.9)	2.9 (1.2–4.3)
GCDCA	10.6 (7.3–17.9)	10.3 (5–15.1)
GDCA	0.2 (0–0.6)	0.1 (0–0.4)
GLCA	0.1 (0–0.1)	0.1 (0–0.1)
GUDCA	0.3 (0.2–0.5)	0.4 (0.2–0.6)
LCA	0.1 (0.1–0.3)	0.1 (0.1–0.2)
MDCA	0.2 (0.2–0.3)	0.2 (0.2–0.2)
TCA	0.9 (0.7–2.3)	0.7 (0.5–1.7)
TCDCA	4.1 (1.4–8.2)	3.0 (0.9–5.7)
TDCA	0.1 (0–0.6)	0.1 (0–0.4)
TLCA-S	0.4 (0.4–0.6)	0.4 (0.4–0.6)
UDCA	0.1 (0–0.1)	0.1 (0–0.1)
Other	0.2 (0–0.4)	0.2 (0.1–0.5)
Total BA[a]	32.2 (19.5–37.7)	26.2 (14.1–39.2)
CA/CDCA[b]	0.3 (0.2–0.6)	0.3 (0.2–0.6)
Glyco/Tauro conjugates	2.9 (1.4–5.2)	3.3 (1.3–4.6)
Primary/secondary BA	26.5 (5.9–34.3)	14.3 (5.5–30.6)

Note: Data presented as median (interquartile range).

Abbreviations: BA, bile acid(s); CA, cholic acid; CDCA, chenodeoxycholic acid; DCA, deoxycholic acid; GCA, glycocholic acid; GCDCA, glycochenodeoxycholic acid; GDCA, glycodeoxycholic acid; GLCA, glycolithocholic acid; GUDCA, glycoursodeoxycholic acid; LCA, lithocholic acid; MDCA, murideoxycholic acid; TCA, taurocholic acid; TCDCA, taurochenodeoxycholic acid; TDCA, taurodeoxycholic acid; TLCA-S, taurolithocholic acid 3-sulfate; UDCA, ursodeoxycholic acid.

[a]The sum of all detectable BA species.

[b]Ratio calculated from CA (CDCA) and their conjugates.

of a BA largely depends on its polarity. The more polar trihydroxy CA binds to serum albumin to a much lesser extent than does dihydroxy CDCA; so its renal clearance is about 3 times higher. On the other hand, CDCA is preferentially sulfated compared to CA, leading to faster renal elimination; and the net renal excretion in patients with liver cirrhosis seems to be balanced or even higher for CDCA.[28] There are two crucial steps in the classical pathway of BA synthesis: 7α hydroxylation (catalysed by cholesterol 7α-monooxygenase, CYP7A1) is the initial and key regulatory step; common for both primary BA. On the other hand, the action of sterol 12-α-hydroxylase (CYP8B1) directs synthesis exclusively towards CA, thereby determining the CA/CDCA ratio. The lower the CYP8B1 activity, the lower the proportion of CA. Both enzymes are under negative feedback control by BA; however, the mechanisms seem to differ. CYP7A1 has been shown to be primarily controlled by intestinal FXR signalling (via FGF19/FGF15), while hepatic FXR predominantly suppresses CYP8B1 (via SHP).[29] In patients with portal hypertension (or more generally in patients with decreased biliary BA output and elevated serum BA levels) hepatic FXR signalling should predominate over intestinal FXR signalling, leading to the suppression of CYP8B1 and lower CA formation. However, it should be noted that this tissue-specific action has only been studied in mice, and rodent experiments can not always be easily translated to humans, especially in the case of BA. Basal expression of *Cyp7a1* and *Cyp8b1* in tissue-specific *Fxr* knock-out animals also contradicted a later study.[30] The recent observation that BA-driven LIX1L overexpression leads to upregulation of both *CYP7A1* and *CYP8B1* (with the effect more pronounced with CYP7A1) may also partially explain the preferential synthesis of CDCA over that of CA.[31]

There are several limitations in our study. First, the small number of subjects in the exploratory cohort (due to the unavailability of the portal blood sample) may have led to other relevant markers being overlooked. The uneven distribution of HVPG values within our cohorts did not allow us to reliably assess the role of BA in the prediction of portal hypertension other than ≥10 mm Hg. Next, the vast majority of patients in our cohorts had portal hypertension of ethylic aetiology; therefore, perhaps the results can not be directly inferred to work with patients with portal hypertension of other etiologies. Although the predictive performance of TCDCA does not seem to be aetiology dependent, this remains to be proven in a larger cohort study. The high proportion of alcohol-abuse-related portal hypertension subjects in our study may have markedly influenced the

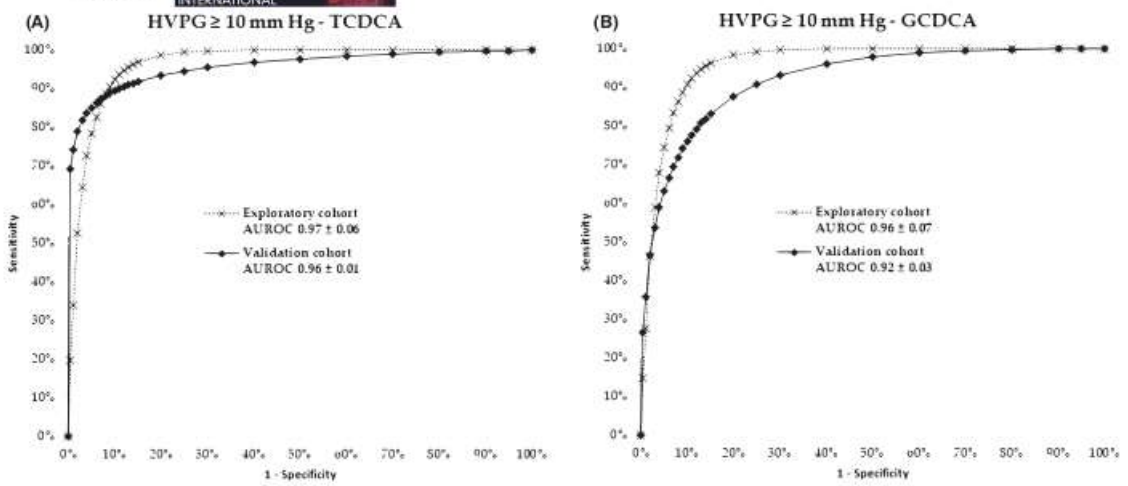

FIGURE 3 TCDCA and GCDCA as predictors of clinically significant portal hypertension. ROC analysis showed excellent predictive power of both TCDCA (panel A) and GCDCA (panel B) for differentiation of cirrhotic patients with HVPG ≥ 10 mm Hg. Curves based both on exploratory cohort ($n = 21$) as well as validation cohort ($n = 214$) are shown. AUROC, area under the ROC; GCDCA, glycochenodeoxycholic acid; HVPG, hepatic venous pressure gradient; ROC, receiver operating characteristics; TCDCA, taurochenodeoxycholic acid.

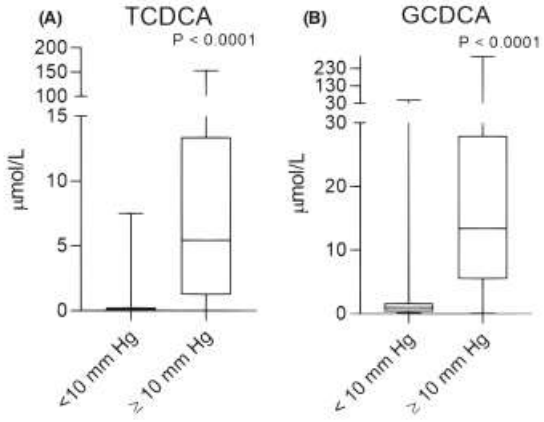

FIGURE 4 Serum concentration of TCDCA and GCDCA according to portal hypertension severity. The concentration of TCDCA and GCDCA markedly differs in cirrhotic patients with/without clinically significant portal hypertension (HVPG ≥ 10 mm Hg). Data (from the validation cohort, $n = 214$) are presented as the median, interquartile range (box), and minimum-maximum (whiskers). GCDCA, glycochenodeoxycholic acid; HVPG, hepatic venous pressure gradient; TCDCA, taurochenodeoxycholic acid.

TABLE 3 Correlation of HVPG with other noninvasive markers in validation cohort

	n[a]	r	p	$p_{corr.}$[b]
ALT [µkat/L]	196	−0.229	.001	.013
AST [µkat/L]	196	0.188	.008	ns
AST/ALT [−]	196	0.543	<.001	<.001
Creatinine [µmol/L]	194	−0.084	.252	ns
Hyaluronic acid [µg/L]	172	0.548	<.001	<.001
Osteopontin [ng/ml]	214	0.282	<.001	<.001
Albumin [g/L]	214	−0.480	<.001	<.001
Spleen diameter [mm]	190	0.244	<.001	.006
Bilirubin [µmol/L]	195	0.359	<.001	<.001

Abbreviations: ALT, alanine aminotransferase; AST, aspartate aminotransferase; HVPG, hepatic venous pressure gradient.

[a]Number of cases is given due to an incomplete dataset.

[b]Bonferroni corrected p-values.

proposed "portal hypertension index", as the AST/ALT ratio (used to calculate the index) is known to be altered in patients with a pattern of alcohol abuse.[32] Also, the utility of the index has not been tested in an independent validation cohort. Finally, it should be mentioned that TCDCA itself is seen elevated in multiple liver diseases, and it is unlikely to be specific for portal hypertension.

In conclusion, the serum concentration of TCDCA can serve as a minimally invasive marker of clinically significant portal hypertension, which can help to identify those patients who need more detailed examination. The predictive value can likely be improved by combining TCDCA with both the AST/ALT ratio and spleen diameter; however, this needs to be verified in an independent cohort.

ACKNOWLEDGEMENTS

This work was funded by the Ministry of Health, Czech Republic—conceptual development of research organization (RVO-VFN 64165/2021), and by the Foundation of the Czech Society of Hepatology.

CONFLICT OF INTEREST

The authors have no conflicts to disclose.

ORCID

Kateřina Žižalová https://orcid.org/0000-0003-1155-4351
Barbora Nováková https://orcid.org/0000-0002-7565-5592
Martin Leníček https://orcid.org/0000-0001-6242-3488

REFERENCES

1. D'Amico G, Morabito A, D'Amico M, et al. Clinical states of cirrhosis and competing risks. *J Hepatol*. 2018;68:563-576. doi:10.1016/j.jhep.2017.10.020
2. de Franchis R. Expanding consensus in portal hypertension: report of the Baveno VI consensus workshop: stratifying risk and individualizing care for portal hypertension. *J Hepatol*. 2015;63:743-752. doi:10.1016/j.jhep.2015.05.022
3. Garcia-Tsao G, Abraldes JG, Berzigotti A, Bosch J. Portal hypertensive bleeding in cirrhosis: risk stratification, diagnosis, and management: 2016 practice guidance by the American association for the study of liver diseases. *Hepatology*. 2017;65:310-335. doi:10.1002/hep.28906
4. Hofmann AF. Bile acids: trying to understand their chemistry and biology with the hope of helping patients. *Hepatology*. 2009;49:1403-1418. doi:10.1002/hep.22789
5. Chiang JYL. Bile acid metabolism and signaling. *Compr Physiol*. 2013;3:1191-1212. doi:10.1002/cphy.c120023
6. Møller S, Bendtsen F. The pathophysiology of arterial vasodilatation and hyperdynamic circulation in cirrhosis. *Liver Int*. 2018;38:570-580. doi:10.1111/liv.13589
7. Gilmore IT, Thompson RP. Plasma clearance of oral and intravenous cholic acid in subjects with and without chronic liver disease. *Gut*. 1980;21:123-127. doi:10.1136/gut.21.2.123
8. Pak JM, Lee SS. Vasoactive effects of bile salts in cirrhotic rats: in vivo and in vitro studies. *Hepatology*. 1993;18:1175-1181.
9. Pak JM, Adeagbo AS, Triggle CR, Shaffer EA, Lee SS. Mechanism of bile salt vasoactivity: dependence on calcium channels in vascular smooth muscle. *Br J Pharmacol*. 1994;112:1209-1215. doi:10.1111/j.1476-5381.1994.tb13212.x
10. Königshofer P, Hofer BS, Brusilovskaya K, et al. Distinct structural and dynamic components of portal hypertension in different animal models and human liver disease etiologies. *Hepatology*. 2022;75:610-622. doi:10.1002/hep.32220
11. Bruha R, Jachymova M, Petrtyl J, et al. Osteopontin: a non-invasive parameter of portal hypertension and prognostic marker of cirrhosis. *World J Gastroenterol*. 2016;22:3441-3450. doi:10.3748/wjg.v22.i12.3441
12. Groszmann RJ, Wongcharatrawee S. The hepatic venous pressure gradient: anything worth doing should be done right. *Hepatology*. 2004;39:280-283. doi:10.1002/hep.20062
13. Prasnicka A, Cermanova J, Hroch M, et al. Iron depletion induces hepatic secretion of biliary lipids and glutathione in rats. *Biochim Biophys Acta Mol Cell Biol Lipids*. 2017;1862:1469-1480. doi:10.1016/j.bbalip.2017.09.003
14. Eng J. *ROC analysis: web-based calculator for ROC curves*. Johns Hopkins University; 2014. http://www.jrocfit.org
15. Herrick FC. An experimental study into the cause of the increased portal pressure IN portal cirrhosis. *J Exp Med*. 1907;9:93-104. doi:10.1084/jem.9.1.93
16. Paton A, Reynolds TB, Sherlock S. Assessment of portal venous hypertension by catheterisation of hepatic vein. *Lancet*. 1953;261:918-921. doi:10.1016/S0140-6736(53)92060-1
17. Harjai KJ, Kamble MS, Ashar VJ, Anklesaria PS, Ratnam KL, Abraham P. Portal venous pressure and the serum-ascites albumin concentration gradient. *Cleve Clin J Med*. 1995;62:62-67. doi:10.3949/ccjm.62.1.62
18. Kropf J, Gressner AM, Tittor W. Logistic-regression model for assessing portal hypertension by measuring hyaluronic acid (hyaluronan) and laminin in serum. *Clin Chem*. 1991;37:30-35.
19. Park SH, Park TE, Kim YM, et al. Non-invasive model predicting clinically-significant portal hypertension in patients with advanced fibrosis. *J Gastroenterol Hepatol*. 2009;24:1289-1293. doi:10.1111/j.1440-1746.2009.05904.x
20. MRC/BHF heart protection study of cholesterol lowering with simvastatin in 20,536 high-risk individuals: a randomised placebo-controlled trial. *Lancet*. 2002;360:7-22.
21. Garcia-Pagán JC, Saffo S, Mandorfer M, Garcia-Tsao G. Where does TIPS fit in the management of patients with cirrhosis? *JHEP Rep*. 2020;2:100122. doi:10.1016/j.jhepr.2020.100122
22. Hayashi H, Beppu T, Okabe H, et al. Combined measurements of serum bile acid level and splenic volume may be useful to noninvasively assess portal venous pressure. *J Gastroenterol*. 2012;47:1336-1341. doi:10.1007/s00535-012-0599-7
23. Liu N, Feng J, Lv Y, et al. Role of bile acids in the diagnosis and progression of liver cirrhosis: a prospective observational study. *Exp Ther Med*. 2019;18:4058-4066. doi:10.3892/etm.2019.8011
24. Caussy C, Hsu C, Singh S, et al. Serum bile acid patterns are associated with the presence of NAFLD in twins, and dose-dependent changes with increase in fibrosis stage in patients with biopsy-proven NAFLD. *Aliment Pharmacol Ther*. 2019;49:183-193. doi:10.1111/apt.15035
25. Carey JB Jr. The serum trihydroxy-dihydroxy bile acid ratio in liver and biliary tract disease. *J Clin Invest*. 1958;37:1494-1503. doi:10.1172/jci103741
26. Einarsson KKHE, Schersten T. The formation of bile acids in patients with portal liver cirrhosis. *Scand J Gastroenterol*. 1975;10:299-304.
27. Vlahcevic ZR, Juttijudata P, Bell CC Jr, Swell L. Bile acid metabolism in patients with cirrhosis. II. Cholic and chenodeoxycholic acid metabolism. *Gastroenterology*. 1972;62:1174-1181.
28. Stiehl A, Earnest DL, Admirant WH. Sulfation and renal excretion of bile salts in patients with cirrhosis of the liver. *Gastroenterology*. 1975;68:534-544.
29. Kong B, Wang L, Chiang JYL, Zhang Y, Klaassen CD, Guo GL. Mechanism of tissue-specific farnesoid X receptor in suppressing the expression of genes in bile-acid synthesis in mice. *Hepatology*. 2012;56:1034-1043.
30. Xu Y, Li F, Zalzala M, et al. Farnesoid X receptor activation increases reverse cholesterol transport by modulating bile acid composition and cholesterol absorption in mice. *Hepatology*. 2016;64:1072-1085. doi:10.1002/hep.28712
31. Li J, Zhu X, Zhang M, et al. Limb expression 1-like (LIX1L) protein promotes cholestatic liver injury by regulating bile acid metabolism. *J Hepatol*. 2021;75:400-413. doi:10.1016/j.jhep.2021.02.035
32. Ruhl CE, Everhart JE. Joint effects of body weight and alcohol on elevated serum alanine aminotransferase in the United States population. *Clin Gastroenterol Hepatol*. 2005;3:1260-1268. doi:10.1016/s1542-3565(05)00743-3

SUPPORTING INFORMATION

Additional supporting information can be found online in the Supporting Information section at the end of this article.

How to cite this article: Žižalová K, Nováková B, Vecka M, et al. Serum concentration of taurochenodeoxycholic acid predicts clinically significant portal hypertension. *Liver Int*. 2023;43:888-895. doi:10.1111/liv.15481